Nonlinear Model Predictive Control
- from industrial process optimization to new biomedical products

John Bagterp Jørgensen
Technical University of Denmark

02610 Optimization and Data Fitting
2020

DTU Compute
Department of Applied Mathematics and Computer Science

Introduction

Industry 4.0 and beyond

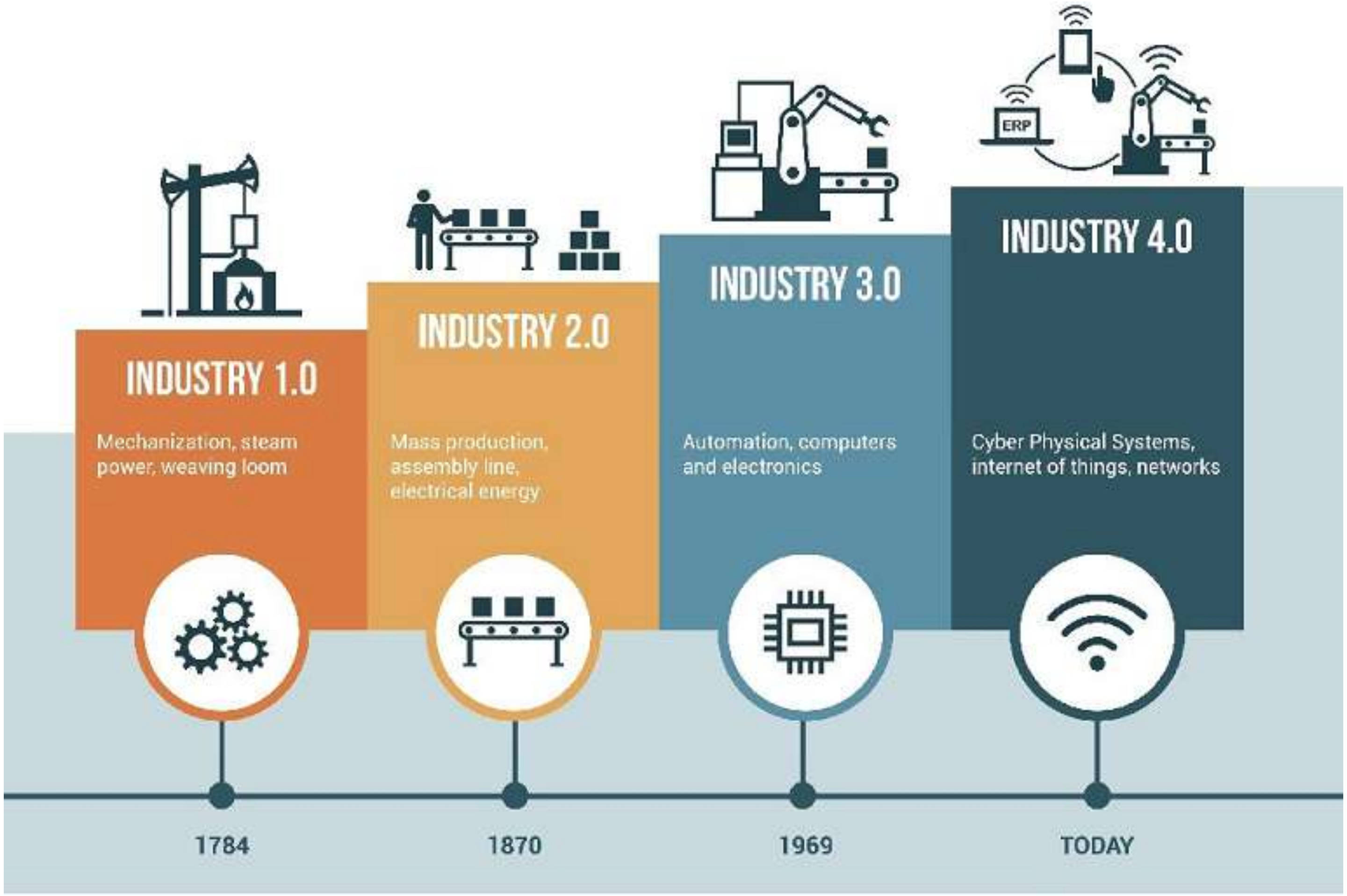

Internet of things, people, and services

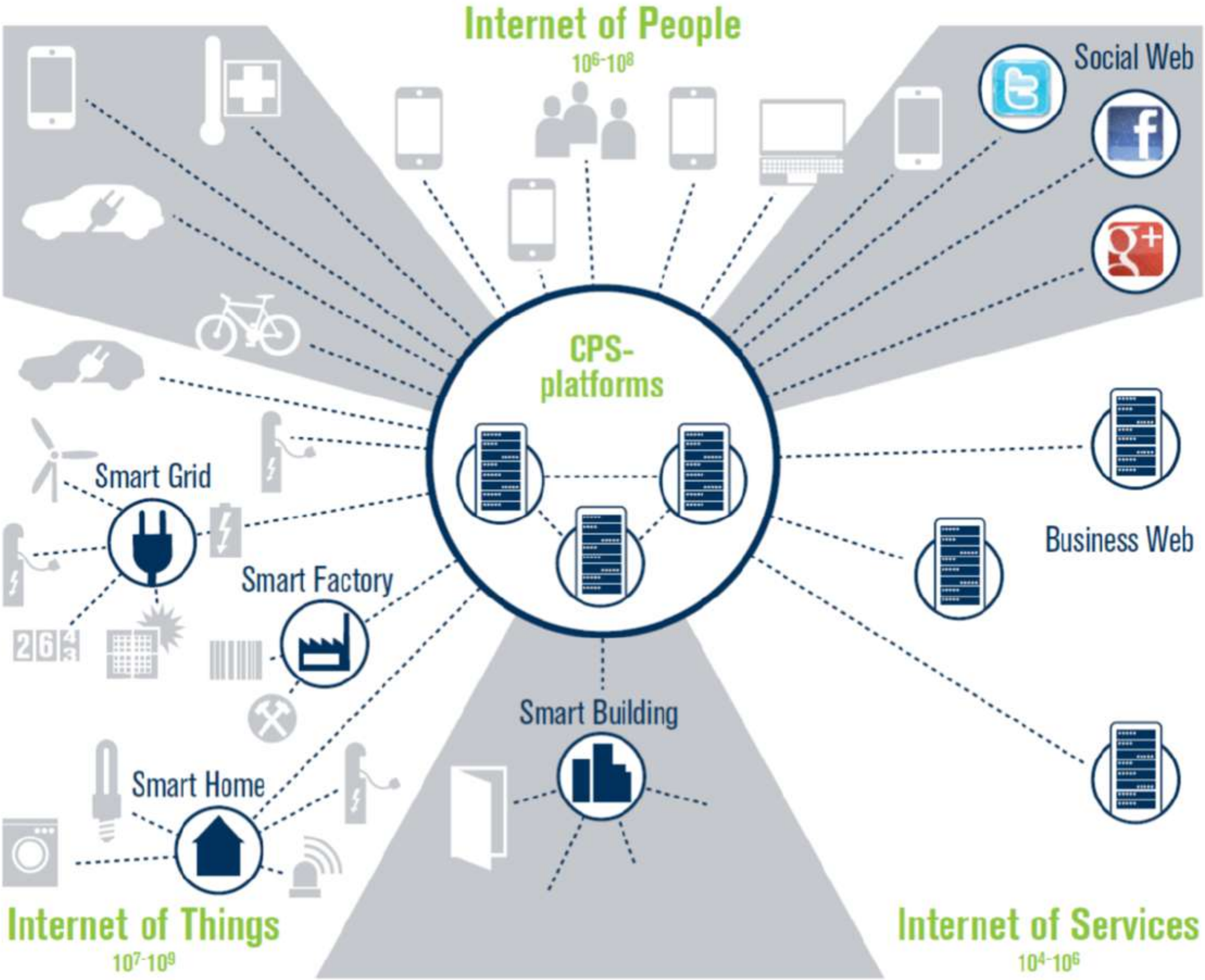

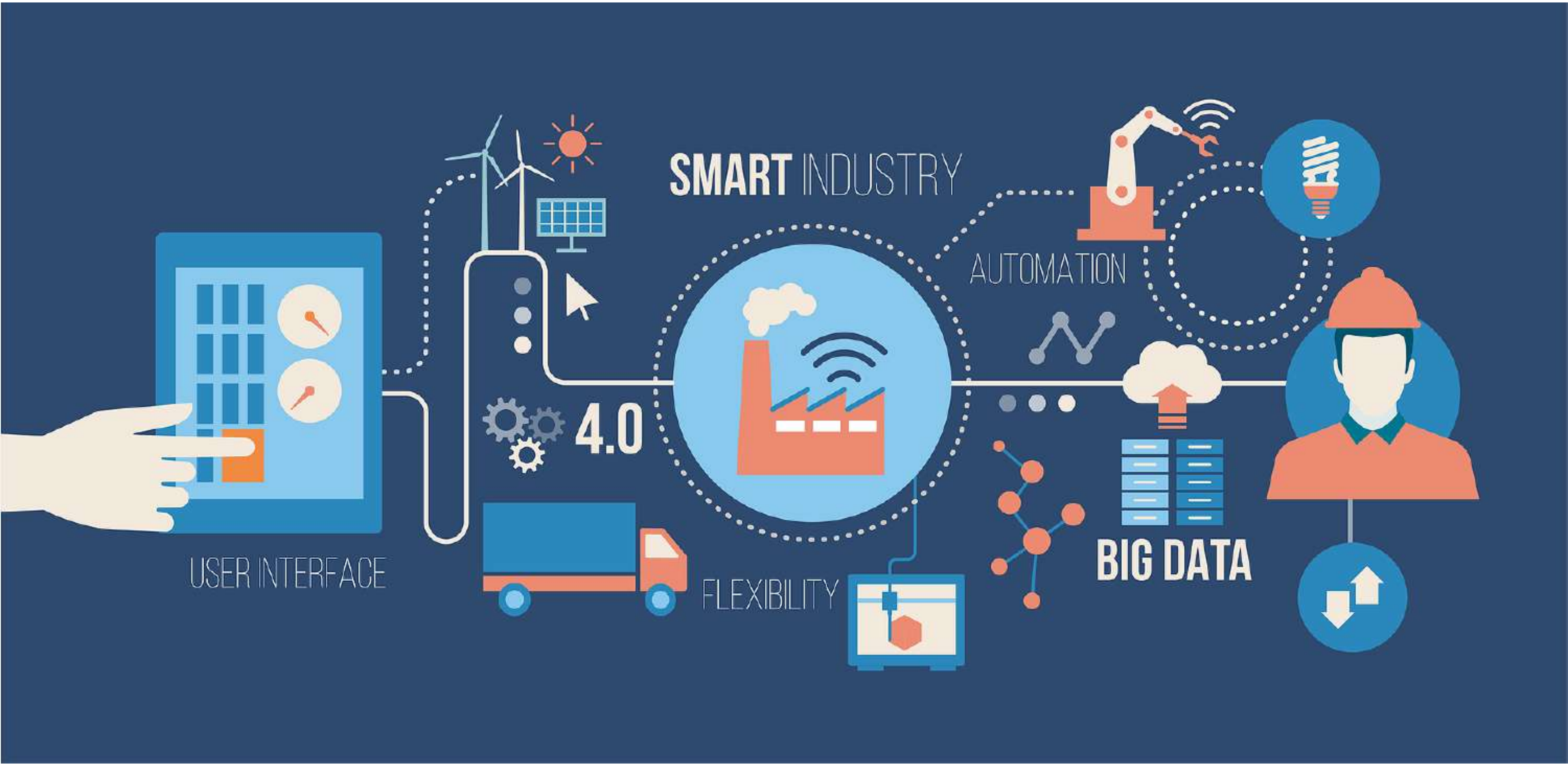
SMART INDUSTRY
AUTOMATION
4.0
USER INTERFACE
FLEXIBILITY
BIG DATA

Model-based control
- and scientific computing

Continuous-discrete system

$$
\begin{aligned}
d\boldsymbol{x}(t) &= f(\boldsymbol{x}(t), u(t), \theta)dt + \sigma(\boldsymbol{x}(t), u(t), \theta)d\boldsymbol{\omega}(t) \\
\boldsymbol{y}(t_k) &= g(\boldsymbol{x}(t_k), \theta) + \boldsymbol{v}(t_k) \\
\boldsymbol{z}(t) &= h(\boldsymbol{x}(t), \theta)
\end{aligned}
$$

$$
\begin{aligned}
\boldsymbol{x}(t_0) &\sim N(\bar{x}_0, P_0) \\
d\boldsymbol{w}(t) &\sim N_{iid}(0, Idt) \\
\boldsymbol{v}(t_k) &\sim N_{iid}(0, R_k(\theta))
\end{aligned}
$$

Continuous-discrete extended Kalman filter

Innovation

$$\hat{y}_{k|k-1} = g(t_k, \hat{x}_{k|k-1}), \quad C_k = \frac{\partial g}{\partial x}(t_k, \hat{x}_{k|k-1}),$$

$$e_k = y_k - \hat{y}_{k|k-1},$$

$$R_{e,k} = C_k P_{k|k-1} C_k' + R_k$$

Filtering

$$K_k = P_{k|k-1} C_k' R_{e,k}^{-1}$$

$$\hat{x}_{k|k} = \hat{x}_{k|k-1} + K_k e_k$$

$$P_{k|k} = P_{k|k-1} - K_k R_{e,k} K_k' = (I - K_k C_k) P_{k|k-1} (I - K_k C_k)' + K_k R_k K_k'$$

Prediction

$$\frac{d\hat{x}_k}{dt}(t) = f(t, \hat{x}_k(t), u_k, \theta),$$

$$A_k(t) = \frac{\partial f}{\partial x}(t, \hat{x}_k(t), u_k, \theta),$$

$$\frac{dP_k}{dt}(t) = A_k(t) P_k(t) + P_k(t) A_k(t)' + \sigma(t, \hat{x}_k(t), u_k, \theta) \sigma(t, \hat{x}_k(t), u_k, \theta)'$$

System identification

Maximum likelihood parameter estimation: Minimize

$$V_{ML}(\theta) = \frac{N+1}{2} \cdot n_y \ln(2\pi) + \frac{1}{2} \sum_{k=0}^{N} \Big(\ln[\det(R_{e,k}(\theta))] + e_k(\theta)'[R_{e,k}(\theta)]^{-1})e_k(\theta) \Big)$$

Maximum a posteriori parameter estimation: Minimize

$$V_{MAP}(\theta) = V_{ML}(\theta) + \frac{1}{2} n_\theta \ln(2\pi) + \frac{1}{2} \ln[\det(P_\theta)] + \frac{1}{2}(\theta - \bar{\theta})' P_\theta^{-1}(\theta - \bar{\theta})$$

Systematic model building

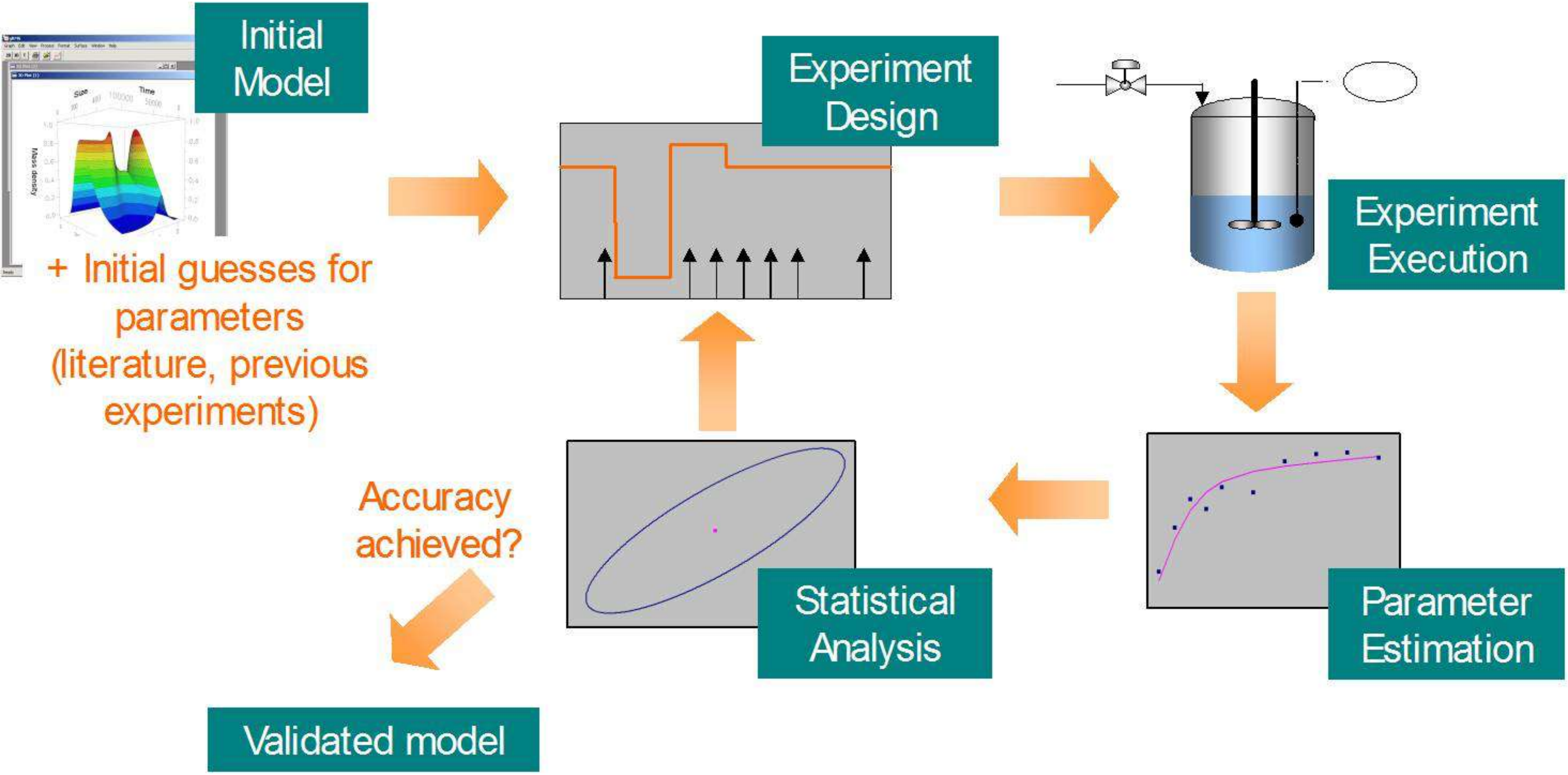

Regulator - Nonlinear Model Predictive Control

Optimal control problem

$$
\begin{aligned}
\min_{x,u} \quad & \phi_k = \phi_{z,k} + \phi_{u,k} + \phi_{\Delta u,k}, & \\
s.t. \quad & x(t_k) = \hat{x}_{k|k}, & \\
& \dot{x}(t) = f(x(t), u(t), \theta), & t_k \le t \le t_k + T_p, \\
& z(t) = h(x(t), \theta), & t_k \le t \le t_k + T_p, \\
& u(t) = u_{k+j|k}, \quad j \in \mathcal{N}, & t_{k+j} \le t < t_{k+j+1}, \\
& u_{\min} \le u_{k+j|k} \le u_{\max}, & j \in \mathcal{N}, \\
& \Delta u_{\min} \le \Delta u_{k+j|k} \le \Delta u_{\max}, & j \in \mathcal{N}
\end{aligned}
$$

$$
\phi_{z,k} = \frac{1}{2} \int_{t_k}^{t_k+T_p} \| z(t) - \bar{z}(t) \|_{Q_z}^2 \, \mathrm{d}t,
$$

$$
\phi_{u,k} = \frac{1}{2} \int_{t_k}^{t_k+T_p} \| u(t) - \bar{u}(t) \|_{Q_u}^2 \, \mathrm{d}t,
$$

$$
\phi_{\Delta u,k} = \frac{1}{2} \sum_{j=0}^{N-1} \| \Delta u_{k+j} \|_{\bar{Q}_{\Delta u}}^2 .
$$

Multiple-shooting (with sensitivities)

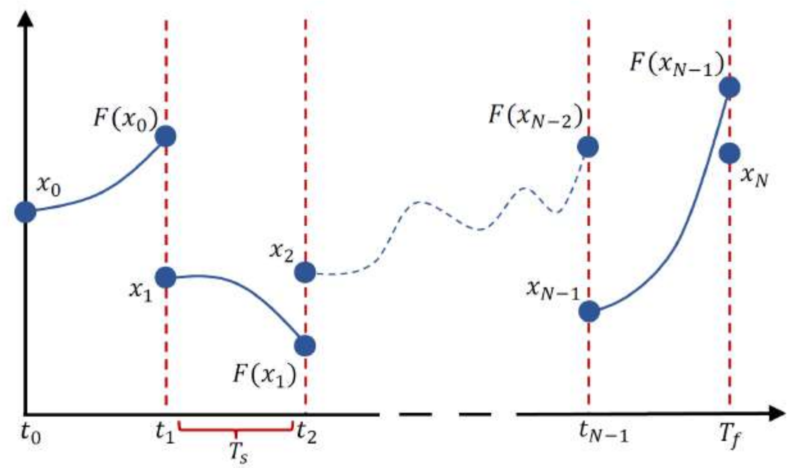

Moving horizon principle

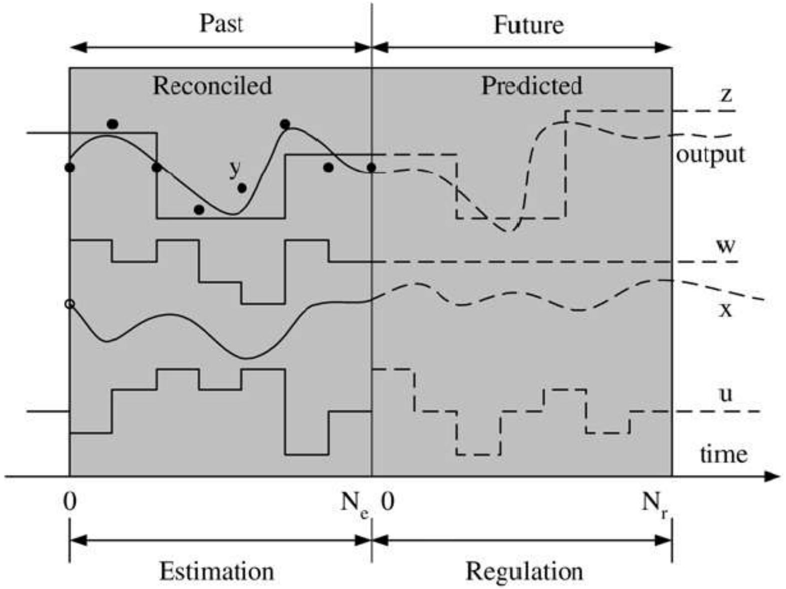

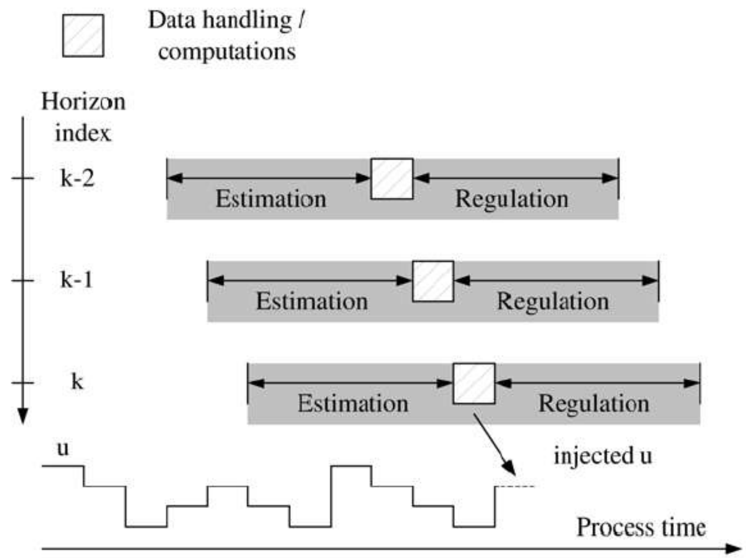

$$
\begin{aligned}
\min_{\{u_k, x_{k+1}\}_{k=0}^{N-1}} \quad & \phi = \phi(\{u_k, x_{k+1}\}_{k=0}^{N-1}; x_0, \theta) \\
s.t. \quad & x_{k+1} = F_k(x_k, u_k, \theta) \qquad k = 0, 1, \ldots, N-1 \\
& u_k \in \mathcal{U}
\end{aligned}
$$

Adiabatic CSTR with an exothermic reaction

Adiabatic CSTR with an Exothermic Reaction

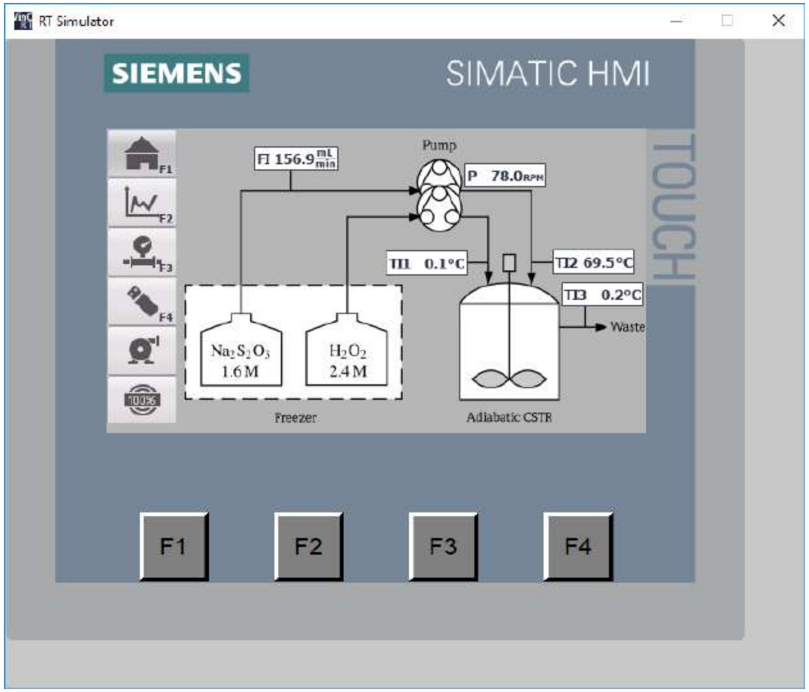

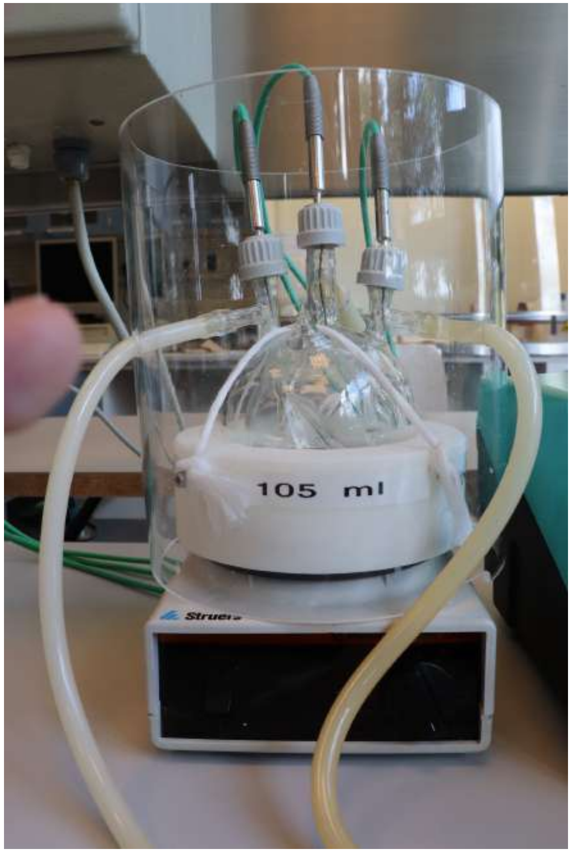

$$\mathrm{Na_2S_2O_3(aq)}+2\mathrm{H_2O_2(aq)} \rightarrow \frac{1}{2}\mathrm{Na_2SO_4(aq)}+\frac{1}{2}\mathrm{Na_2S_3O_6(aq)}+2\mathrm{H_2O(aq)},$$

Model Predictive Controller

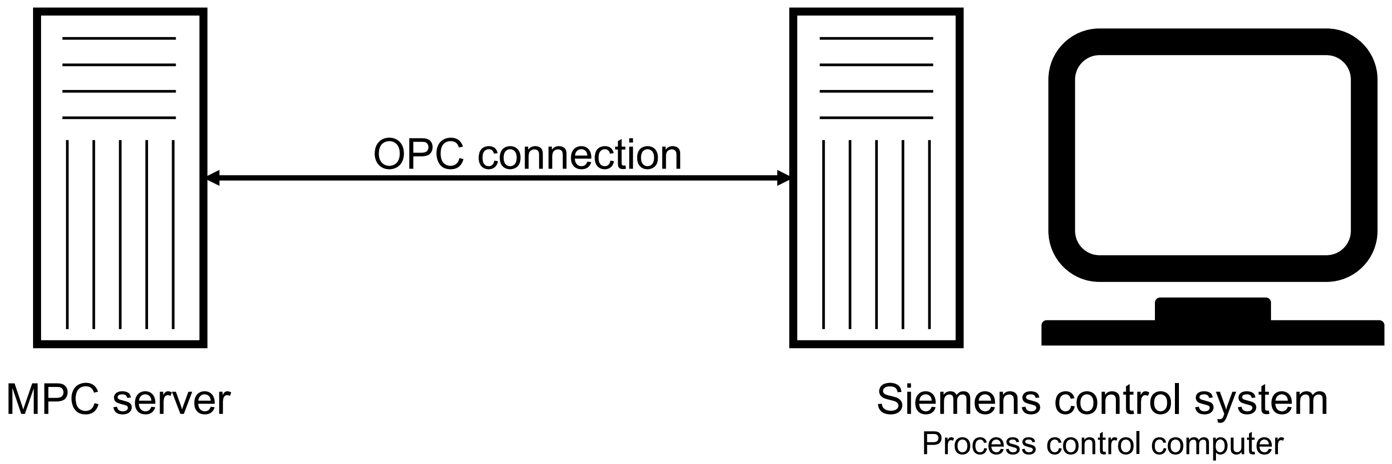

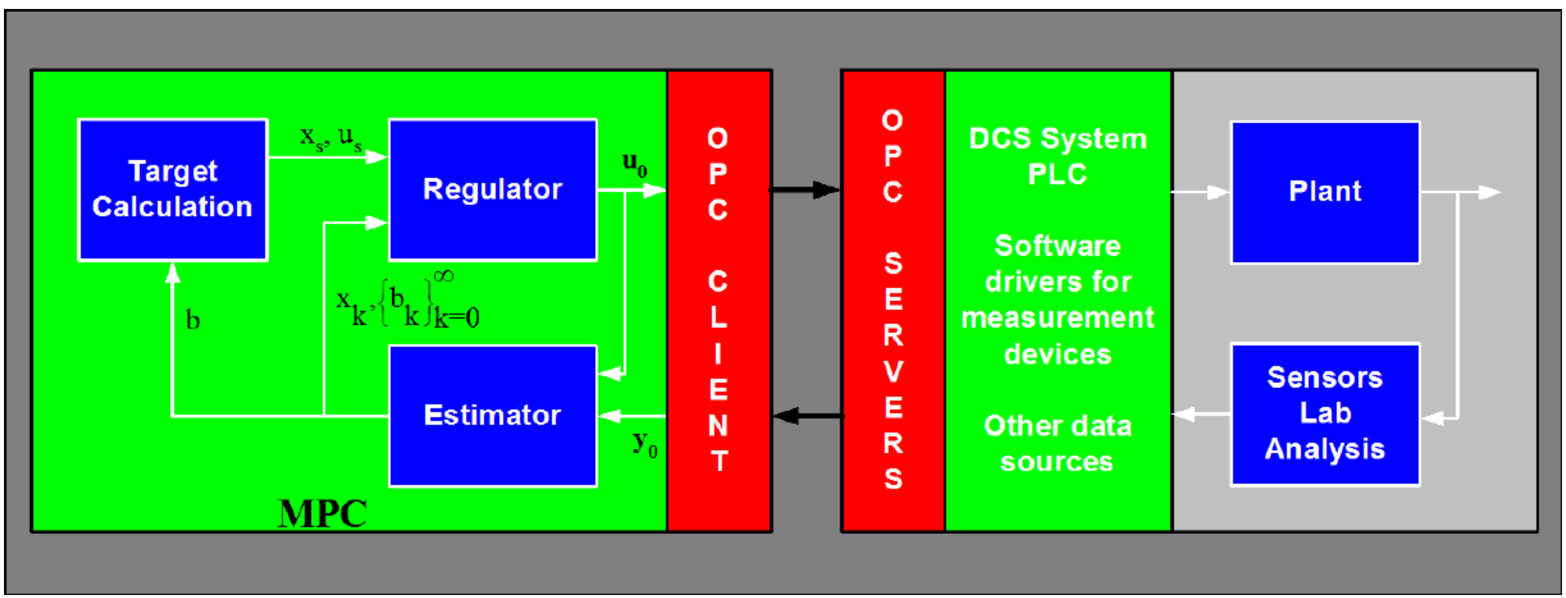

Adiabatic CSTR with an Exothermic Reaction

Adiabatic CSTR with an Exothermic Reaction

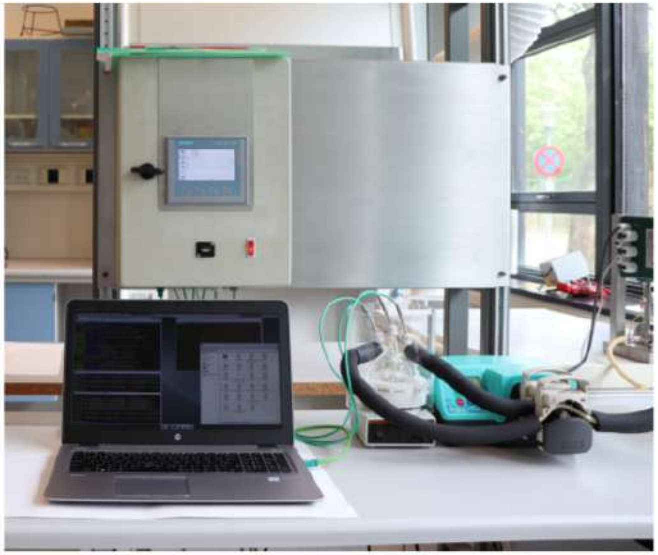

(a) Overview of the experimental setup.

(b) Laboratory-scale adiabatic CSTR.

(c) Low level control system based on the Siemens S7-1200 platform.

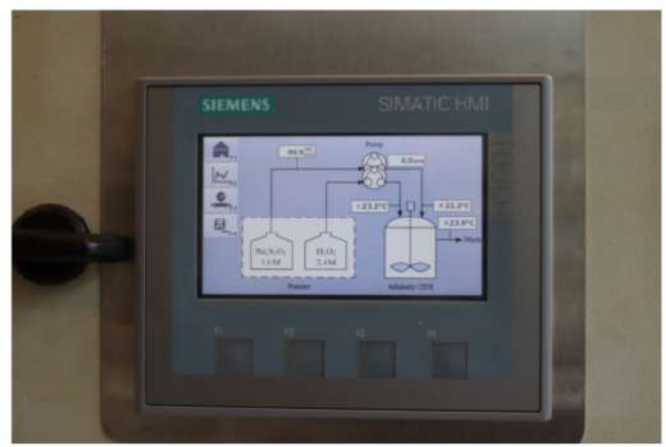

(d) Human Machine Interface (HMI) showing mimic diagram.

Adiabatic CSTR with an Exothermic Reaction

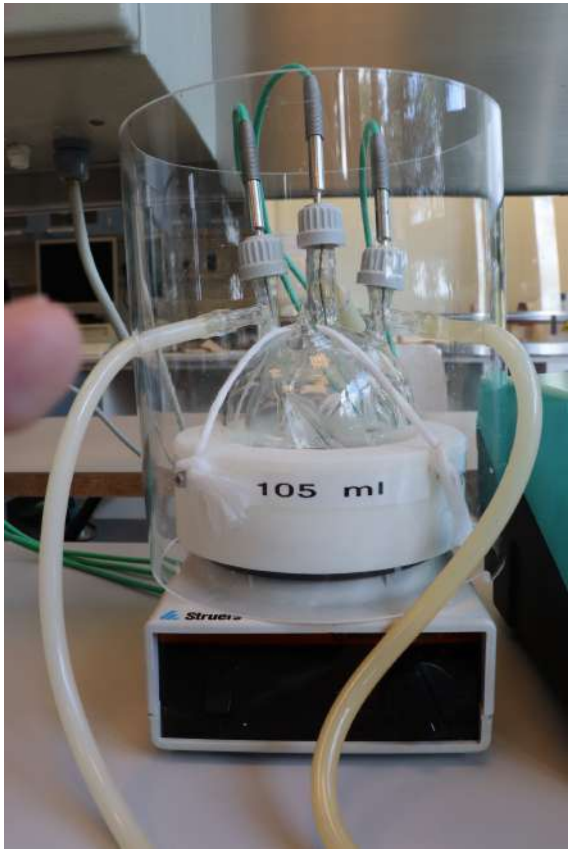

Mass and Energy Balance - SDE

$$
\begin{aligned}
dC_A &= \left[\frac{F}{V} (C_{A,in} - C_A) + R_A(C_A, C_B, T) \right] dt, \\
dC_B &= \left[\frac{F}{V} (C_{B,in} - C_B) + R_B(C_A, C_B, T) \right] dt, \\
dT &= \left[\frac{F}{V} (T_{in} - T) + R_T(C_A, C_B, T) \right] dt + \frac{F}{V} \sigma_T d\omega.
\end{aligned}
$$

Continuous-Discrete System

$$
\begin{aligned}
d\boldsymbol{x}(t) &= f(\boldsymbol{x}(t), u(t), p)dt + \sigma(\boldsymbol{x}(t), u(t), p)d\boldsymbol{\omega}(t), \\
\boldsymbol{y}(t_k) &= g(\boldsymbol{x}(t_k), p) + \boldsymbol{v}(t_k; p), \\
\boldsymbol{z}(t) &= h(\boldsymbol{x}(t), p),
\end{aligned}
$$

Bifurcations and nonlinear dynamics

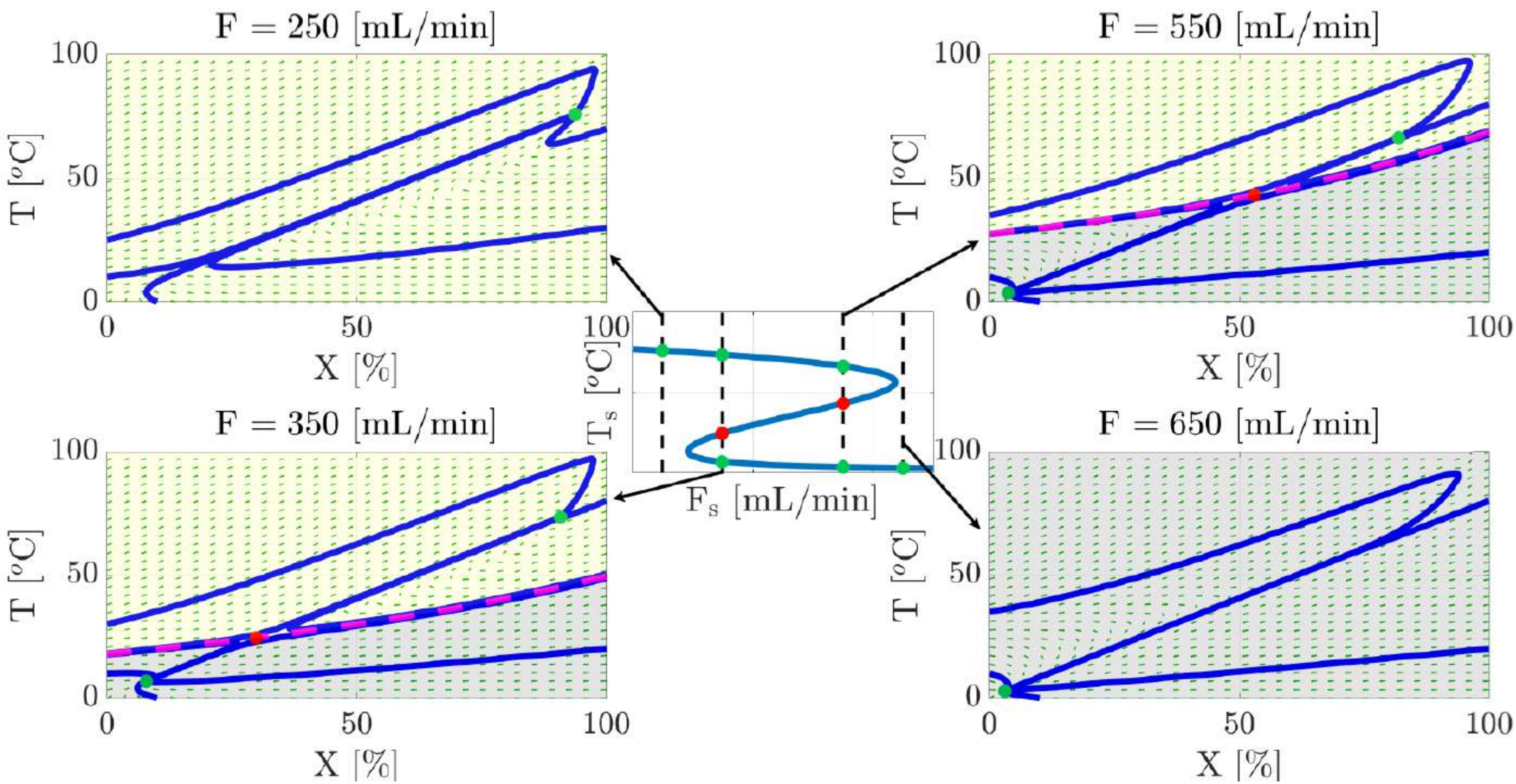

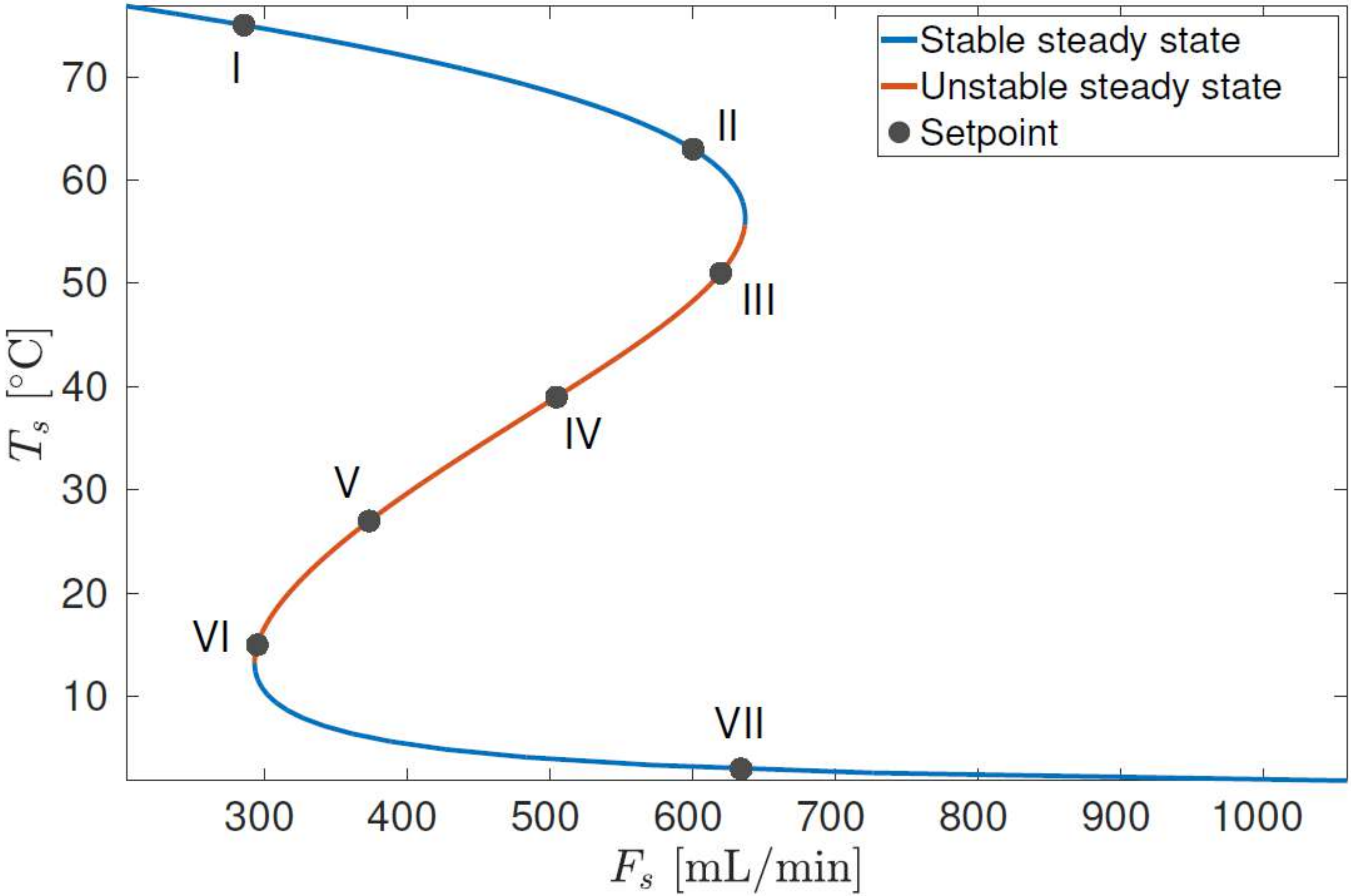
Stable steady state
Unstable steady state
Setpoint
I
II
III
IV
V
VI
VII
70
60
50
40
30
20
10
300
400
500
600
700
800
900
1000
T_s [°C]
F_s [mL/min]

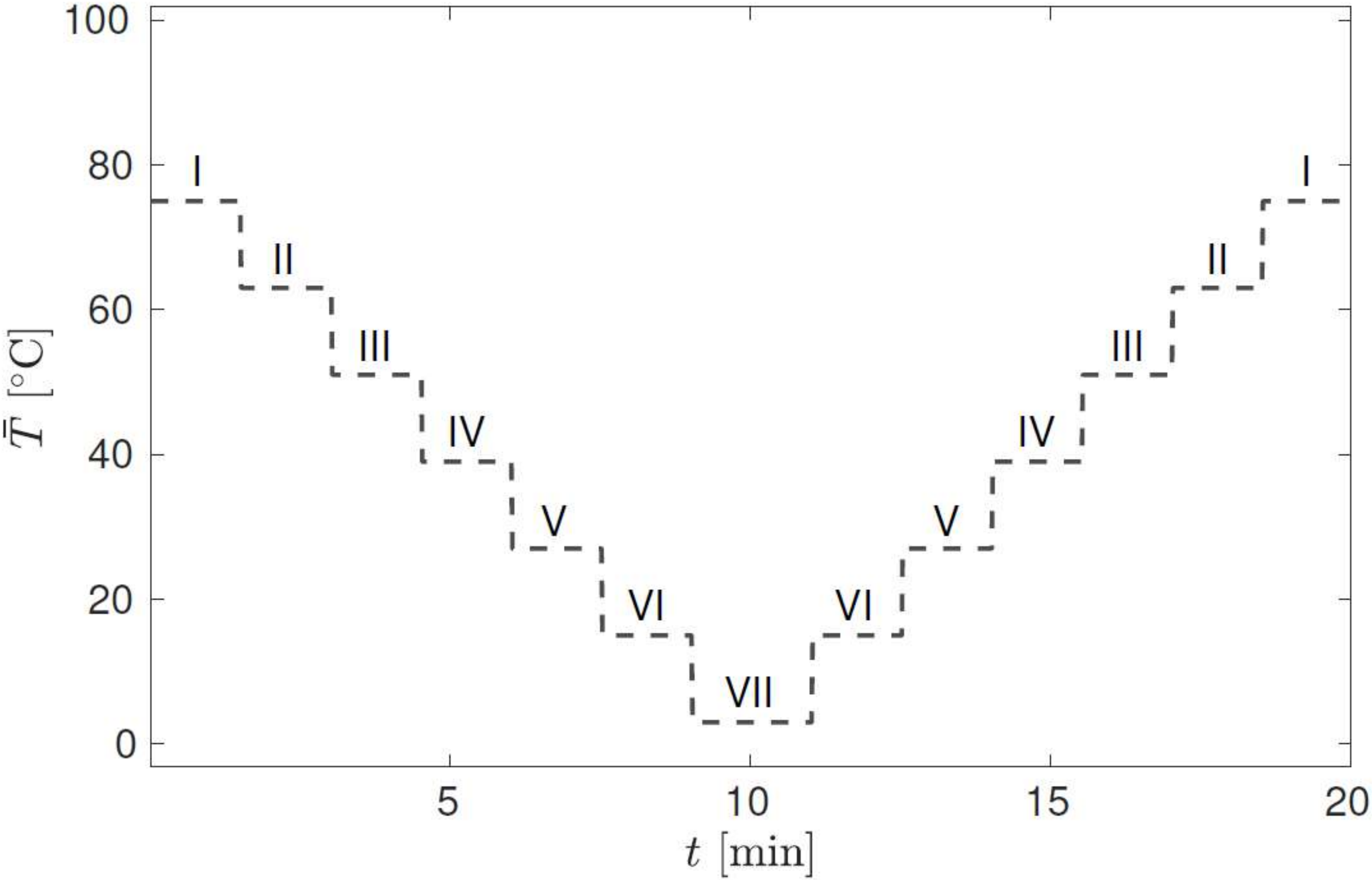

100
80
60
40
20
0
$\bar{T}$ [°C]
5
10
15
20
t [min]
I
II
III
IV
V
VI
VII
VI
V
IV
III
II
I

ODE vs SDE simulation

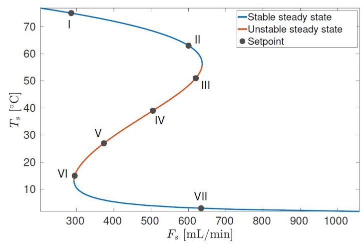

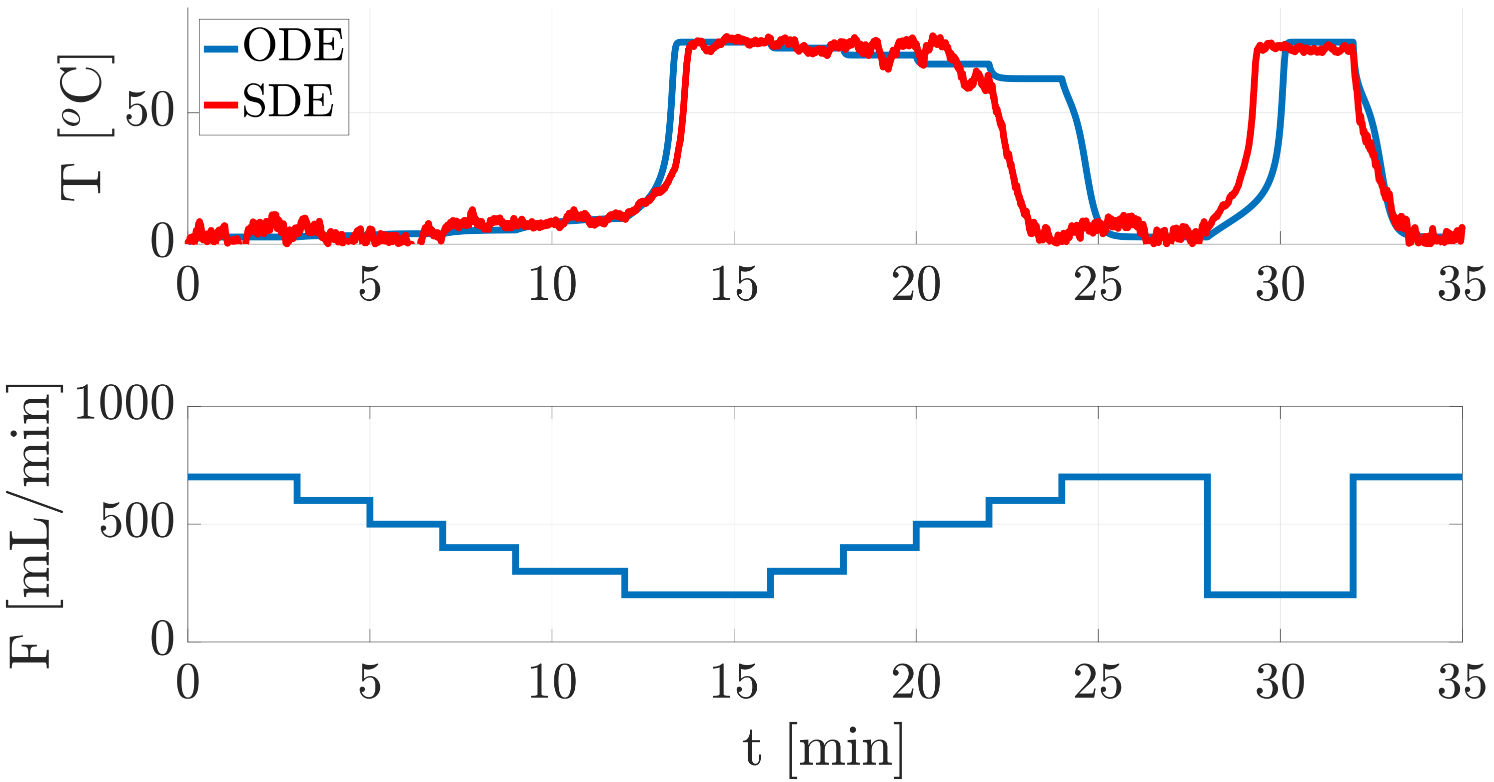

3D model and reduced-order 1D model

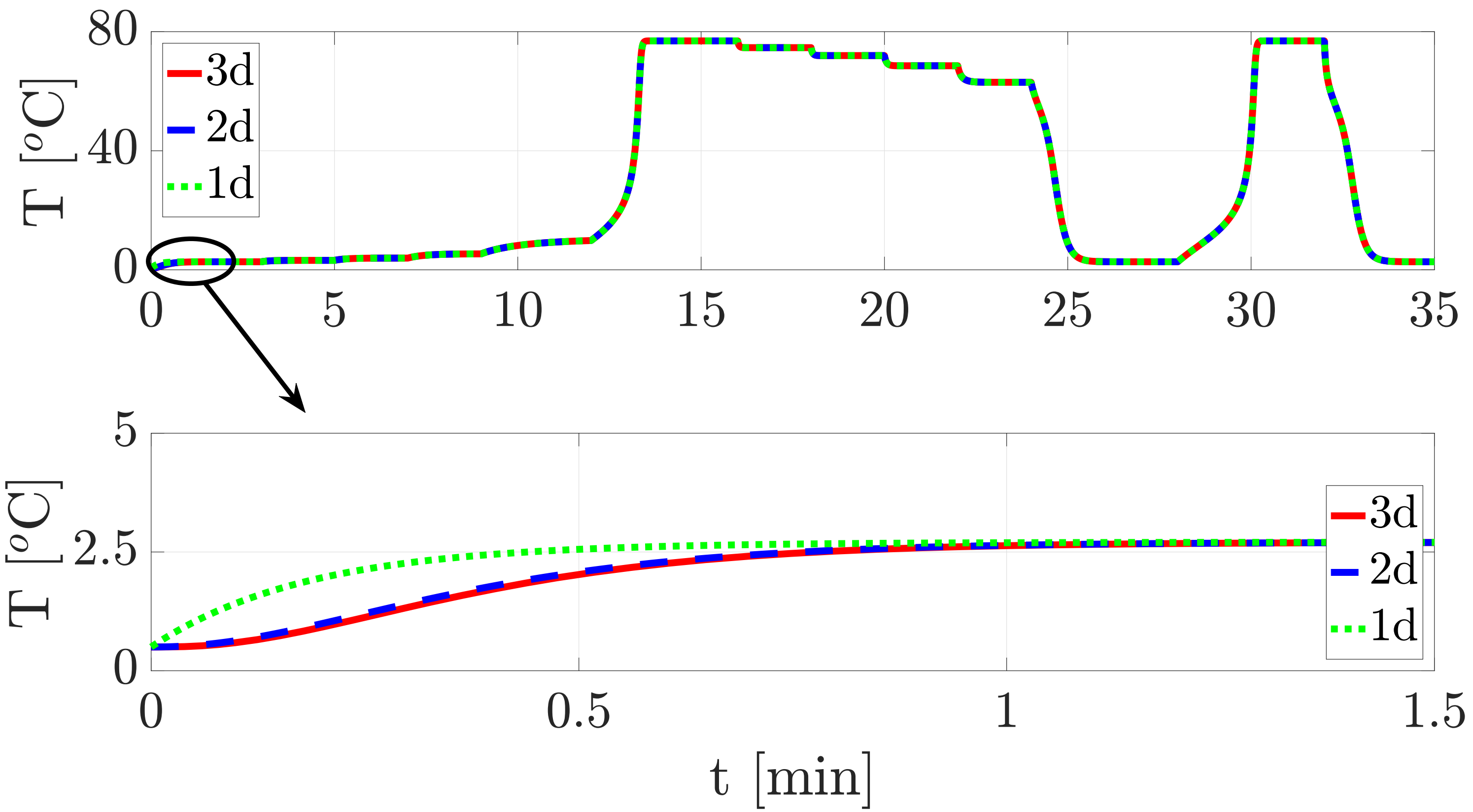

Training and validation data

Data for training and validation

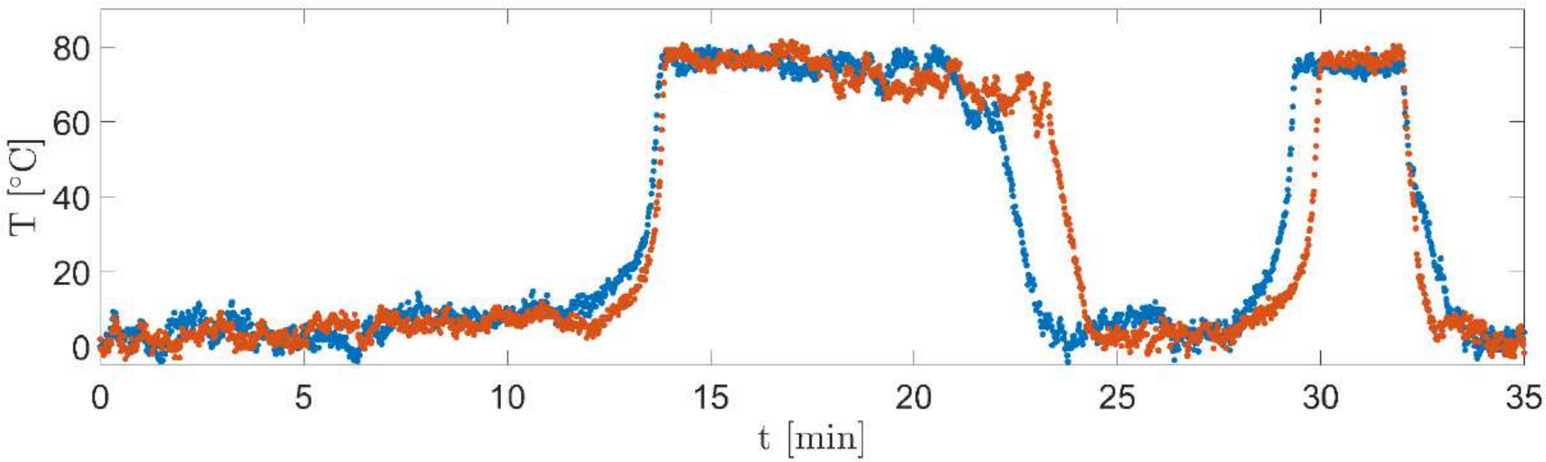

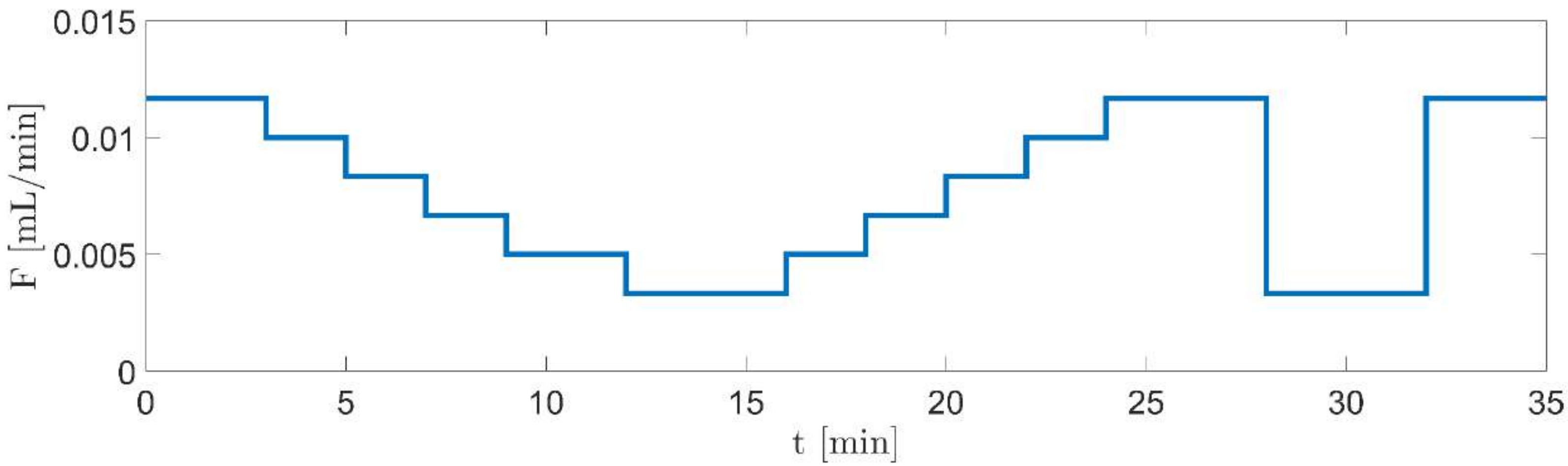

System Identification
Prediction Error Method – Maximum Likelihood

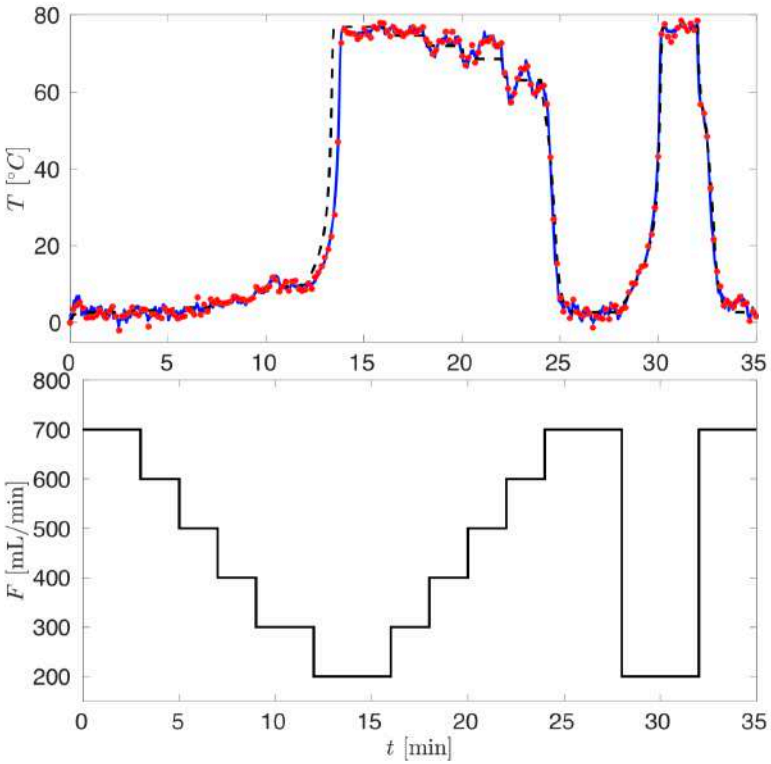

$$
\begin{aligned}
V_{ML}(\theta) = &\frac{1}{2}(N_e+1)n_y \ln(2\pi) \\
&+ \frac{1}{2}\sum_{k=0}^{N_e}\left(\ln\left[\det R_{e,k}\right] + e_k' R_{e,k}^{-1} e_k\right),
\end{aligned}
$$

$$
\begin{aligned}
e_k &= e_k(\theta) = y_k - \hat{y}_{k|k-1}(\theta), \\
R_{e,k} &= R_{e,k}(\theta) = \bar{R}_k(\theta) + C_k(\theta)P_{k|k-1}(\theta)C_k(\theta)',
\end{aligned}
$$

System Identification
Prediction Error Method – Maximum Likelihood

Parameter	Value	MLE value	Std	MAPE value	Std
β	133.78	133.3639	0.1384	133.4740	0.0993
$\log(k_0)$	24.6	24.7046	0.2272	24.8362	0.1431
E_a/R	8500	8537.7	74.113	8577.6	42.0107
p_v	0.15	0.0884	0.0069	0.1314	0.0061
p_w	5	11.4345	0.2694	8.7344	0.0825

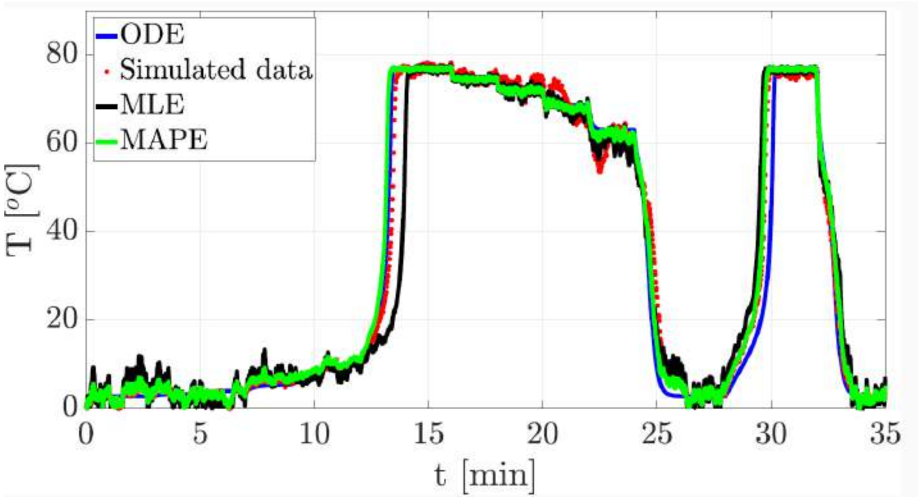

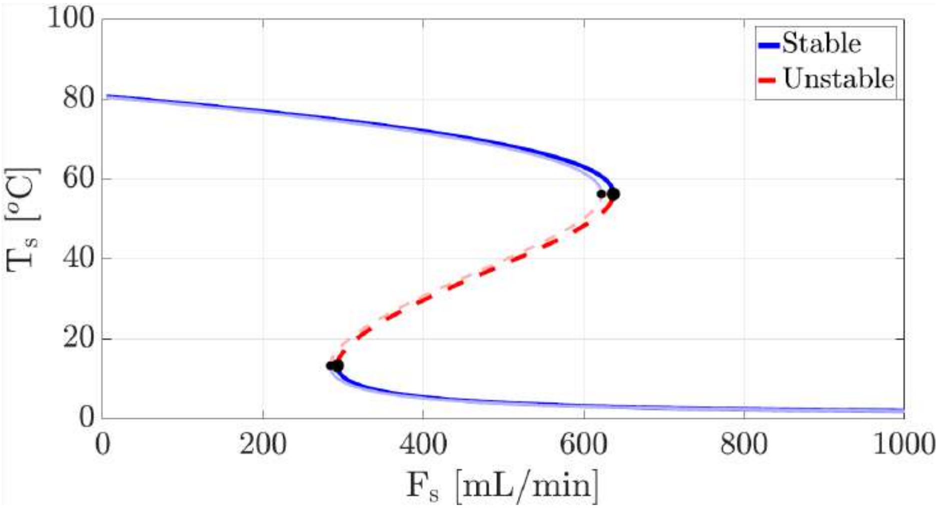

N-step predictions – MLE (3D)

1-step predictions – MLE (3D)

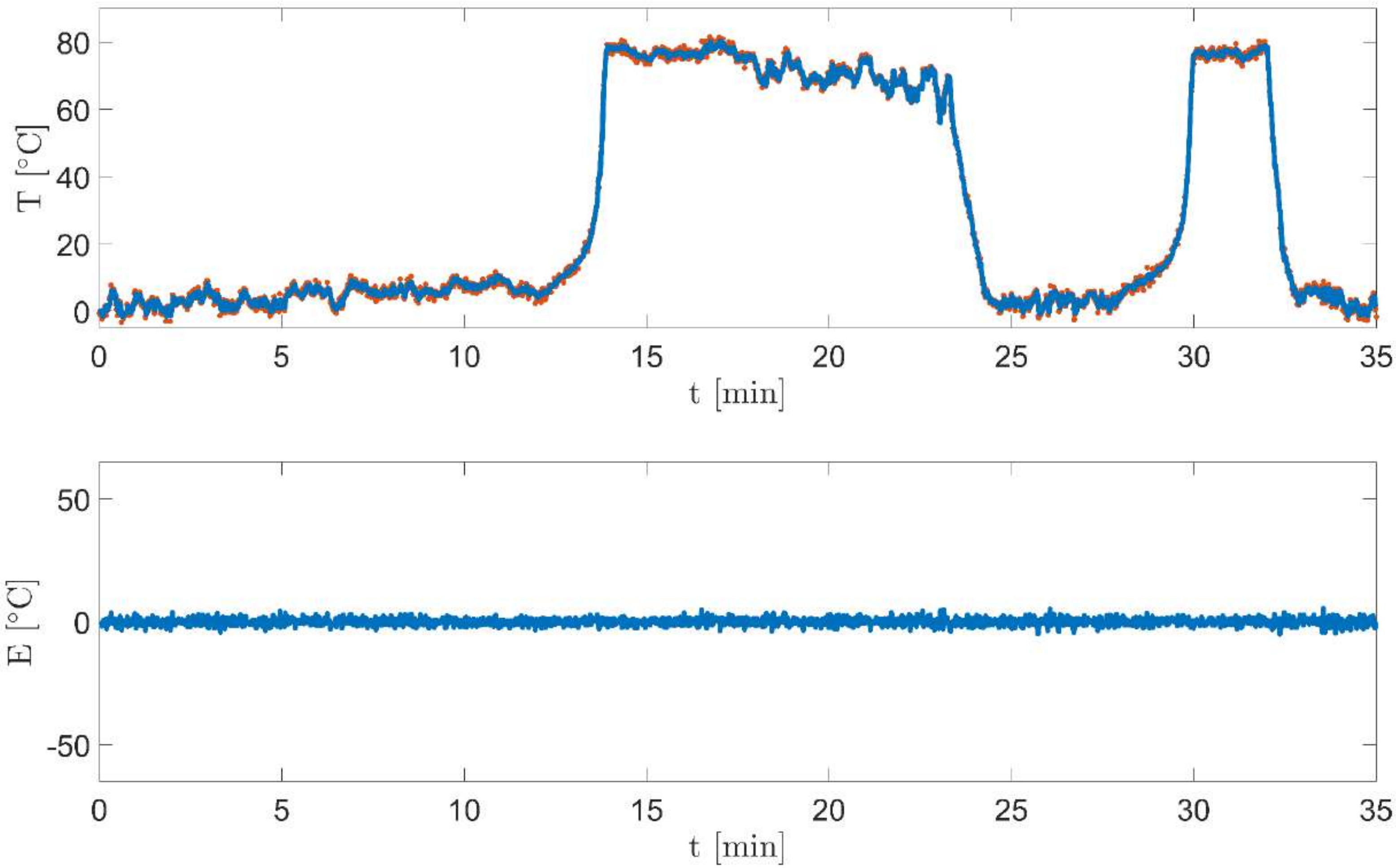

30-step predictions – MLE (3D)

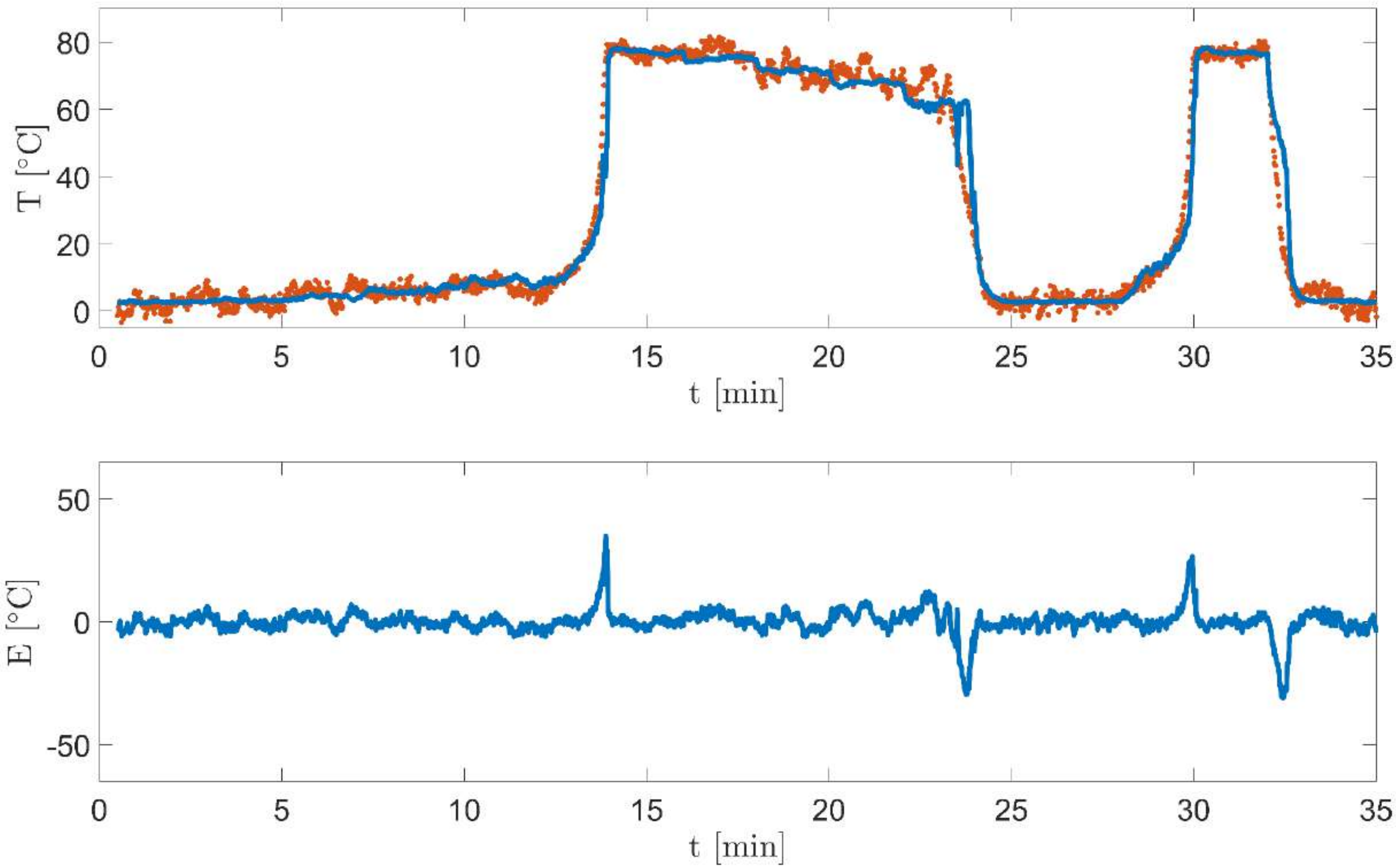

60-step predictions – MLE (3D)

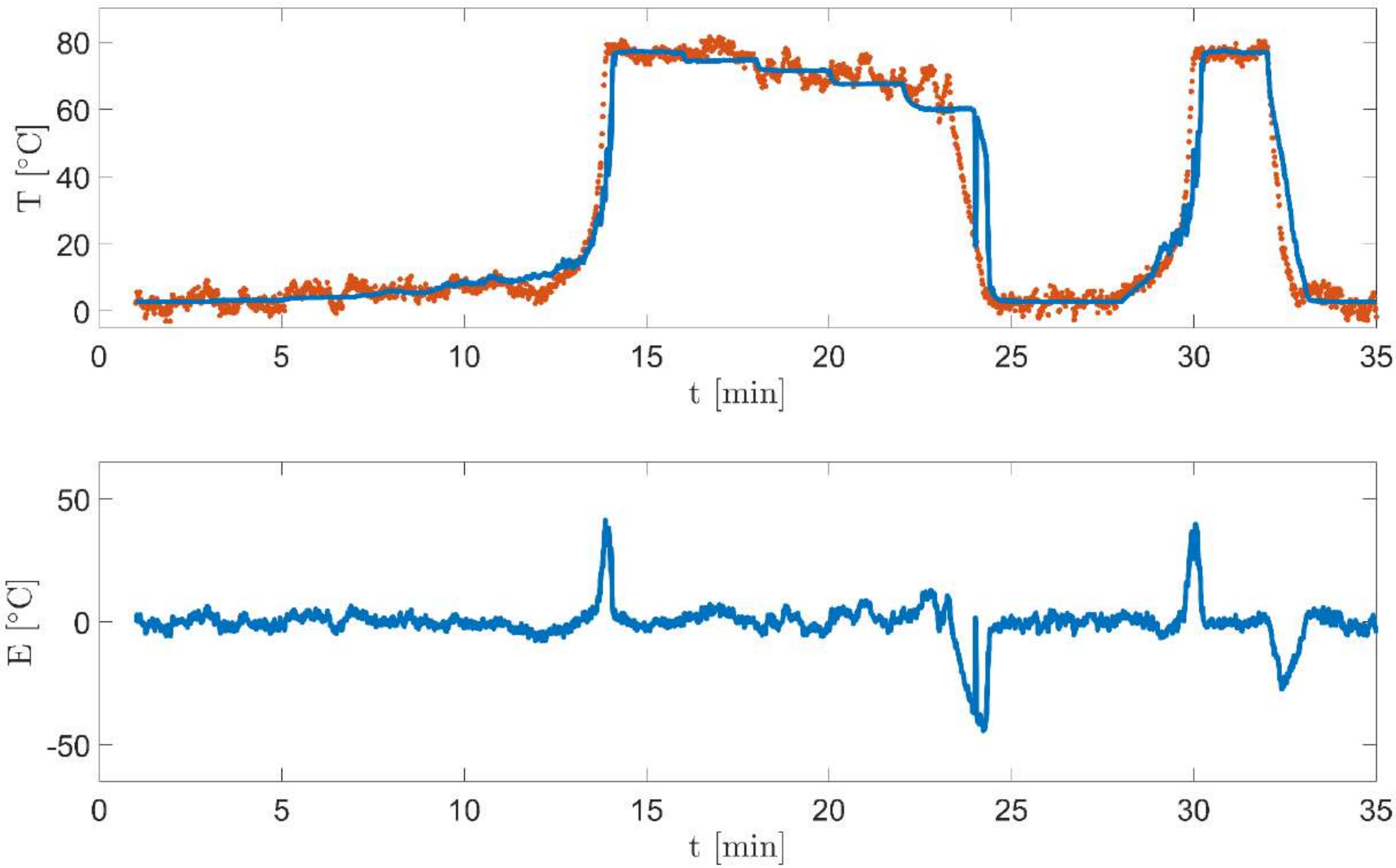

120-step predictions – MLE (3D)

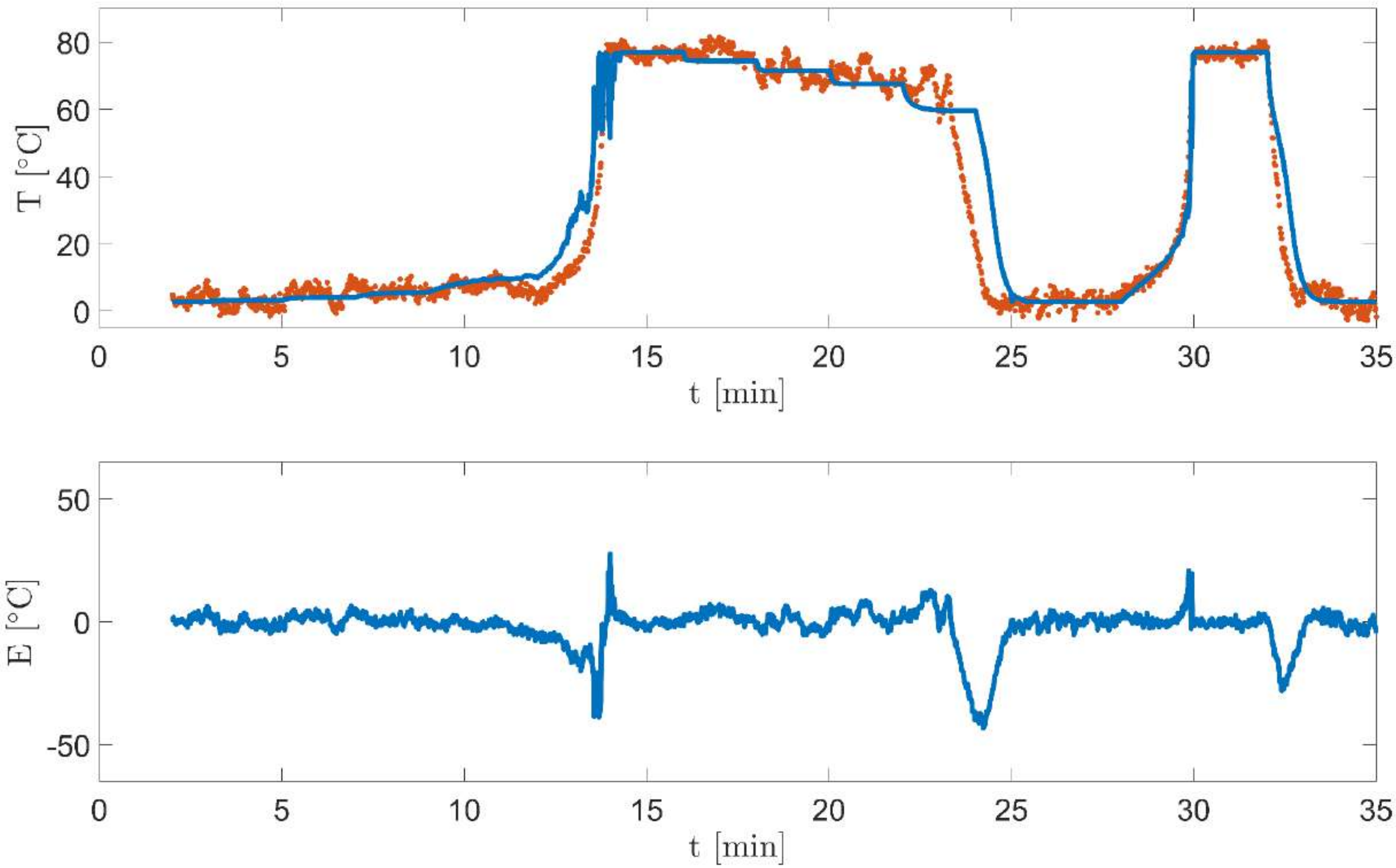

180-step predictions – MLE (3D)

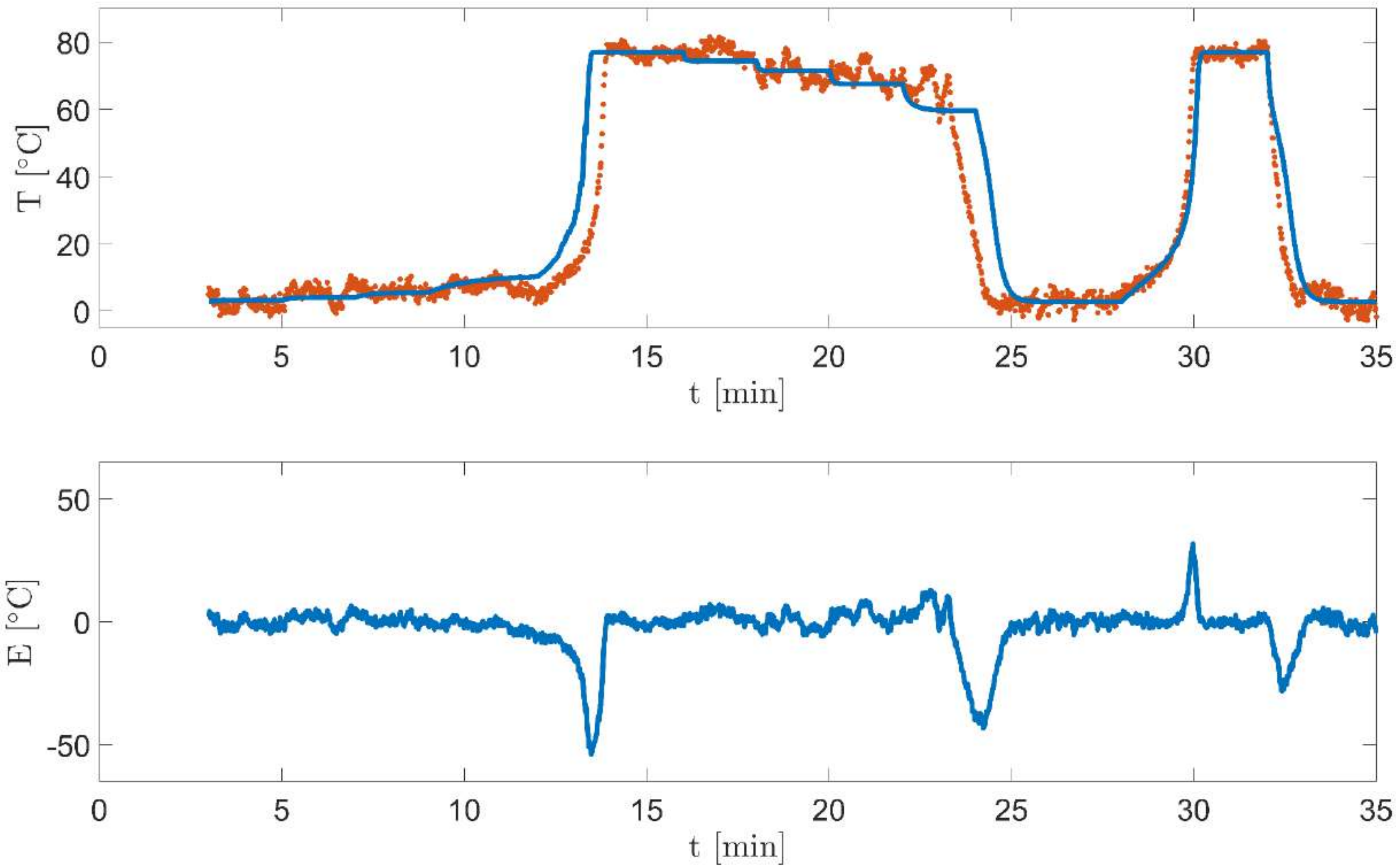

N-step predictions – MLE (1D)

1-step predictions – MLE (1D)

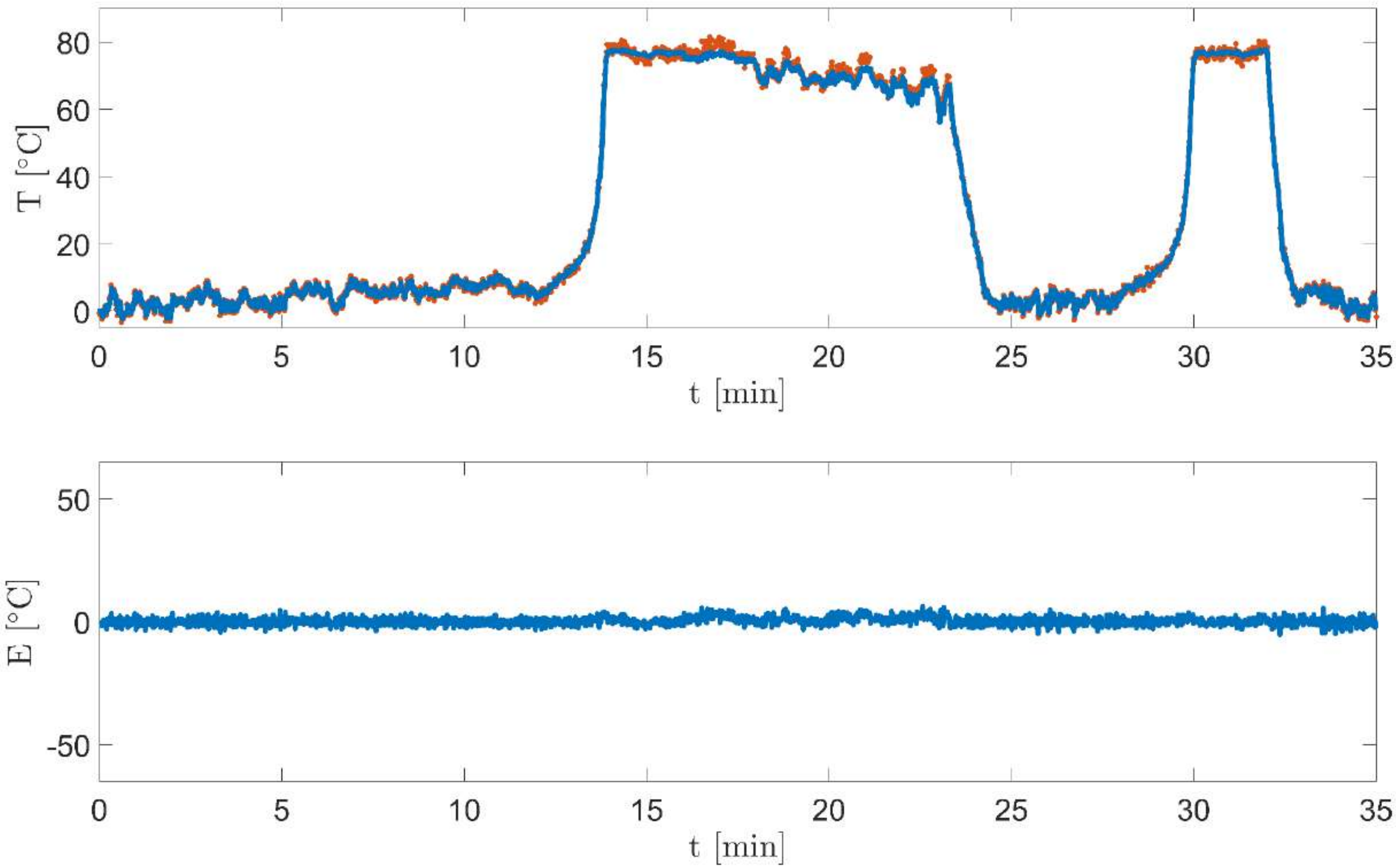

30-step predictions – MLE (1D)

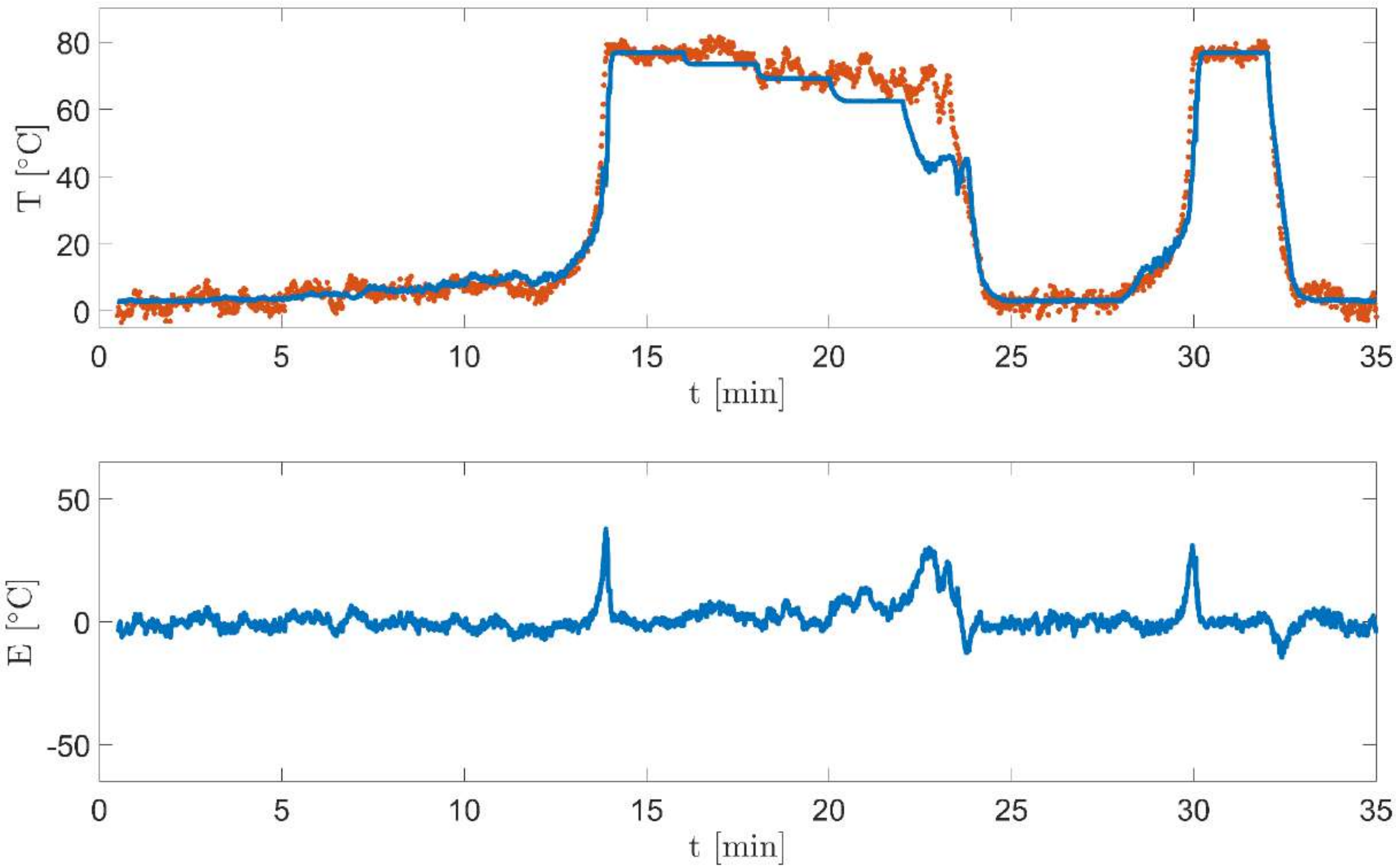

60-step predictions – MLE (1D)

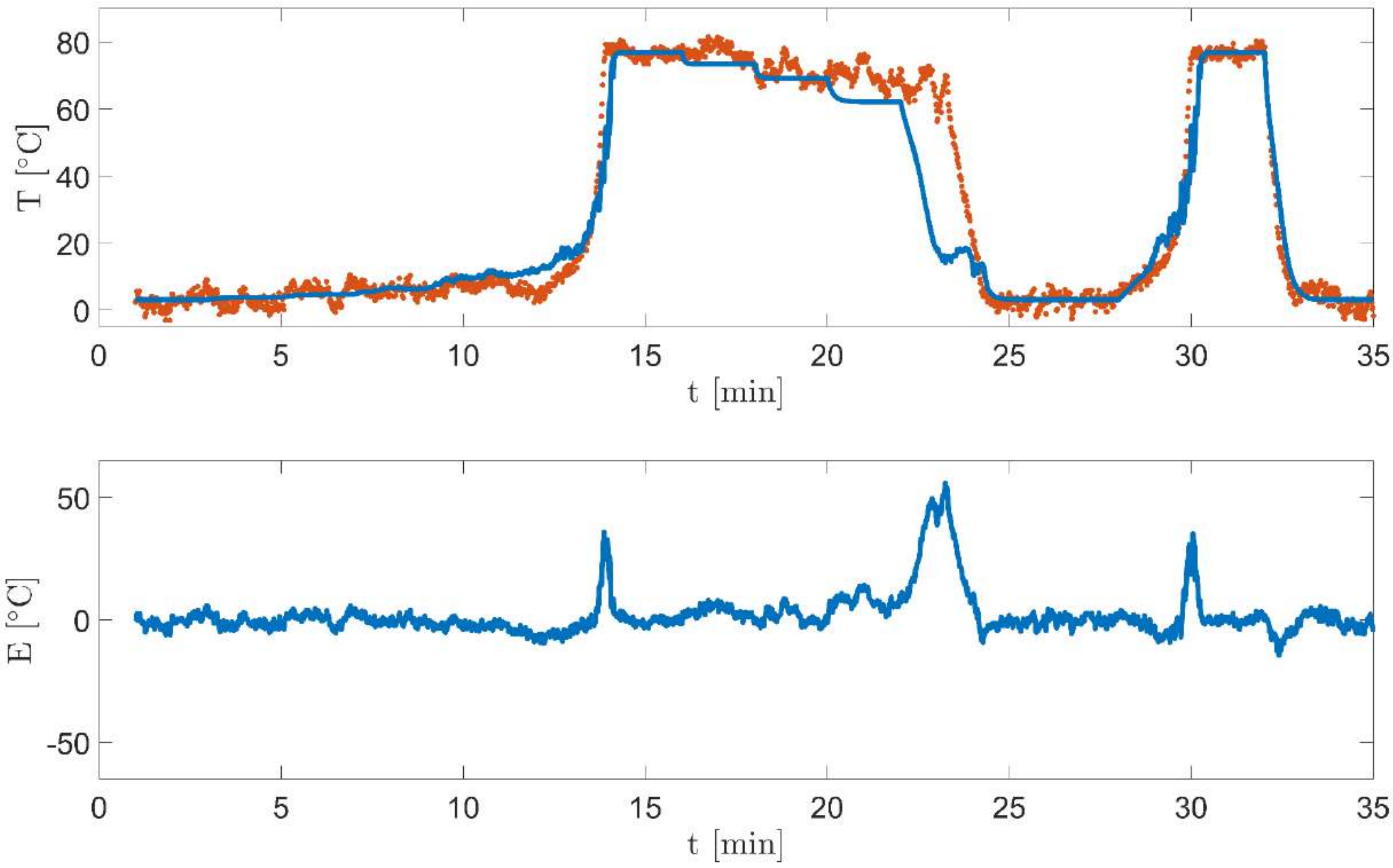

120-step predictions – MLE (1D)

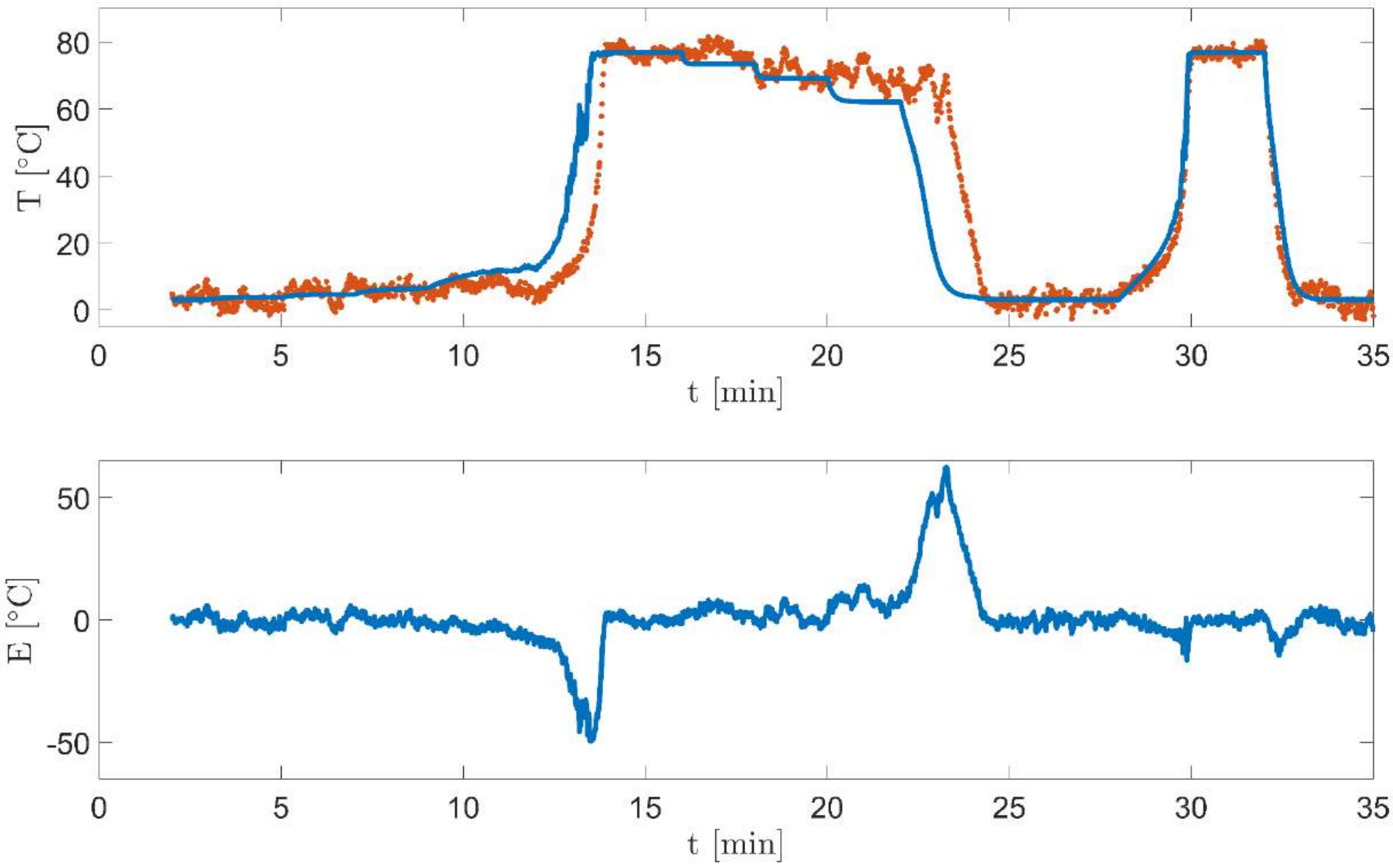

180-step predictions – MLE (1D)

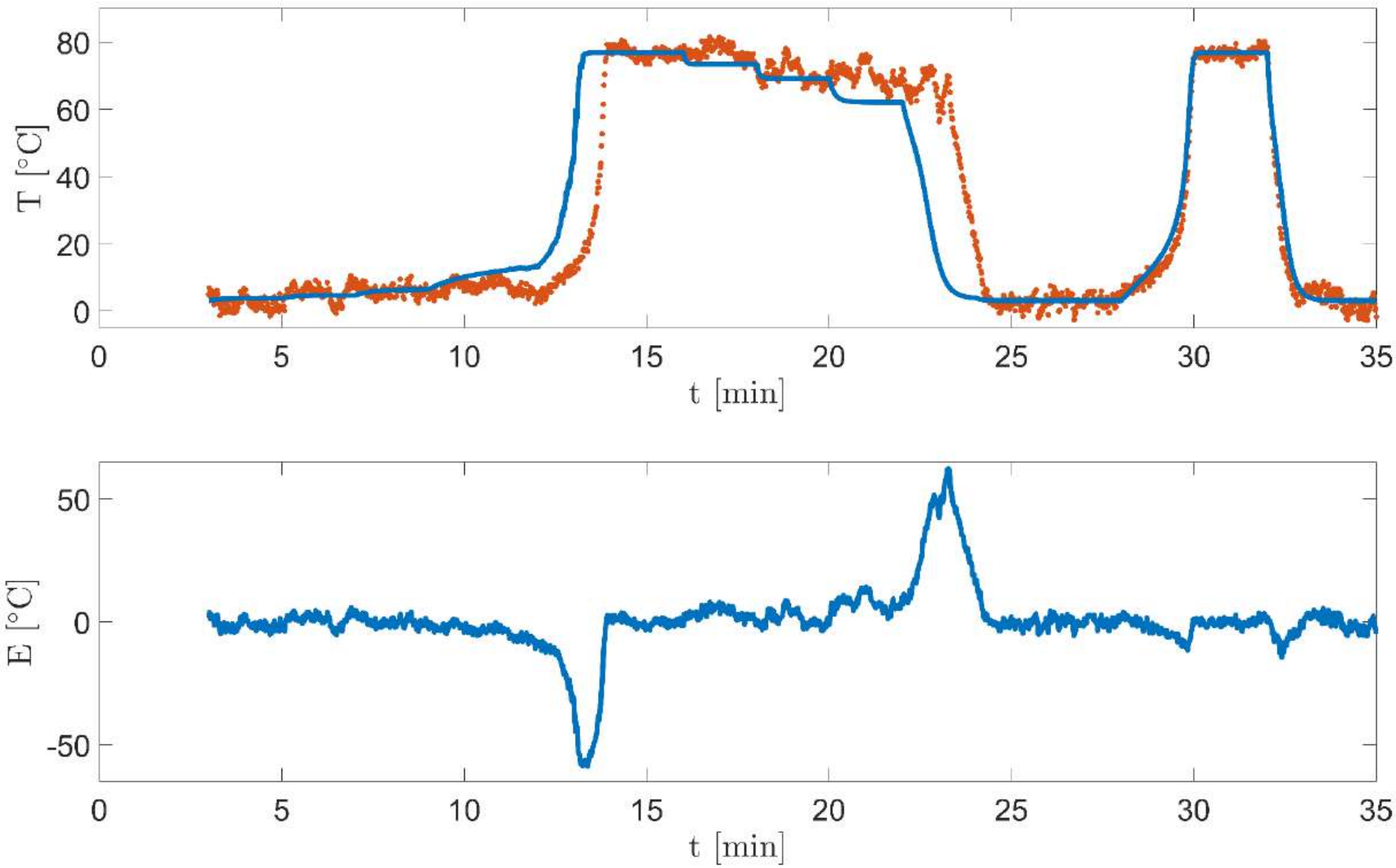

Nonlinear Model Predictive Control

Multiple Steady States

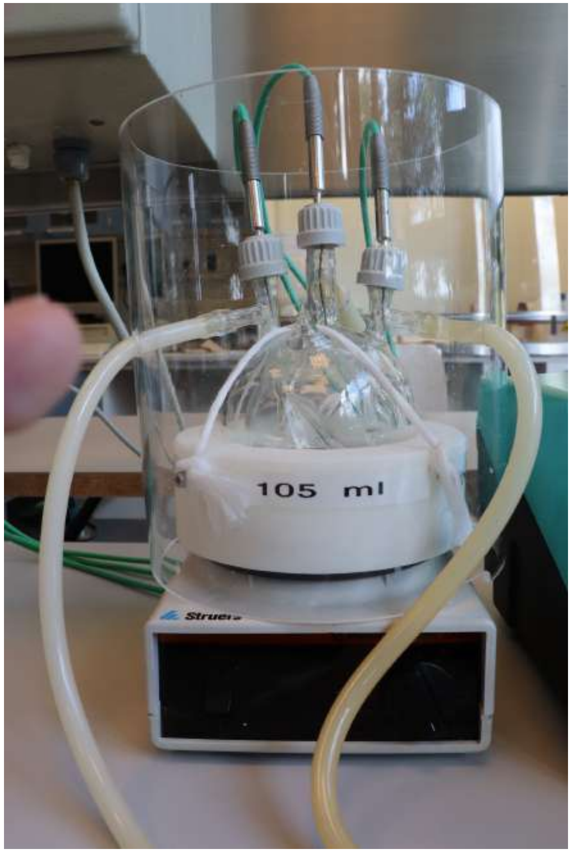

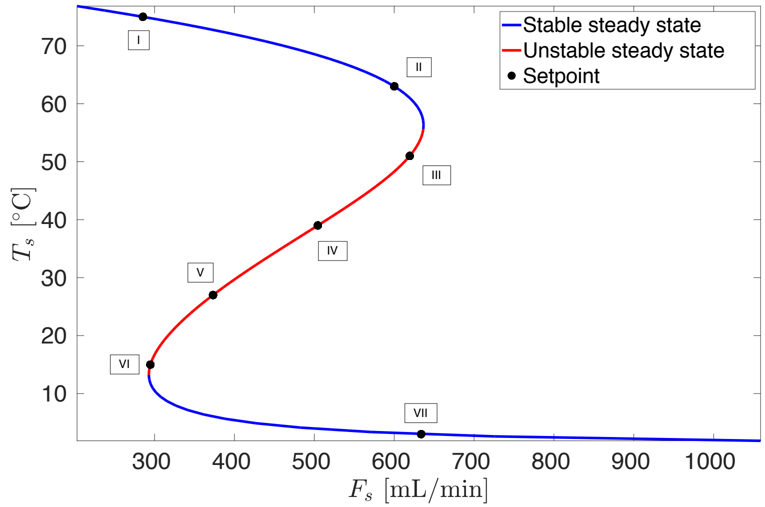

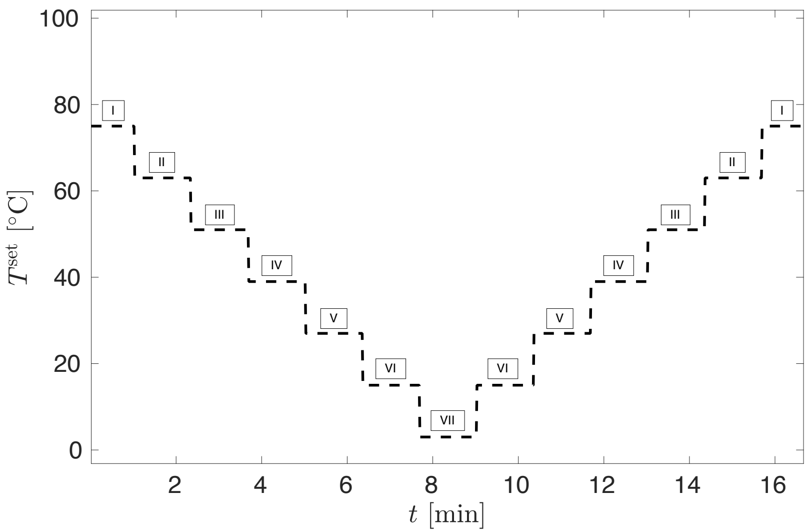

Movie of NMPC

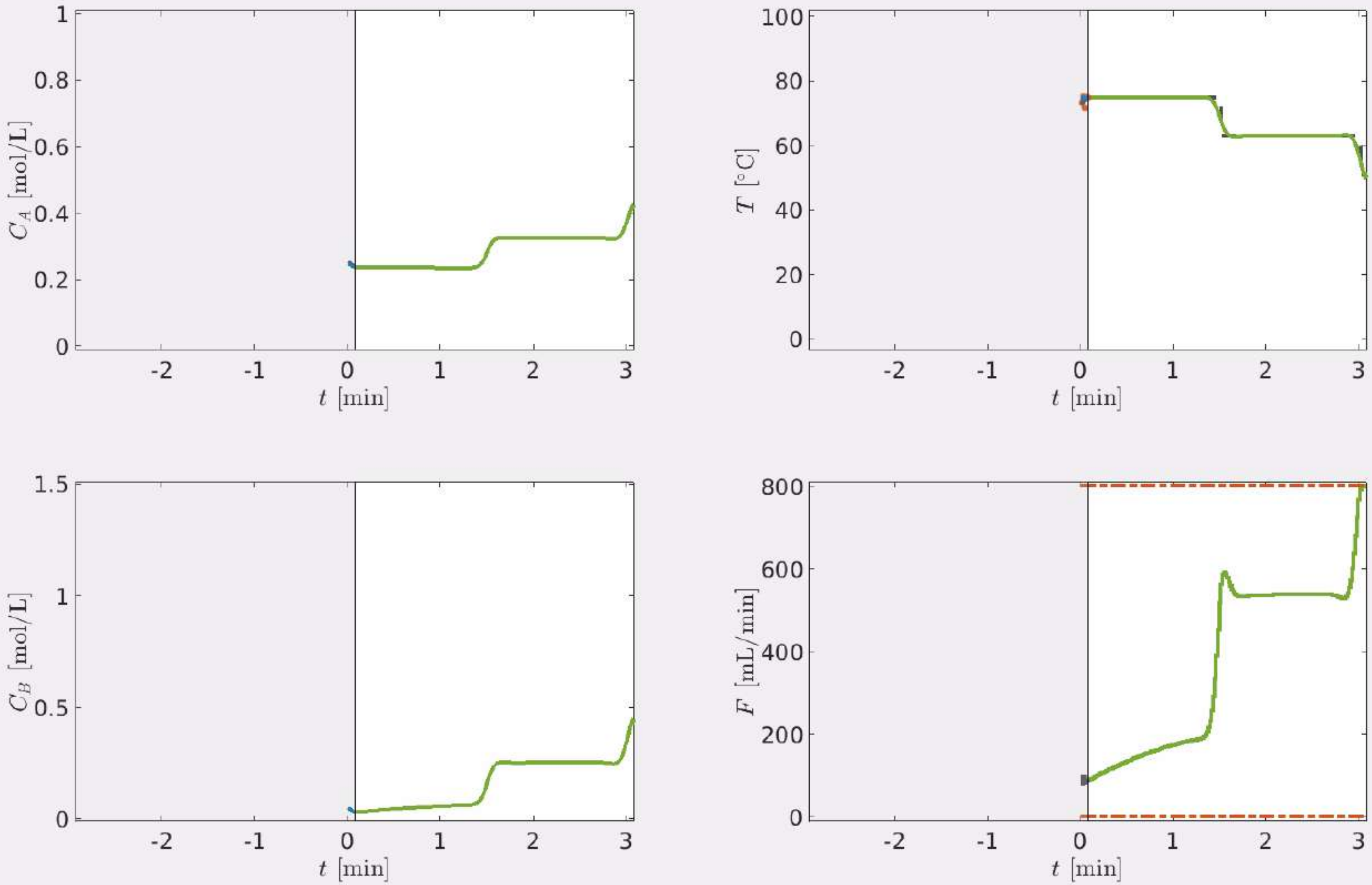

Movie of NMPC
(with true profiles in the prediction window)

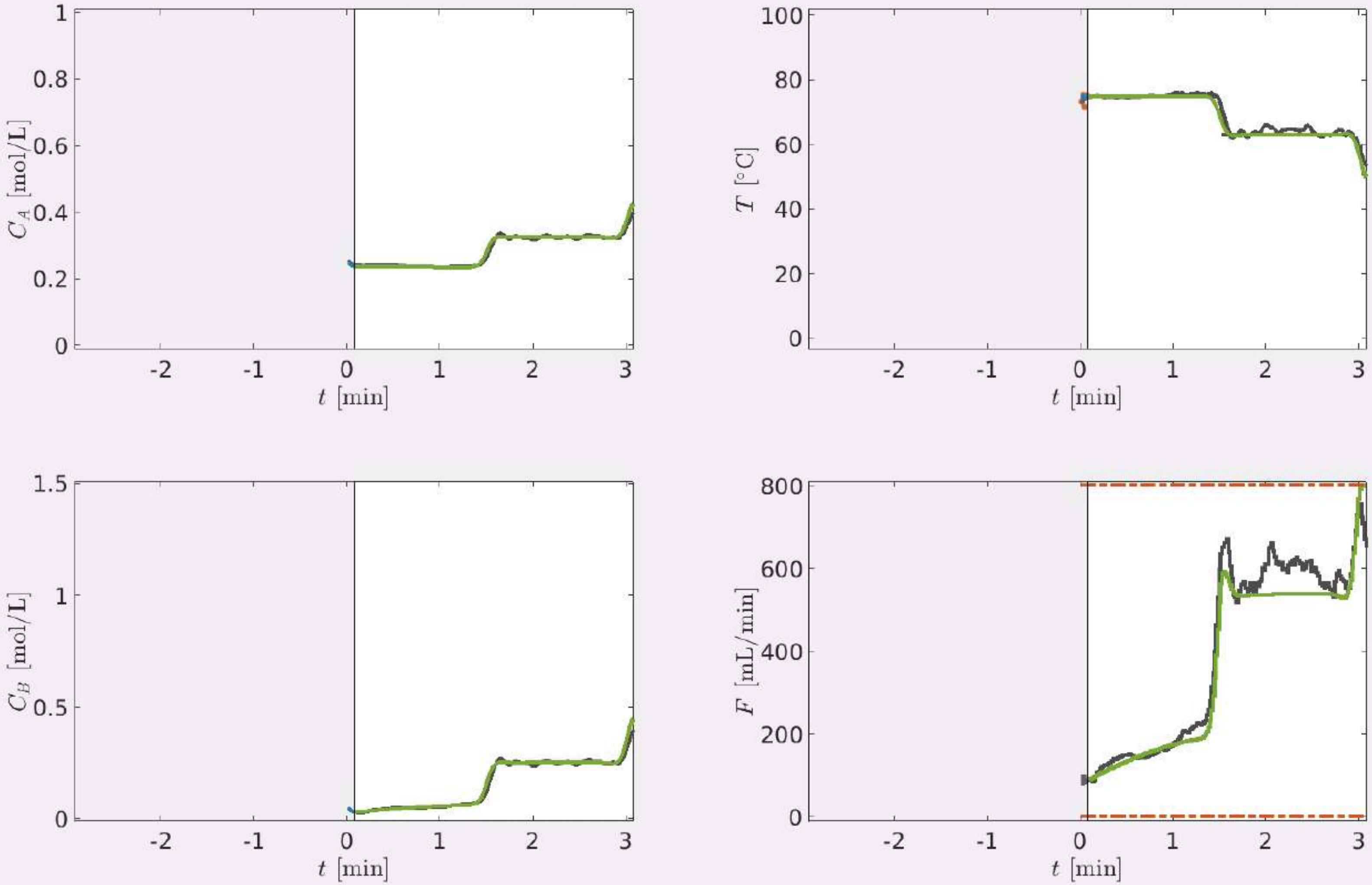

Nonlinear MPC - Closed-Loop Results

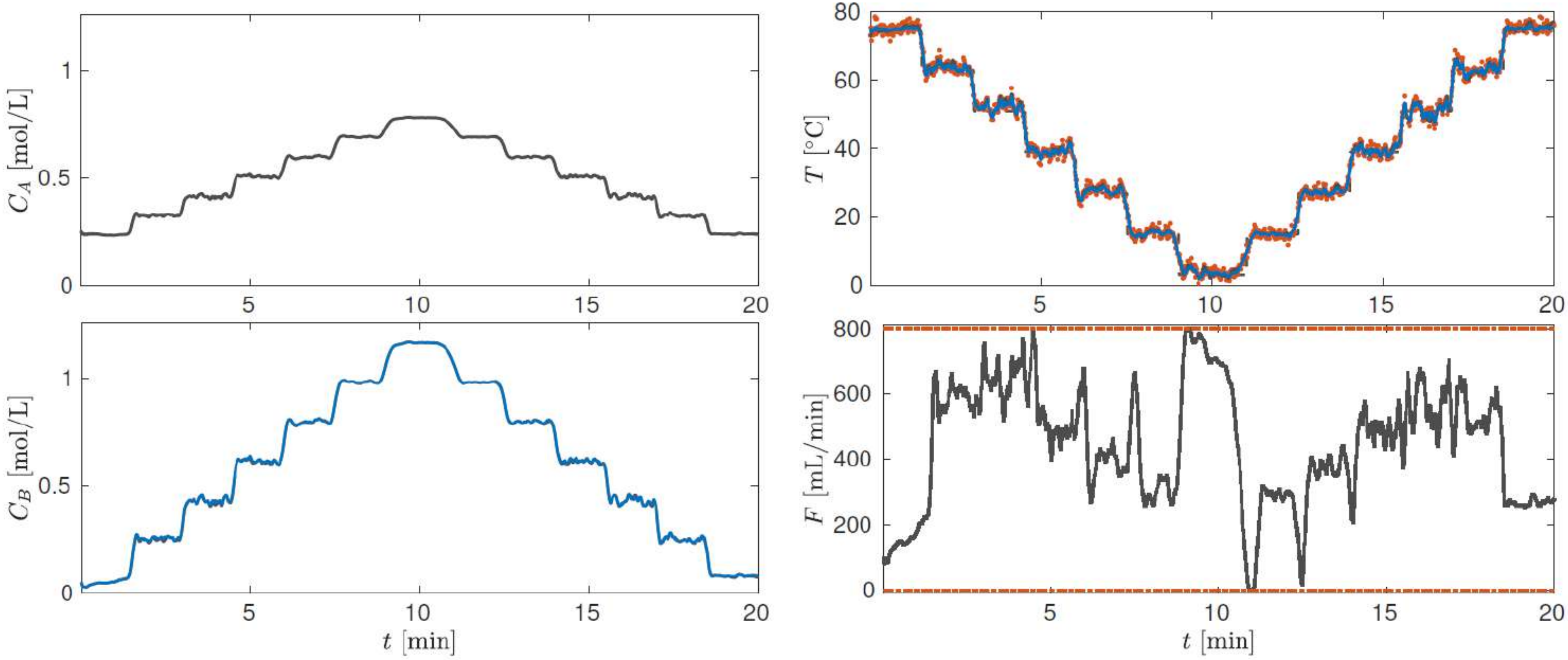

Nonlinear MPC - Closed-Loop Results (temperature)

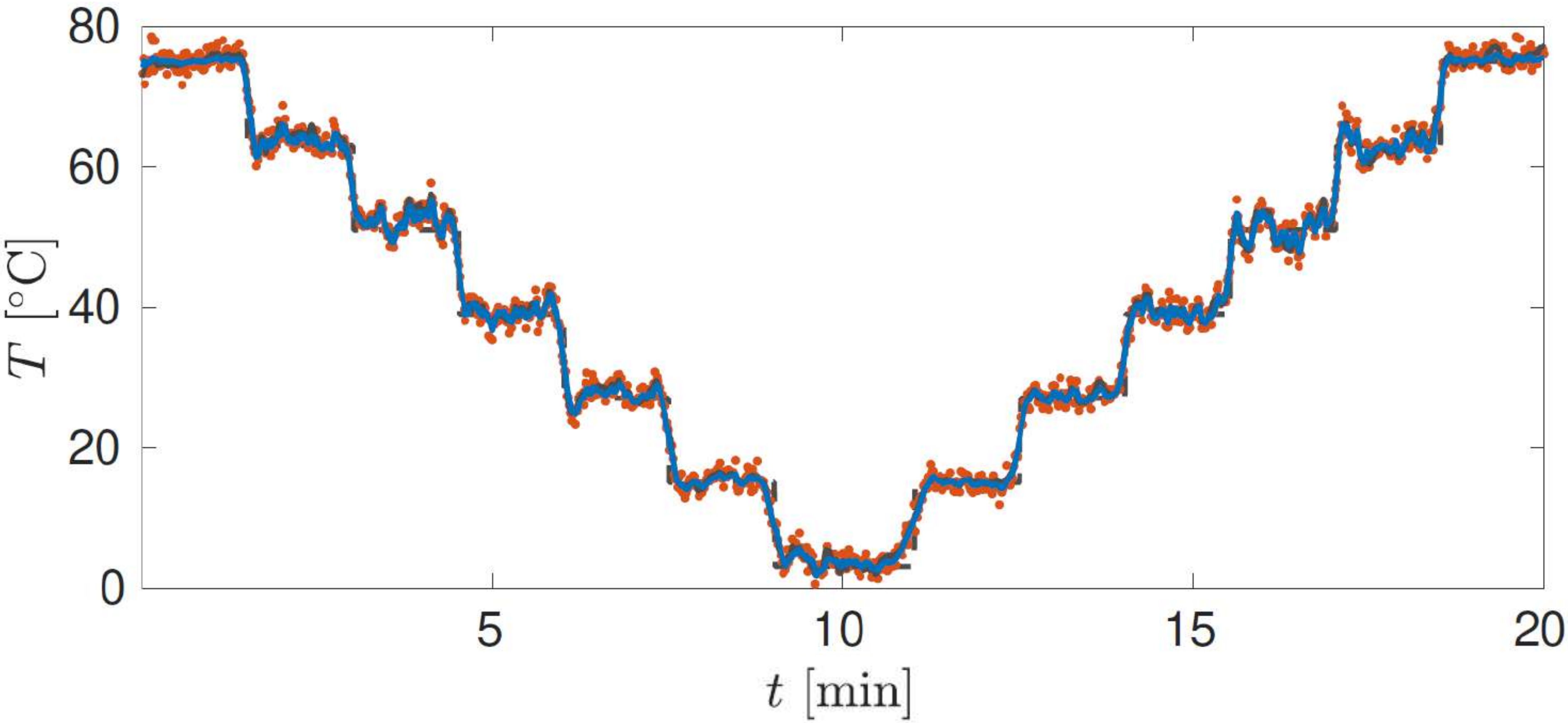

Closed-loop NMPC – 3D model – 1D model

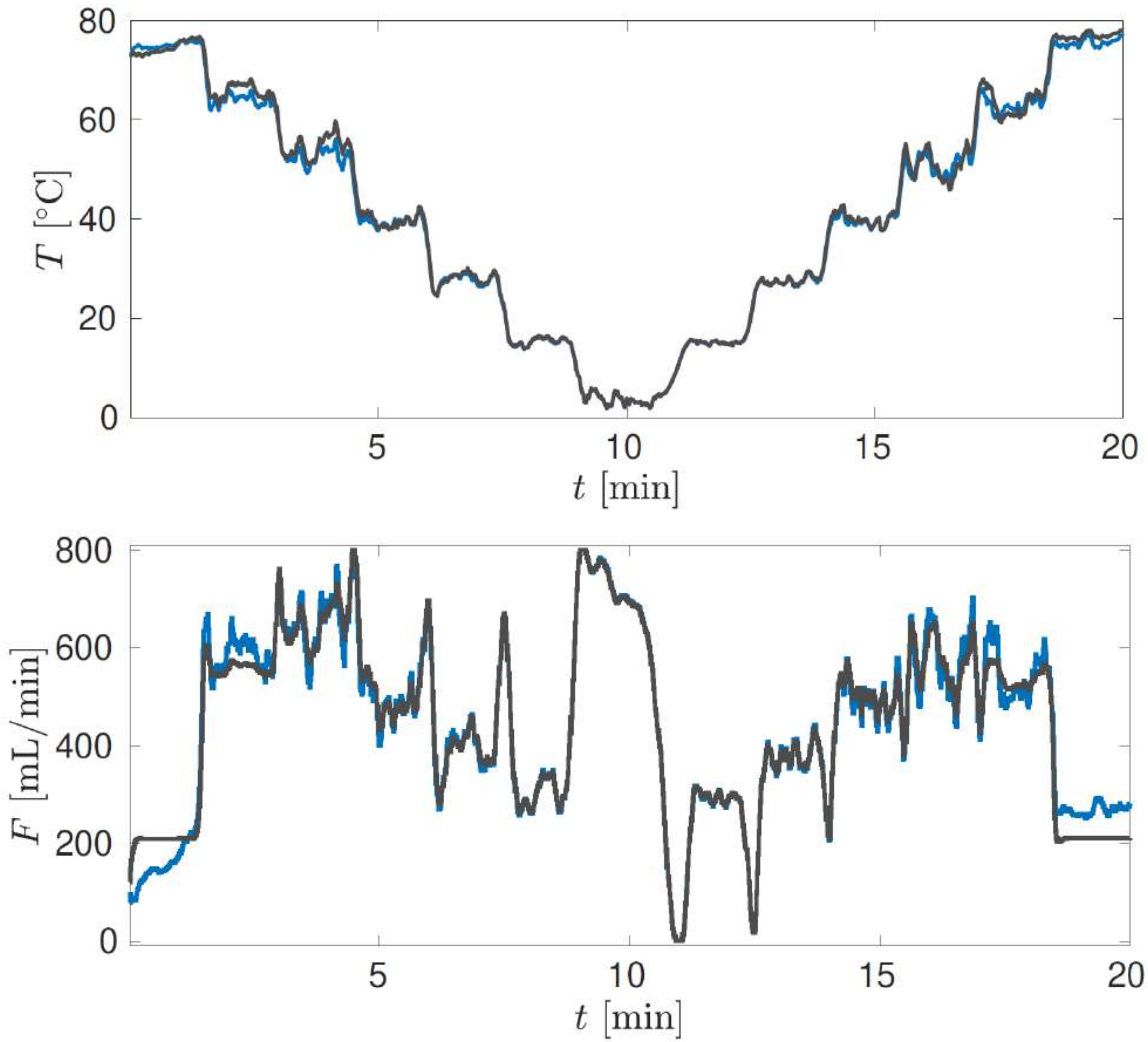

CPU time for the NMPC – 3D model – 1D model

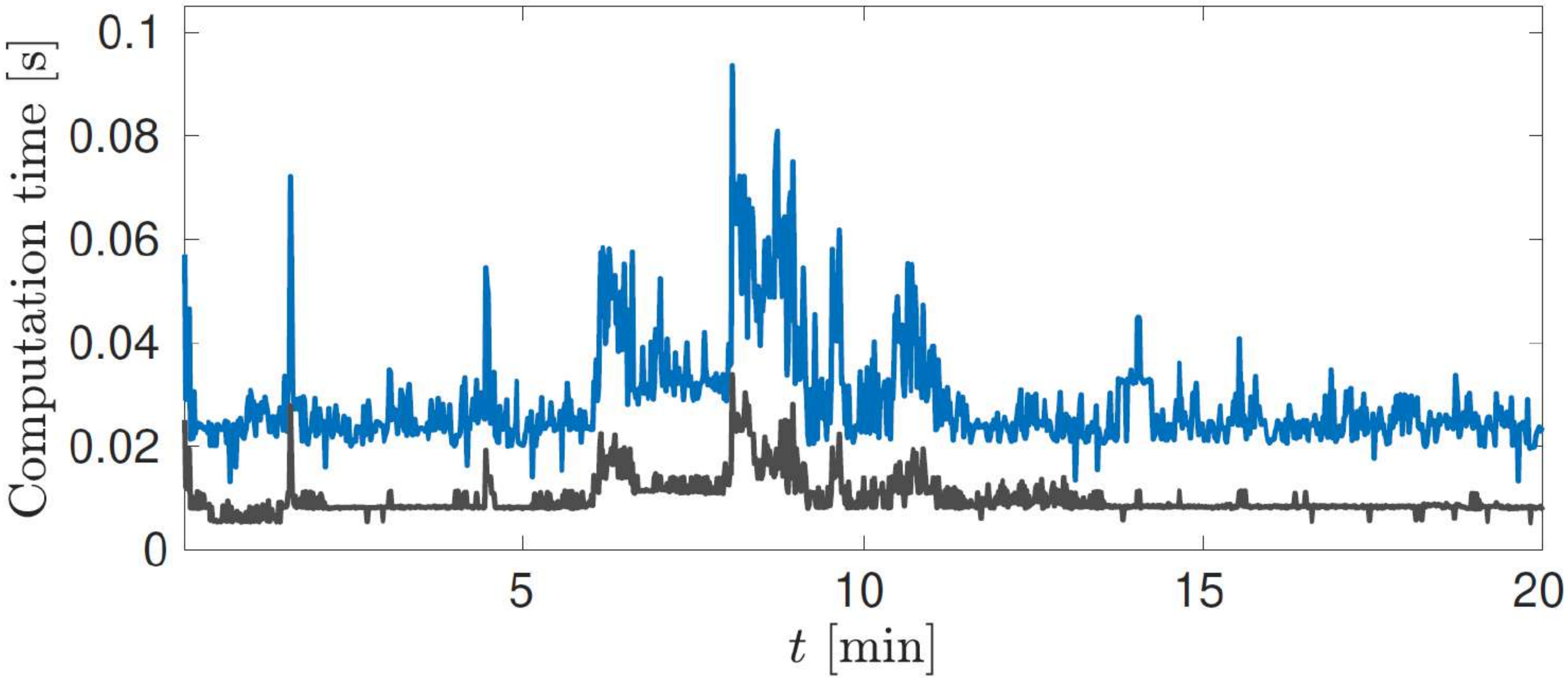

DIACON

An artificial pancreas for people with diabetes

DTU Compute
Department of Applied Mathematics and Computer Science

Artificial pancreas for people with diabetes

DIACON

SINGLE- AND DUAL-HORMONE
ARTIFICIAL PANCREAS

Diabetes is a global problem

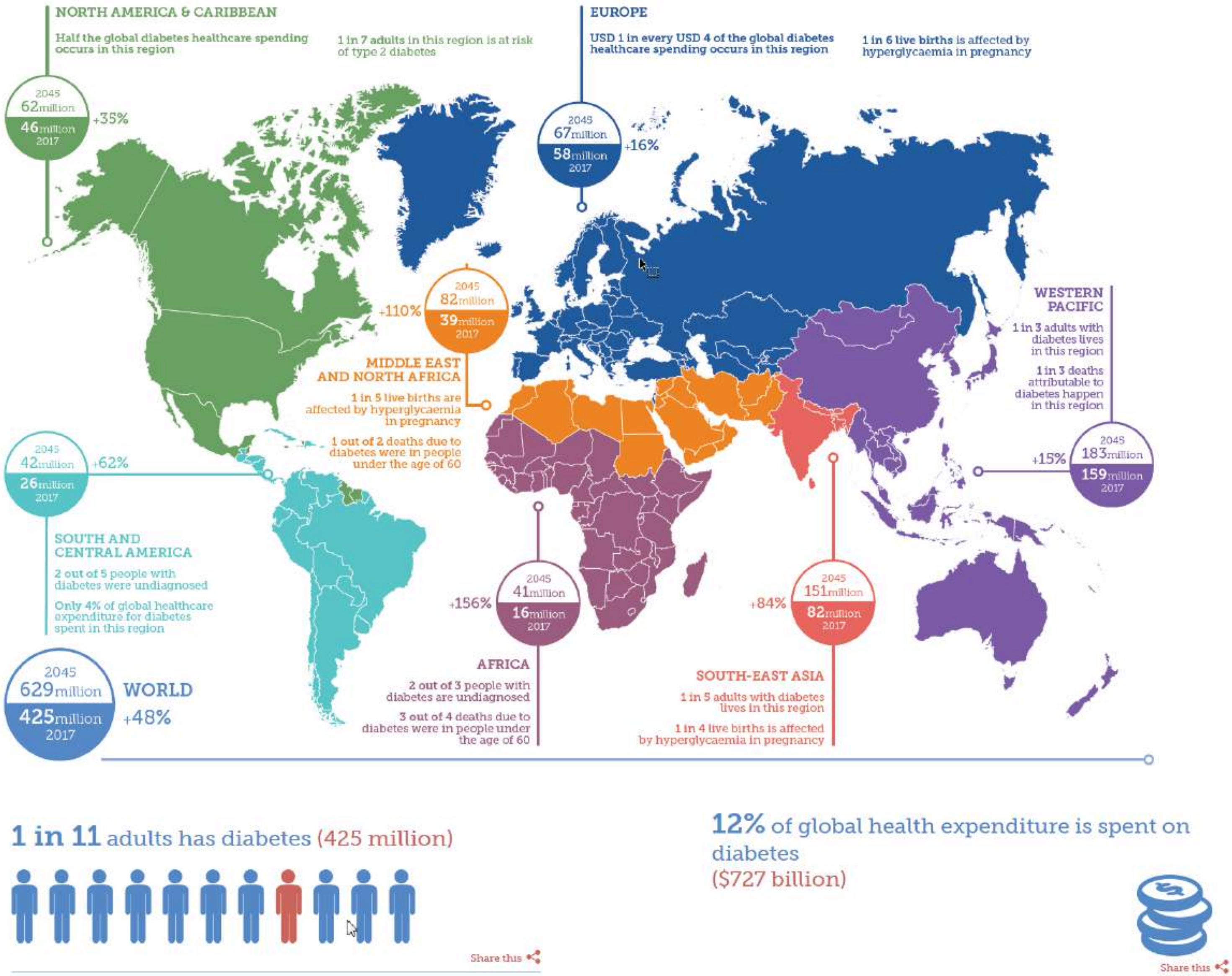

Conventional insulin therapy

+

5-8 blood glucose measurements per day

Detailed carbohydrate counting & adjustment for other events

Computation of insulin dosage by pen or pump

Insulin administration

Blood glucose concentration for conventional insulin therapy

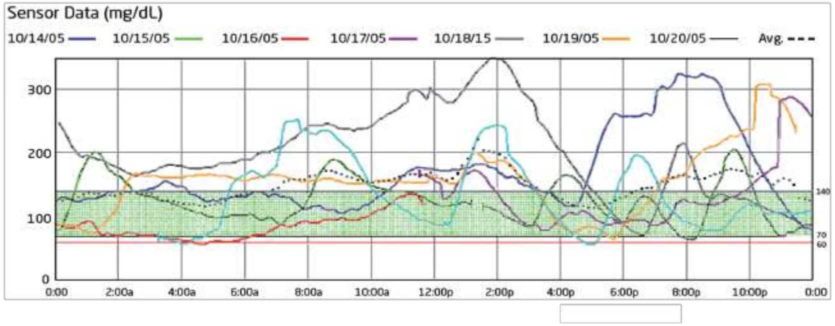

The blood glucose concentration must be in a certain range

- **Too low:** **Coma (immediate effect)**
- **Too high:** **Cardiovascular, kidney, nerve and eye diseases**

Conventional insulin therapy

+

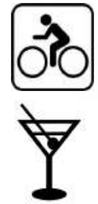

5-8 blood glucose measurements per day

Detailed carbohydrate counting & adjustment for other events

Computation of insulin dosage by pen or pump

Insulin administration

Blood glucose concentration for conventional insulin therapy

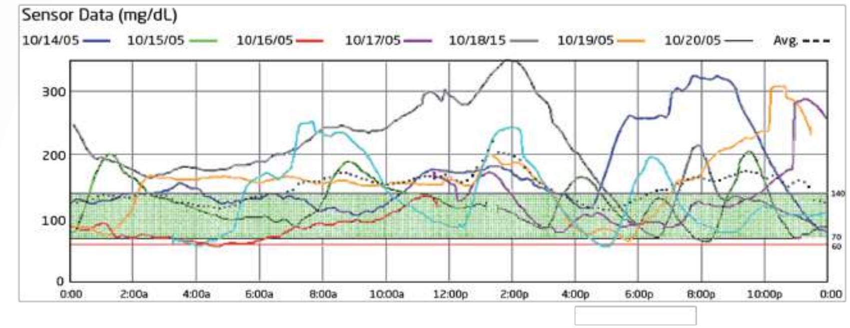

The blood glucose concentration must be in a certain range

- **Too low:** **Coma (immediate effect)**
- **Too high:** **Cardiovascular, kidney, nerve and eye diseases**

Physiology & metabolism

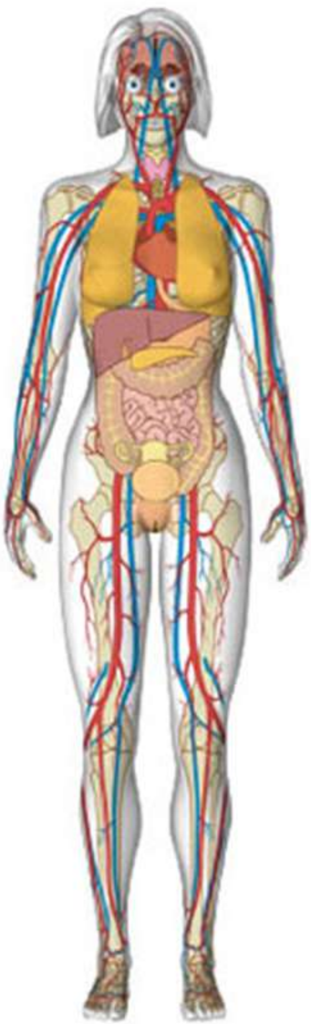

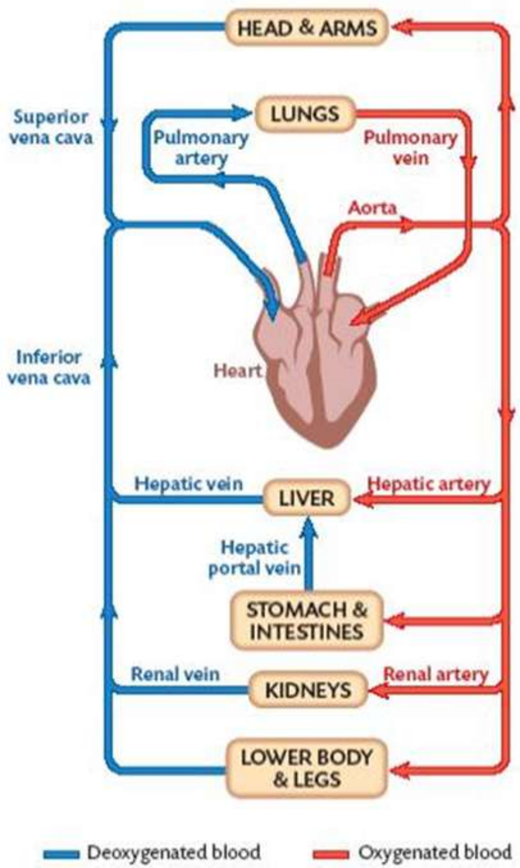

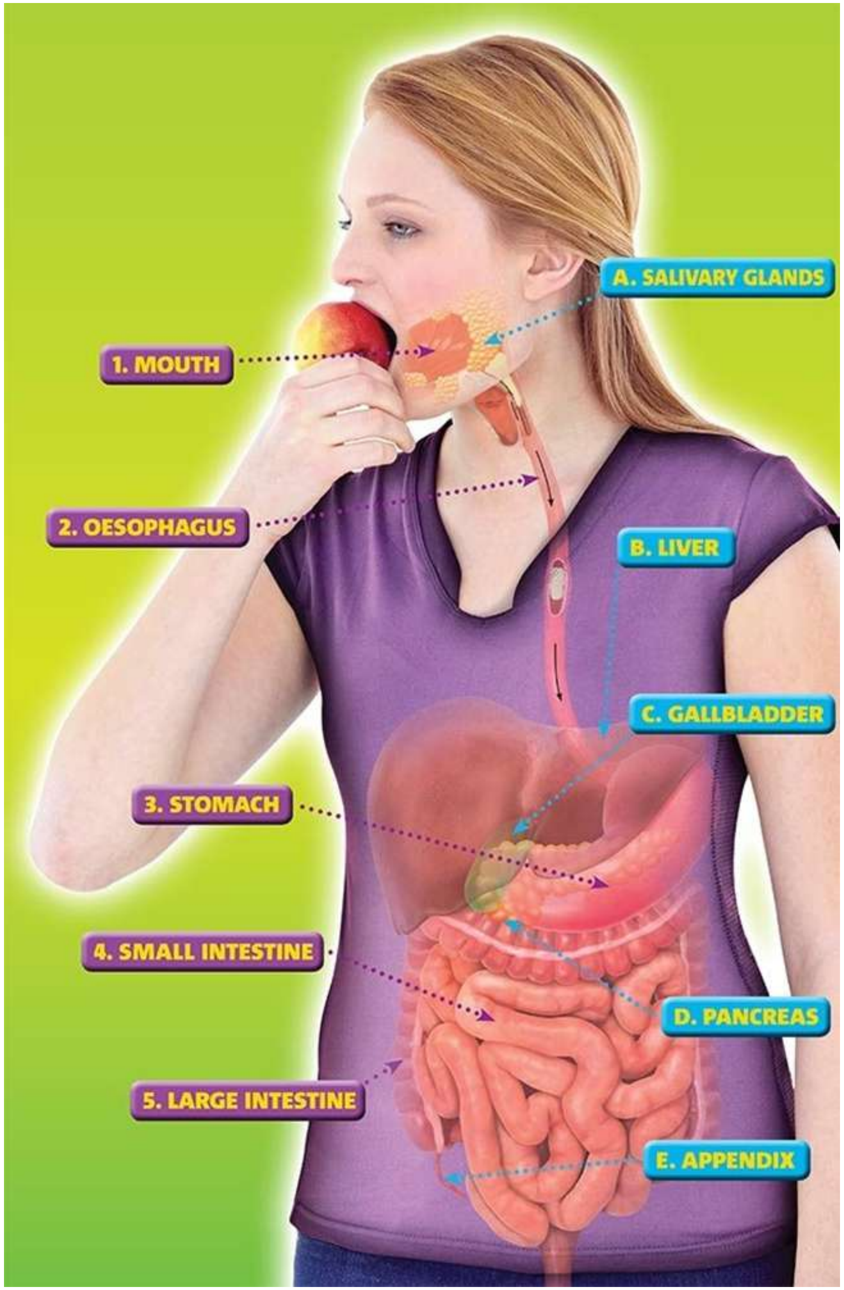

Physiology & metabolism

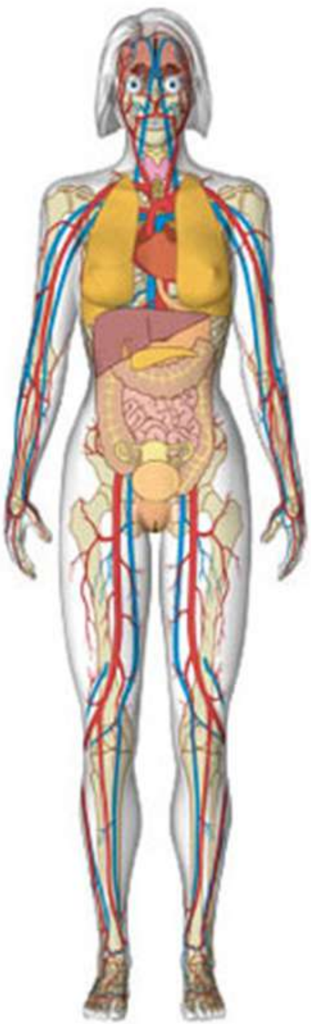

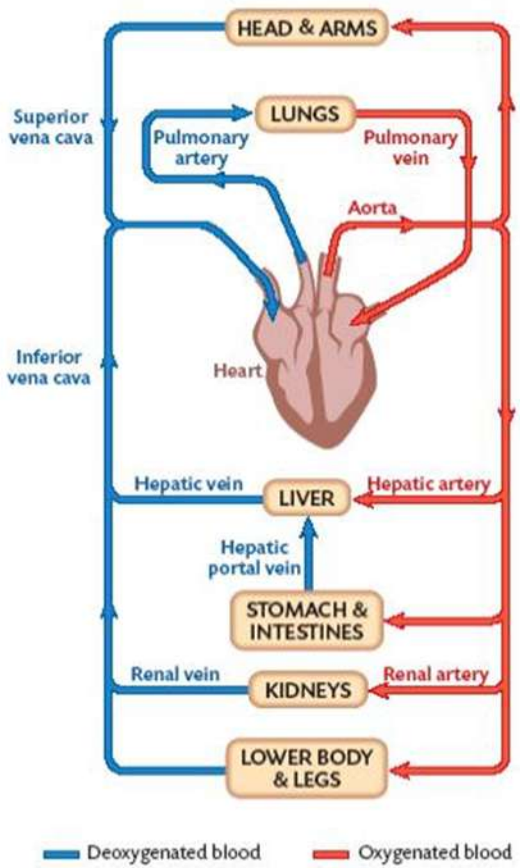

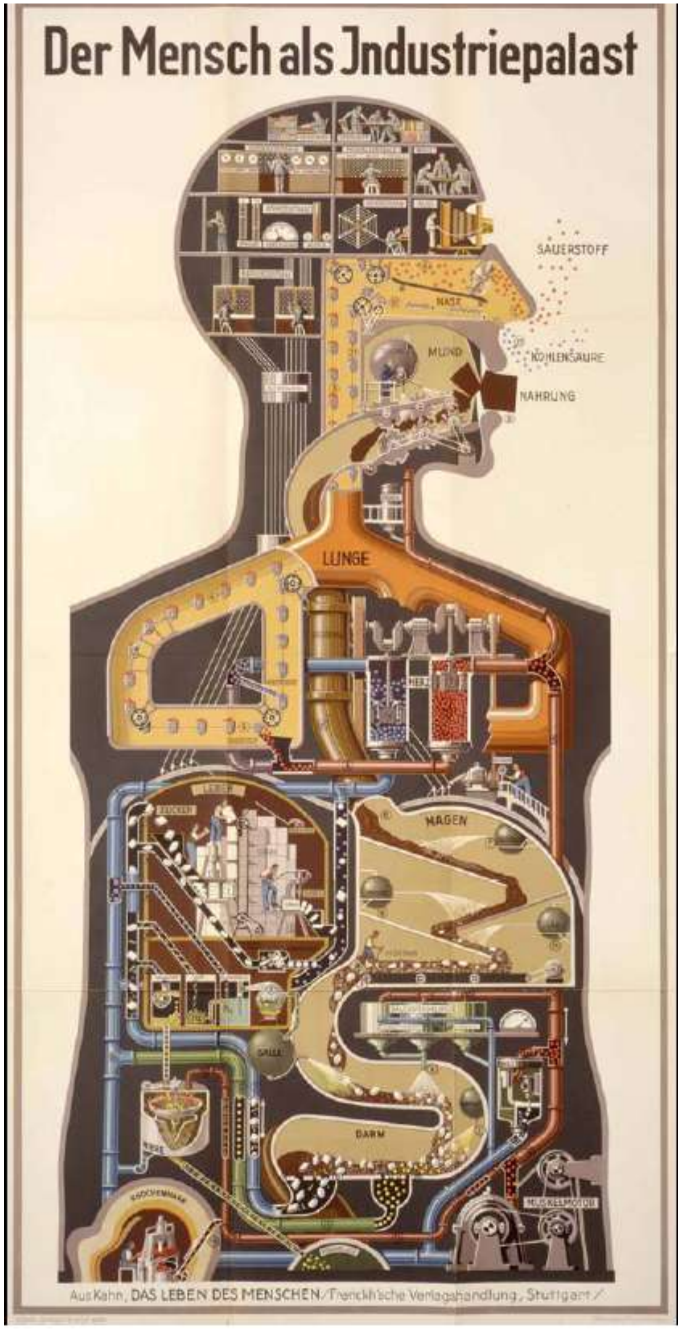

Dual hormone artificial pancreas
- feedback enabled model based control

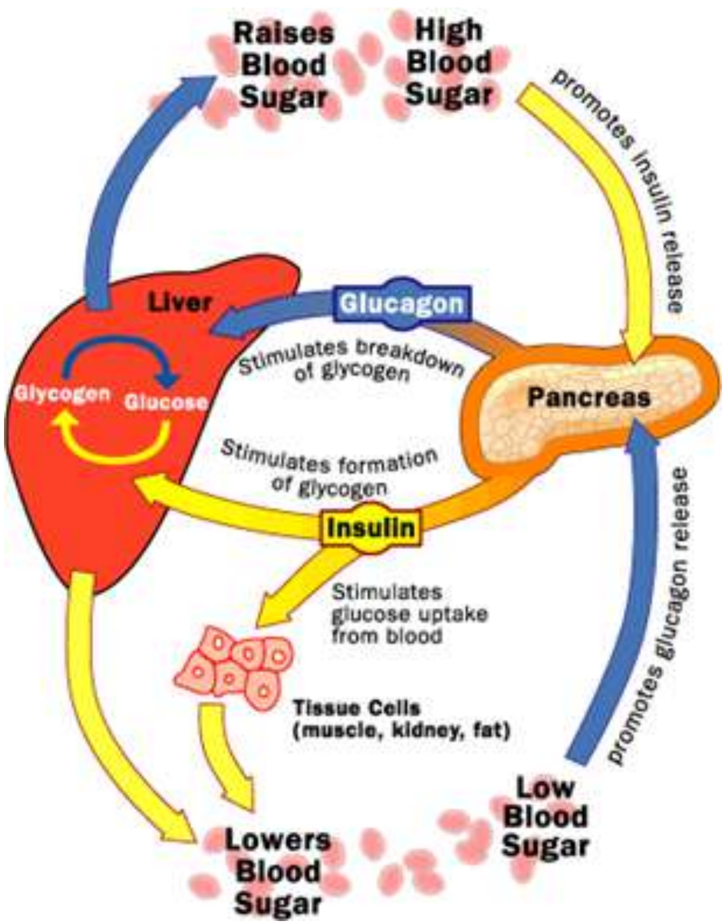

DIACON

SINGLE- AND DUAL-HORMONE ARTIFICIAL PANCREAS

DANISH DIABETES ACADEMY
DIACON
Steno Diabetes Center Copenhagen
cachet
Copenhagen Center for Health Technology

Artificial pancreas for people with diabetes

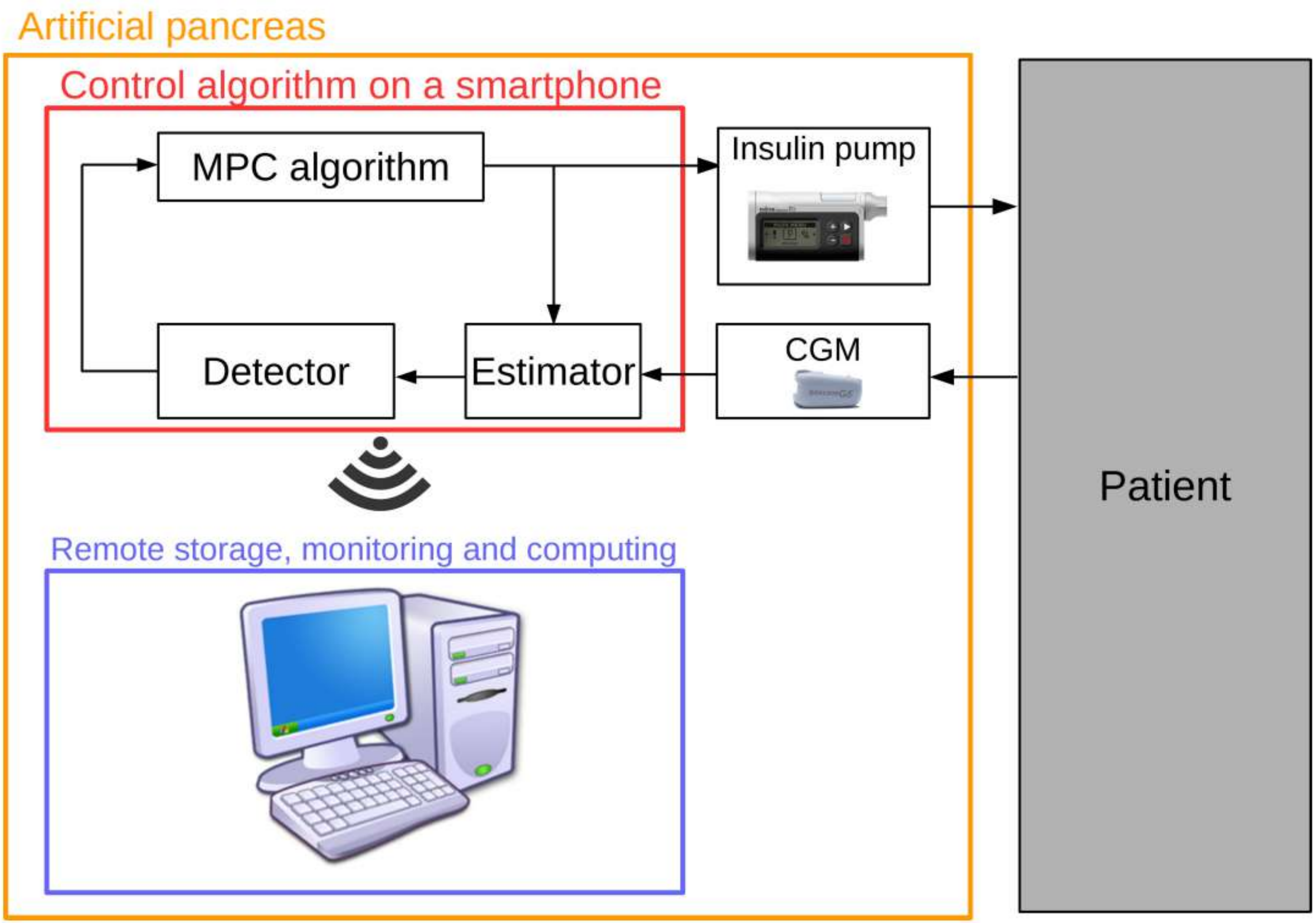

Model identification

Simulated data using a stochastic Hovorka model

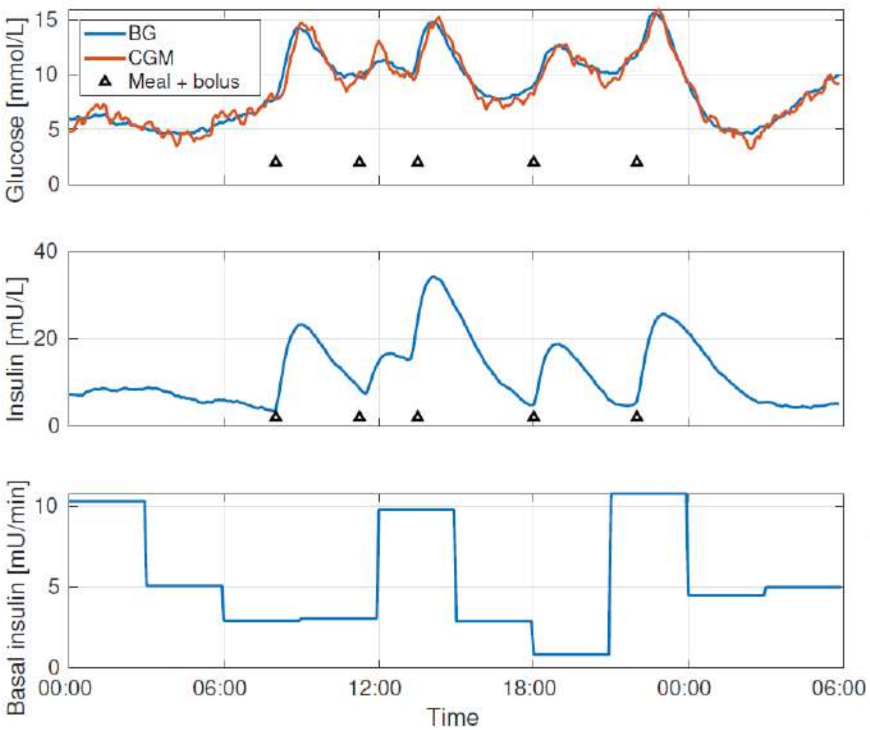

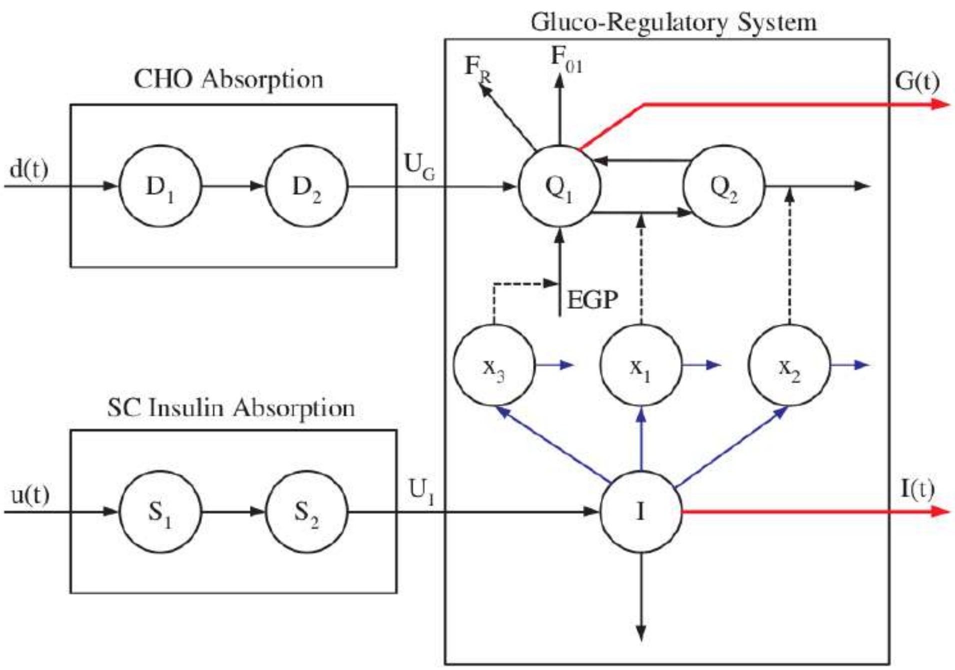

Model identification

- Maximum likelihood estimation
- 10 random Hovorka patients
- Maximum performance of a closed-loop system obtained when $k_1/k_m = \tau_m/\tau_1$ is high

Patient	k_1, k_2, p_2 (min^{-1})	S_I (mL/mU/min)	EGP_0 (mg/dL/min)	$1/V_G$ (dL^{-1})	k_m (min^{-1})	σ_G (mg/dL/min)	k_1/k_m (-)
1	0.023	0.0017	1.17	0.0082	0.0226	2.91	1.02
2	0.015	0.0011	0.98	0.004	0.022	3.15	0.68
3	0.021	0.0014	0.87	0.007	0.026	3.15	0.81
4	0.018	0.0019	1.47	0.0059	0.018	3.07	1.00
5	0.012	0.0024	1.57	0.021	0.015	3.28	0.80
6	0.012	0.0018	1.49	0.0020	0.014	3.60	0.86
7	0.014	0.0016	1.07	0.013	0.017	3.13	0.82
8	0.016	0.0011	0.94	0.0036	0.040	3.08	**0.44**
9	0.014	0.0005	0.35	0.0044	0.041	2.78	**0.34**
10	0.017	0.0008	0.67	0.0039	0.034	3.14	**0.50**
Mean	0.017	0.0013	0.958	0.0074	0.027	3.05	0.63

Nonlinear model-based control

Optimal control problem (OCP) in continuous time

$$
\begin{aligned}
\min_{[x(t),u(t)]_{t_0}^{t_f}} \quad & \phi = \int_{t_0}^{t_f} g(x(t),u(t))dt + h(x(t_f)) \\
\text{s.t.} \quad & x(t_0) = x_0 \\
& \dot{x}(t) = f(x(t),u(t),d(t)) && t \in [t_0, t_f] \\
& u_{\min} \leq u(t) \leq u_{\max} && t \in [t_0, t_f]
\end{aligned}
$$

- Solved using a multiple shooting-based SQP algorithm
- Numerical integration and forward sensitivity computation using a high-order explicit RK scheme
- Line search
- Riccati recursion

Asymmetric penalty function

Split between basal insulin, $u_{ba,k}$, and insulin boluses, $u_{bo,k}$.

$$\phi = \underbrace{\int_{t_0}^{t_f} \rho_z(z(t))dt}_{\text{BG penalty function}} + \underbrace{\sum_{k=0}^{N-1} W_{u,bo}\|u_{bo,k}\|_1 + W_{\Delta u,ba}\|\Delta u_{ba,k}\|_2^2}_{\text{Insulin penalty terms}}$$

The quadratic glucose penalty functions are

$$\rho_{\bar{z}}(z) = \frac{1}{2}(z-\bar{z})^2$$

$$\rho_{z_{\min}}(z) = \frac{1}{2}\left(\min\{z - z_{\min}, 0\}\right)^2$$

The resulting penalty function is

$$\rho_z(z) = \alpha_{\bar{z}}\rho_{\bar{z}}(z) + \alpha_{z_{\min}}\rho_{z_{\min}}(z)$$

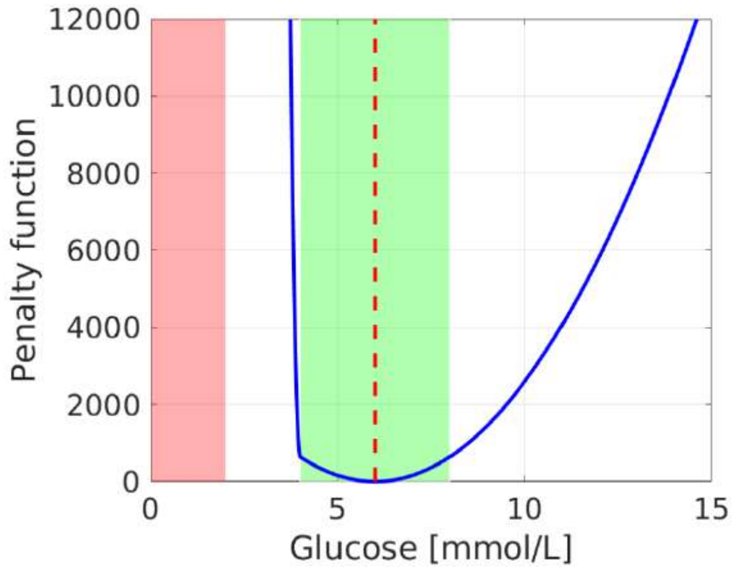

NMPC simulations

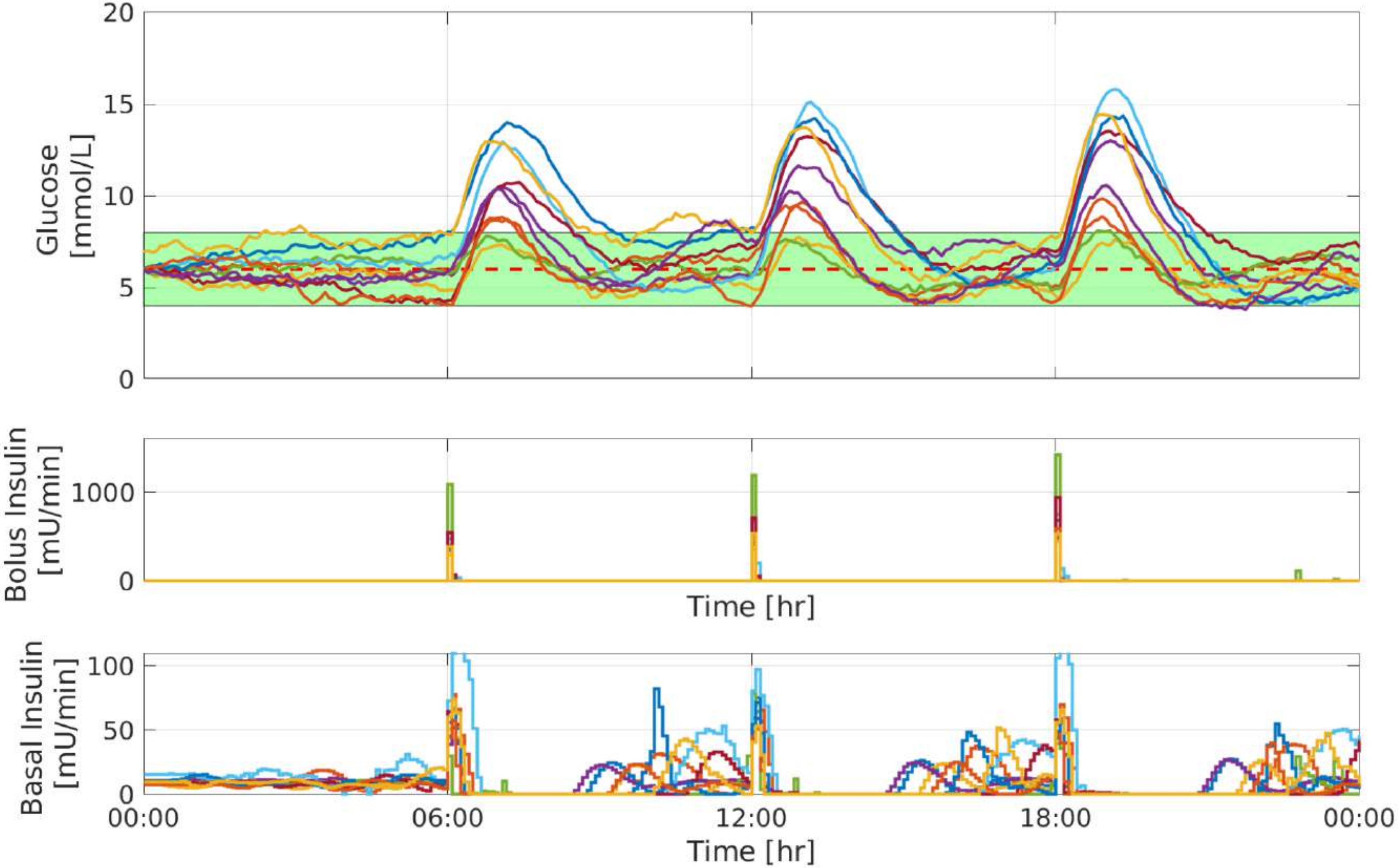

NMPC simulations

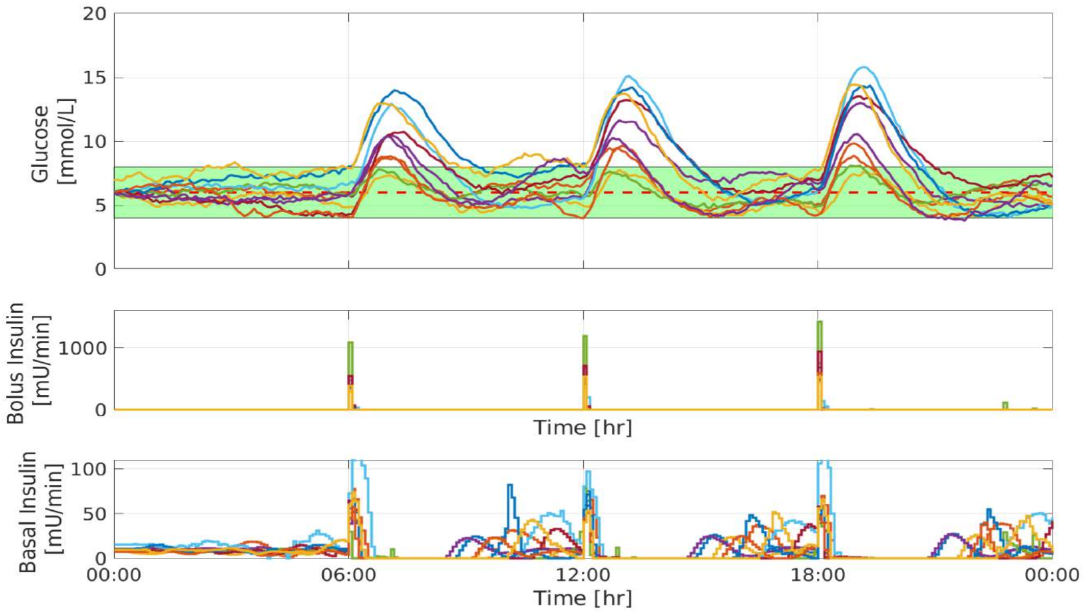

Range (mmol/L)	Mean (%)	Standard deviation (%)	Median (%)	IQR (%)
$G > 10$	7.45	7.75	6.51	0 - 14.96
$3.9 < G < 10$	92.24	7.48	83.35	85.04 - 100
$3.9 < G < 8$	83.57	10.39	81.58	75.36 - 89.75
$G < 3.9$	0.31	0.87	0	0 - 0
$G < 3$	0	0	0	0 - 0

NMPC simulations – correct meal size

60 g carbohydrates announced

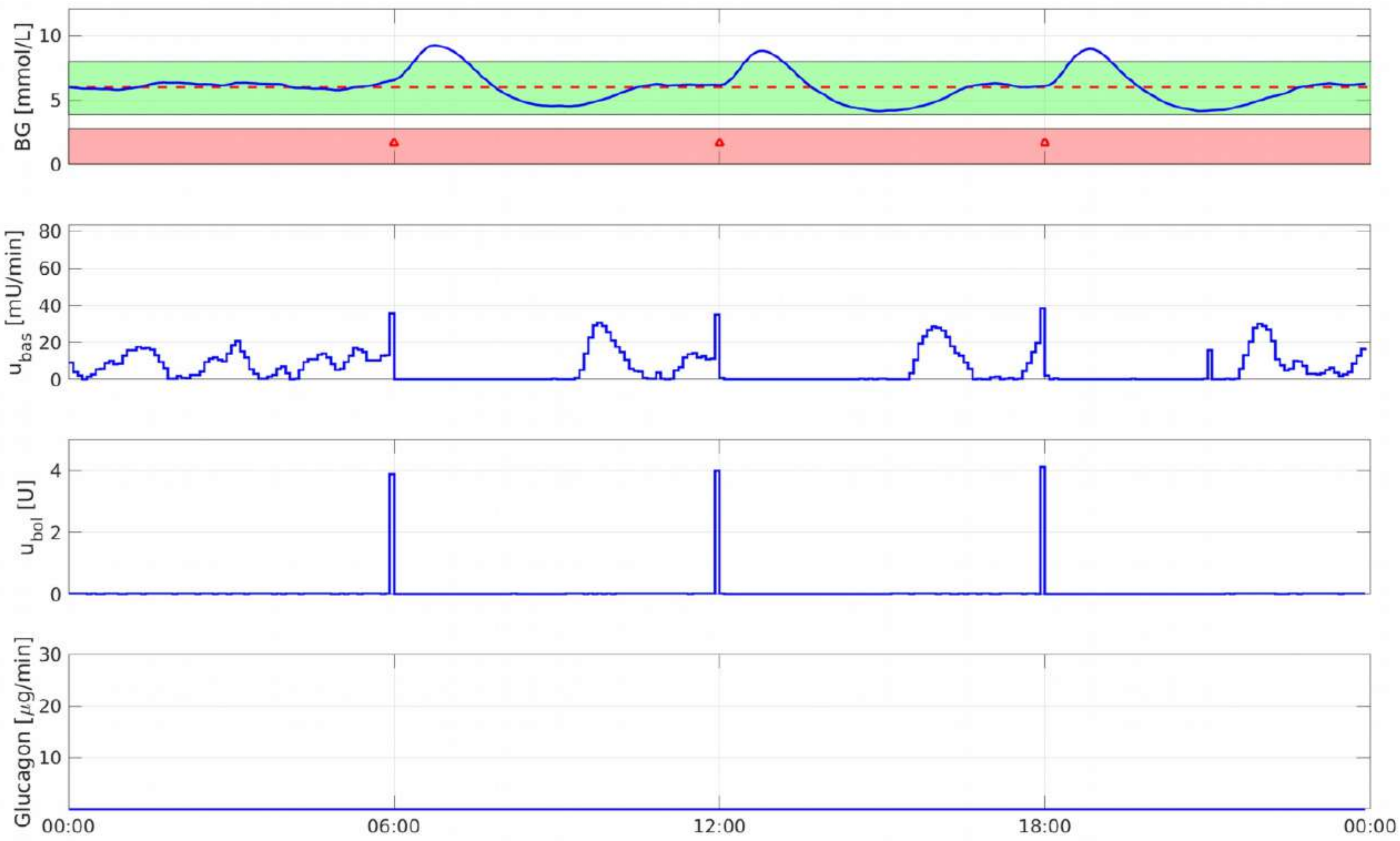

NMPC simulations – underestimated meals

60 g carbohydrates announced

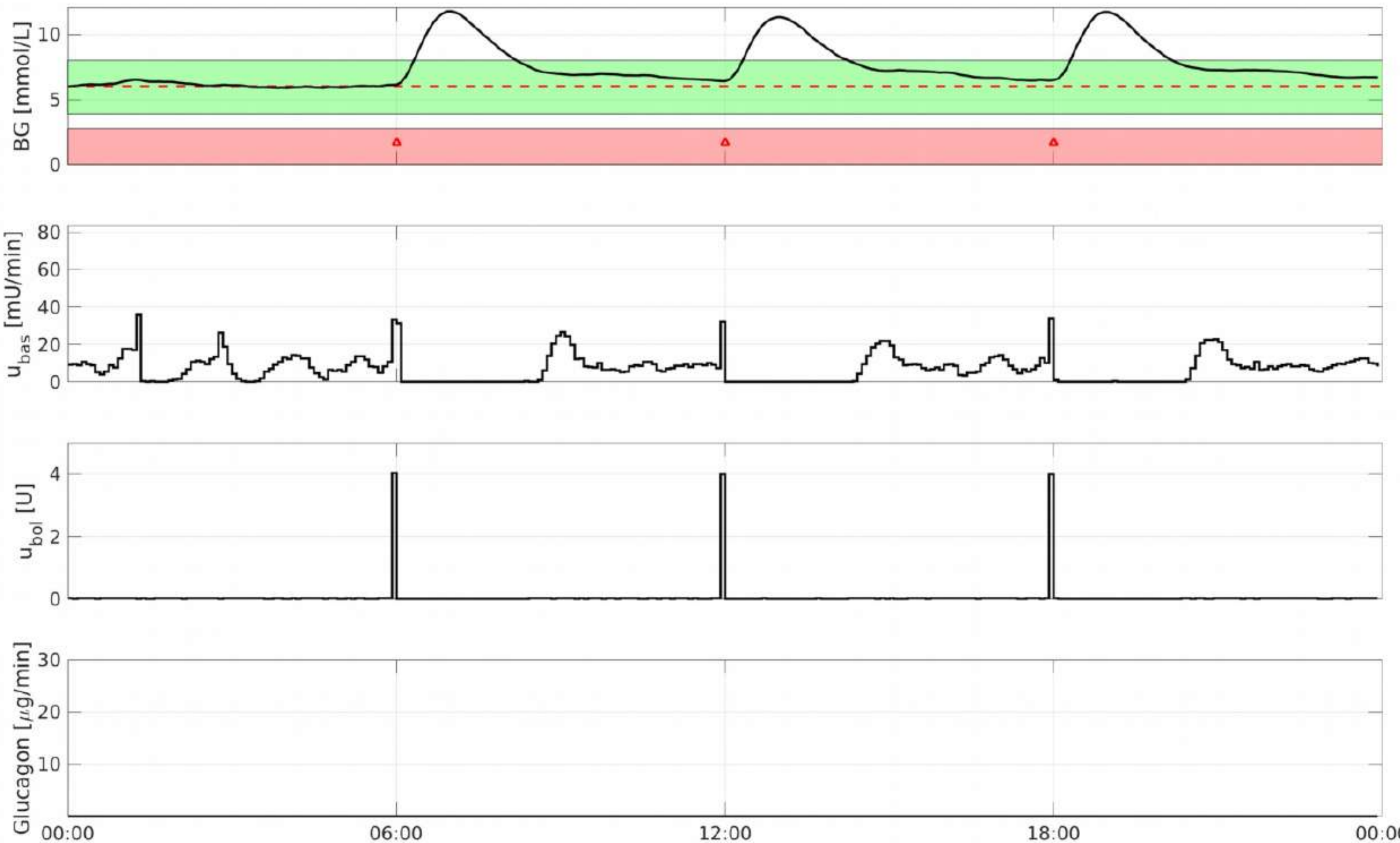

NMPC simulations – overestimated meals

60 g carbohydrates announced

Movie – Single Hormone AP (NMPC algorithm)

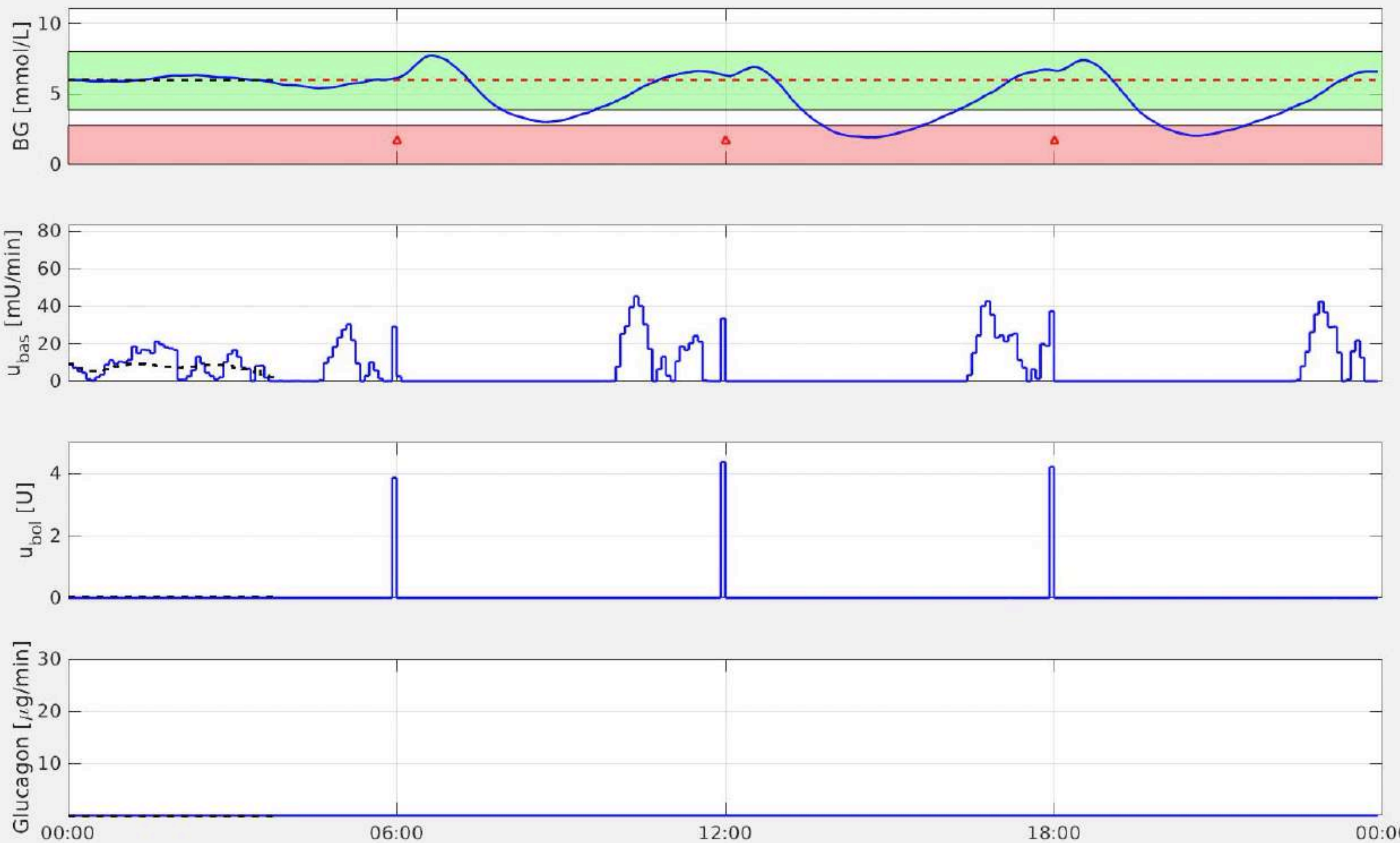

NMPC simulations

60 g carbohydrates announced

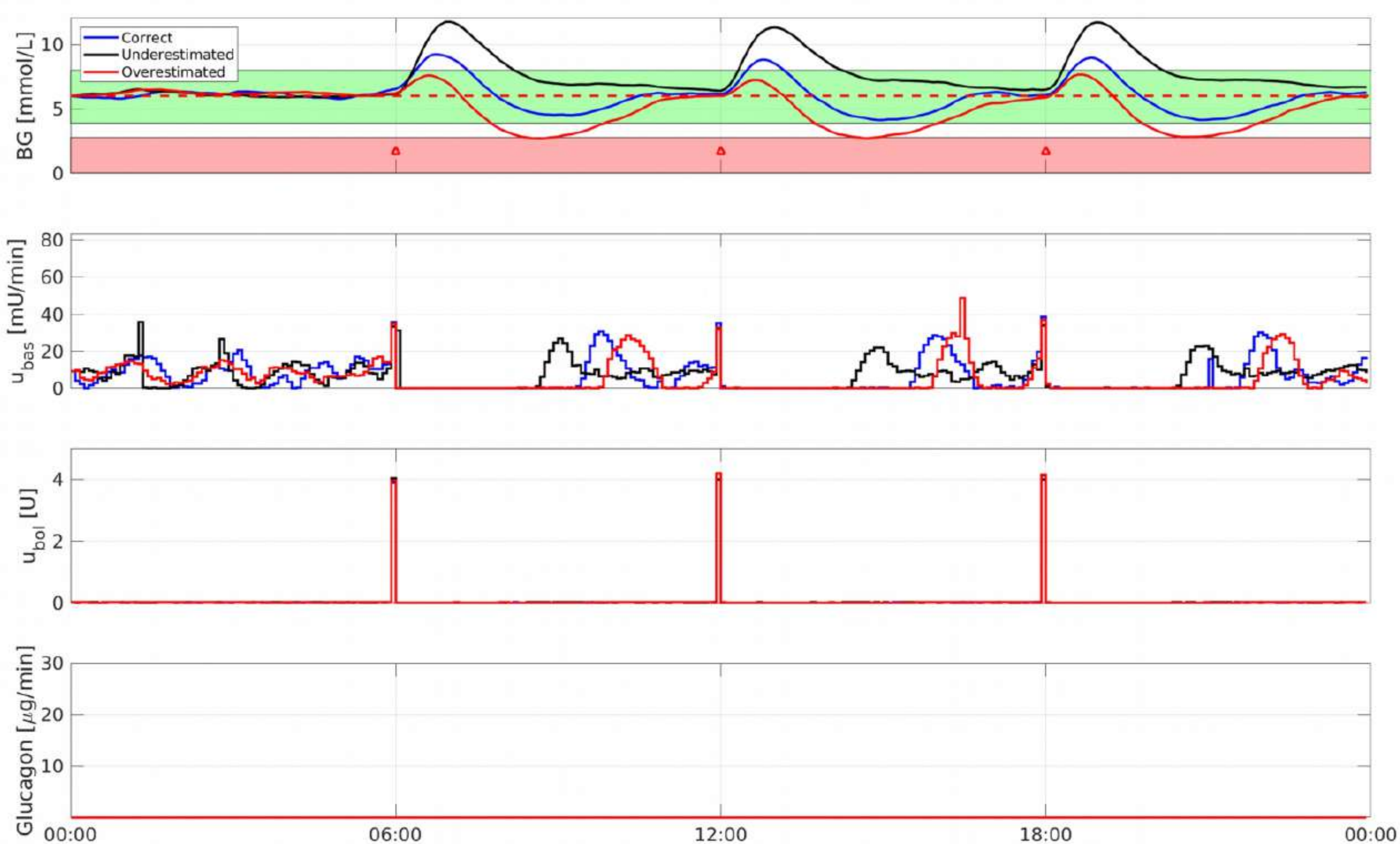

Movie – Dual Hormone AP (NMPC algorithm)

NMPC simulations – Overestimated meals

Single vs. dual hormone AP.

Single- and Dual-Hormone AP in clinical test at Steno Diabetes Center Copenhagen

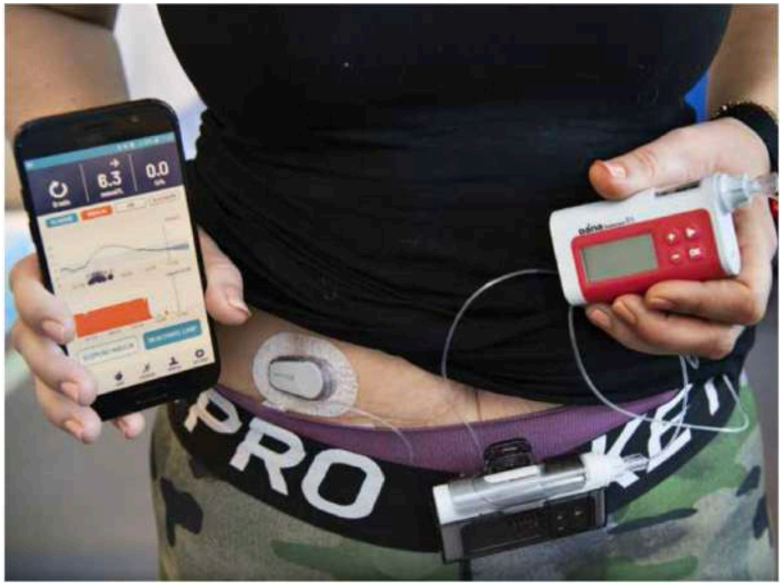

Postprandial dynamics

Maximum BG concentration for different meal sizes.

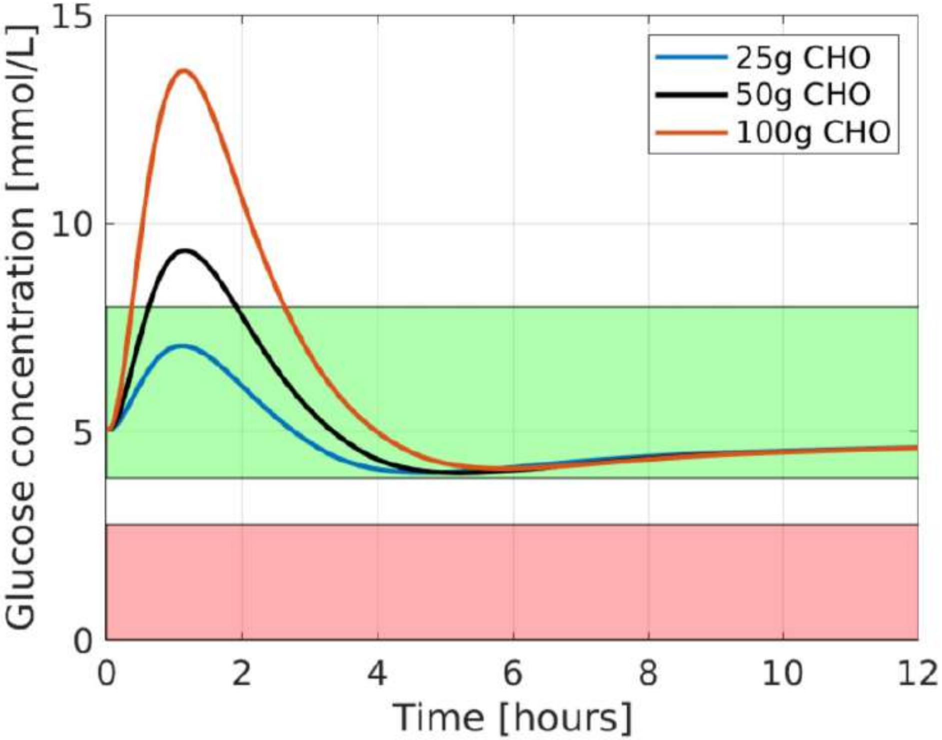

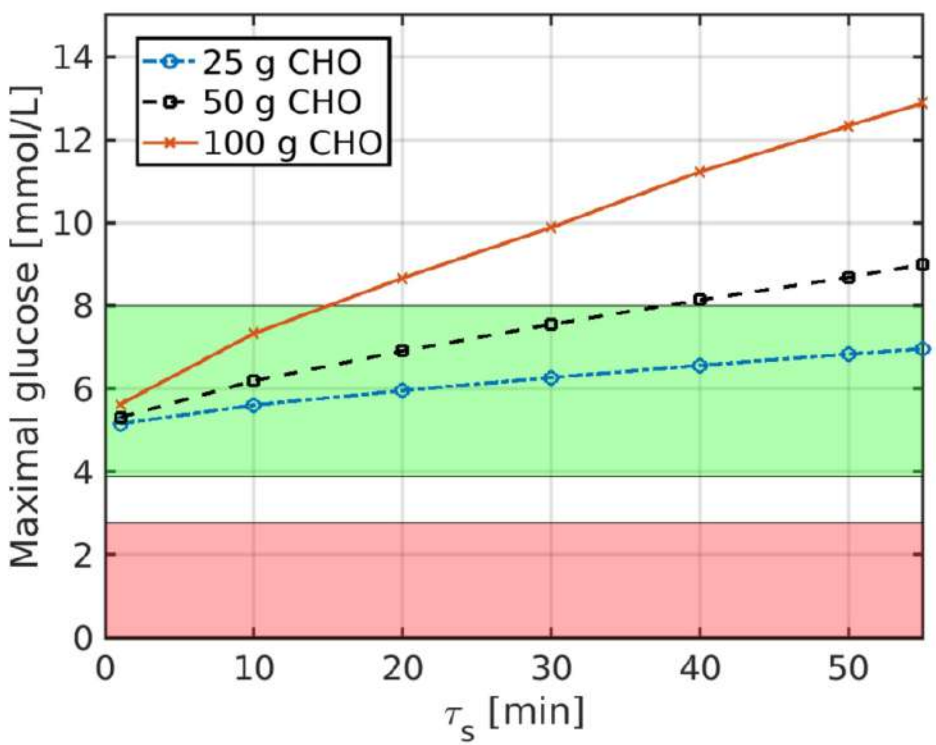

- Ways to reduce postprandial peaks:
  - Faster insulin
  - Glucagon
  - Slower gastric emptying (e.g. amylin)

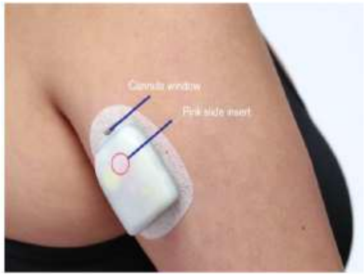

Perspectives

1 Suspend

Next steps:
Clinical adoption

2 Predictive Suspend

Next steps:
U.S. approval, reimbursement, clinical adoption

3a Automated Insulin Delivery (AID)

Next steps: Faster insulin action, miniaturization,
integration, individualized control

3b Multihormone (MH)

Next steps:
Glucagon: Soluble pumpable glucagon, chronic glucagon exposure studies, dual-chamber pump development, algorithm finalization, head-to-head vs. AID
Amylin: Coformulation vs. dual-chamber pump, ratio determination, algorithm finalization, head-to-head vs. AID

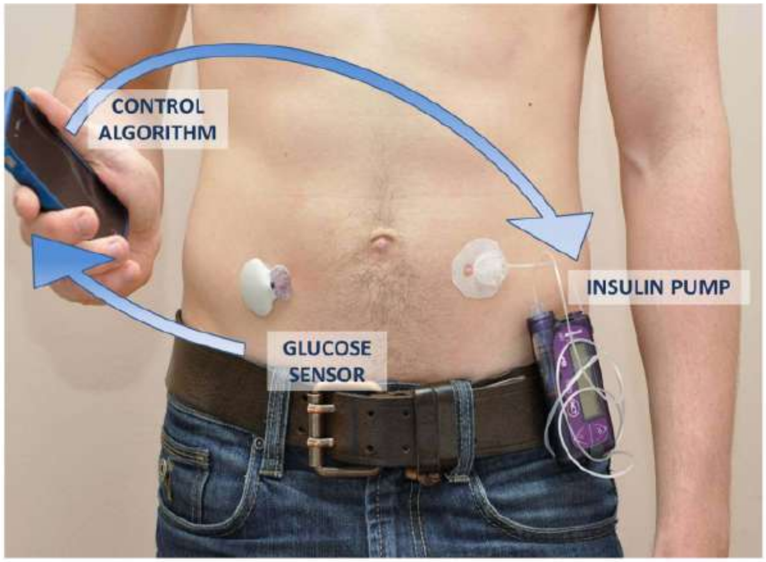

Artificial pancreas for people with diabetes

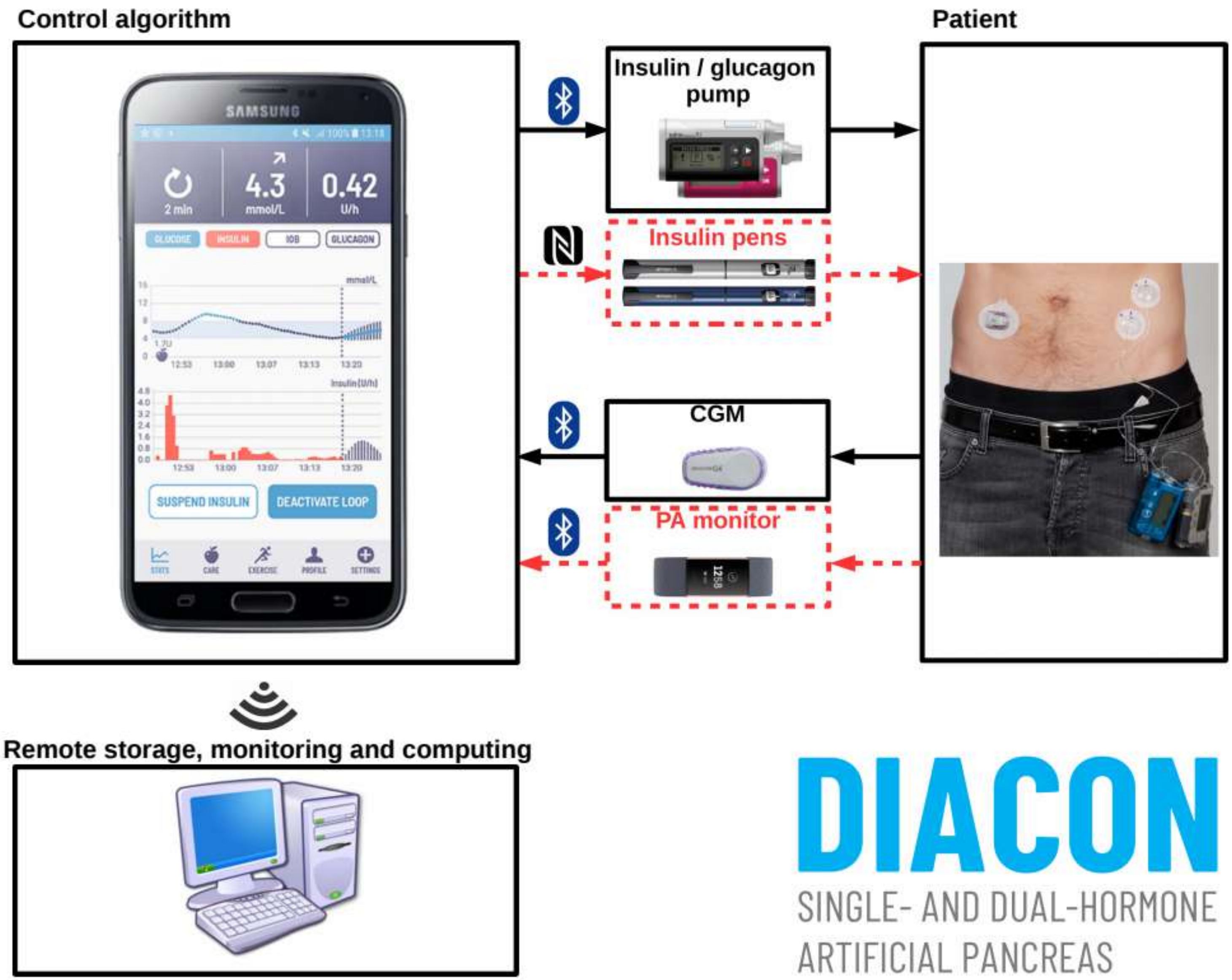

DIACON

SINGLE- AND DUAL-HORMONE ARTIFICIAL PANCREAS

The Artificial Pancreas and Industry 4.0

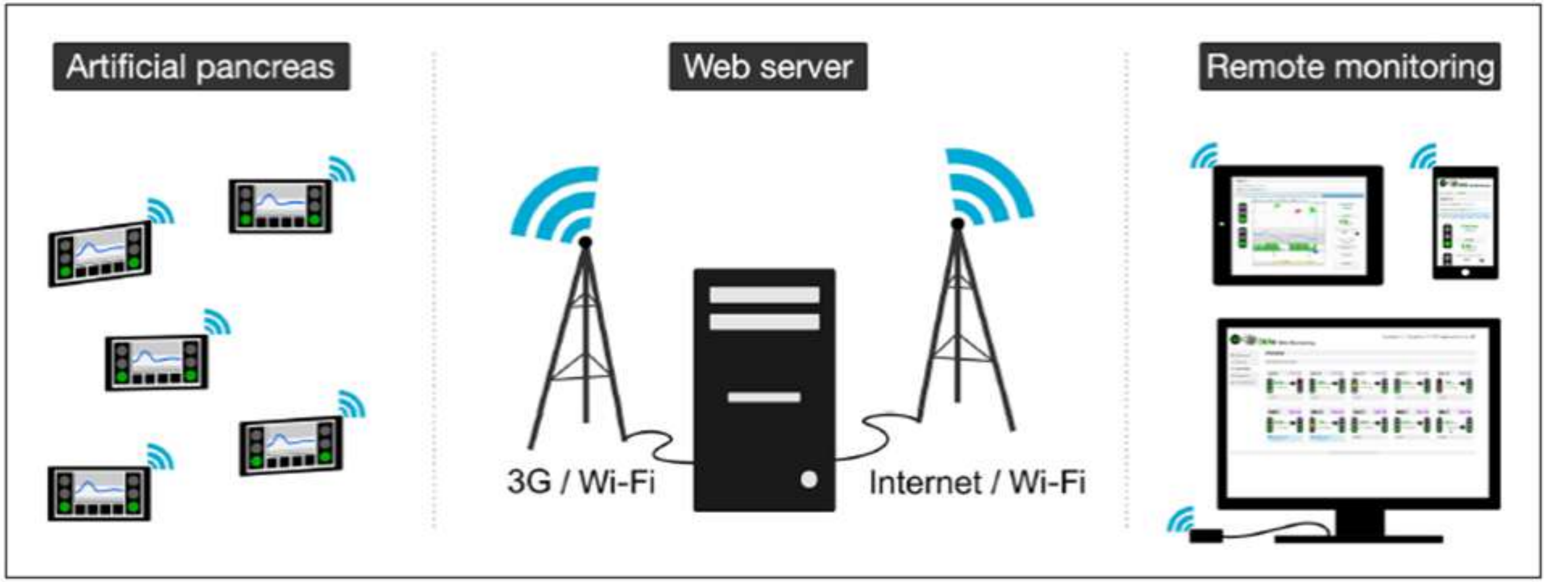

Personalized treatment of type 2 diabetes using model based control in the cloud

novo nordisk

Steno Diabetes Center Sjælland

glooko

Artificial pancreas technology – 2014 perspective

Notat om udvikling af kunstig bugspyt-kirtel teknologi

Objective:
Patients in Denmark must have acces to Artificial Pancreas Technology in 2020

Anders Overgaard Bjarklev
Rektor, cand.polyt., ph.d., dr.techn.
Danmarks Tekniske Universitet

Lars Berendt
Formand for bestyrelsen
Børnediabetesfonden JDRF

John J Nolan
MD, FRCPI, FRCP (Ed), Professor
CEO and Head
Steno Diabetes Center

Tore Christiansen
Managing Director, Ph.D
Dansk Diabetes Akademi

Mette-Marie Harild
Formand for bestyrelsen
Medtronic R&D
Diabetes Danmark

Torben Sandgren
Global Vice President
Sales, Marketing and R&D
ConvaTec A/S

Steen Werner Hansen
Deputy Chief Executive (DCE)
Board of Directors
Herlev Hospital

Birger Thorsteinsson
Professor, overlæge, dr. med.
Endokrinologisk afdeling
Nordsjællands Hospital

David Horn Solomon
President & Chief Executive Officer
Zealand Pharma A/S

Torben Mogensen
Vicedirektør dr.med.
Hvidovre Hospital

Mads Krogsgaard Thomsen
Executive Vice President & Chief Science Officer
Novo Nordisk A/S

Per Michael Johansen
Rektor, professor
Aalborg Universitet

Rasmus Stig Jensen
Adm. direktør
HypoSafe A/S

Jane Kraglund
Adm. Sygehusdirektør, cand.scient.pol.
Odense Universitetshospital

Ny teknologi mod type 1 diabetes
Venstre ønsker at styrke forskningen i kunstig bugspytkirtelteknologi. Denne teknologi kan give mennesker med type 1 diabetes et normalt liv, spare betydelige beløb på det offentlige sundhedsbudget og skabe arbejdspladser og økonomisk vækst i Danmark.

Derfor vil Venstre tilføre midler til Dansk Diabetes Akademi, der forsker i kunstig bugspytkirtelteknologi. Det skal ske via samfinansiering mellem offentlige og private midler. En tilførsel af nye midler kan sikre, at udviklingen af teknologien kan fremskyndes og dermed tidligere komme danske patienter til gode.

STYRKET OG MÅLRETTET FORSKNINGSINDSATS

- **Forskning der skaber arbejdspladser.** Styrke forskning inden for teknisk videnskab, fødevarer, produktion, entreprenørskab og biomedicin med 200 mio. kr.
- **Styrke forskning i kunstig bugspytkirtel teknologi.** Teknologien kan give mennesker med type 1 diabetes et normalt liv.

U-loop reactor for single-cell protein production

Single-Cell Protein to feed the world

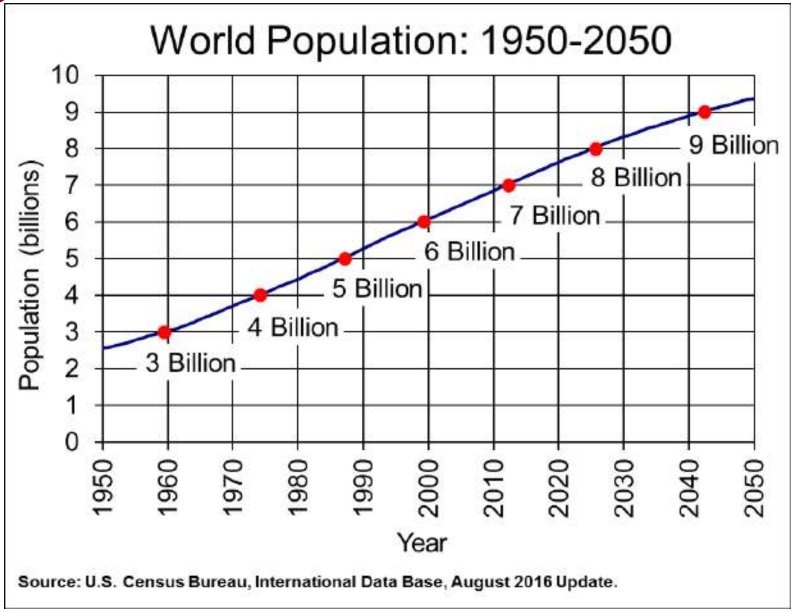

- The population increases and then the demand for protein increases.
- Protein and amino acids are essential for the growth of humans and animals.
- Proteins cannot be substituted by other food components.
- Fish meal is an important protein source for animal feed. But fish reserves decrease

Production of Single-Cell Protein:

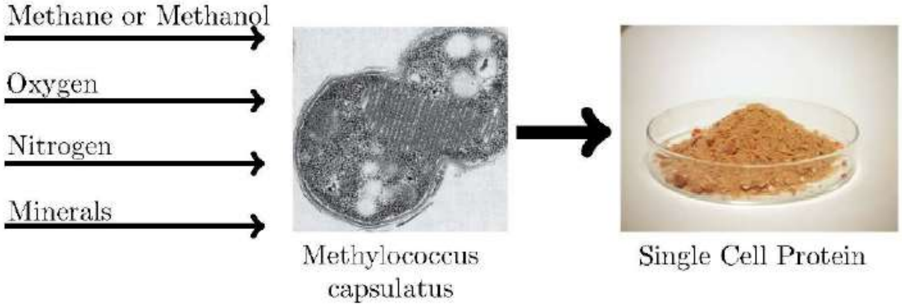

- M. capsulatus can be produced by fermentation on methanol or methane and this protein contains 70% protein.
- Single-Cell Protein (SCP) based on *M. capsulatus* can be used as animal feed.

Industrial complex for SCP production

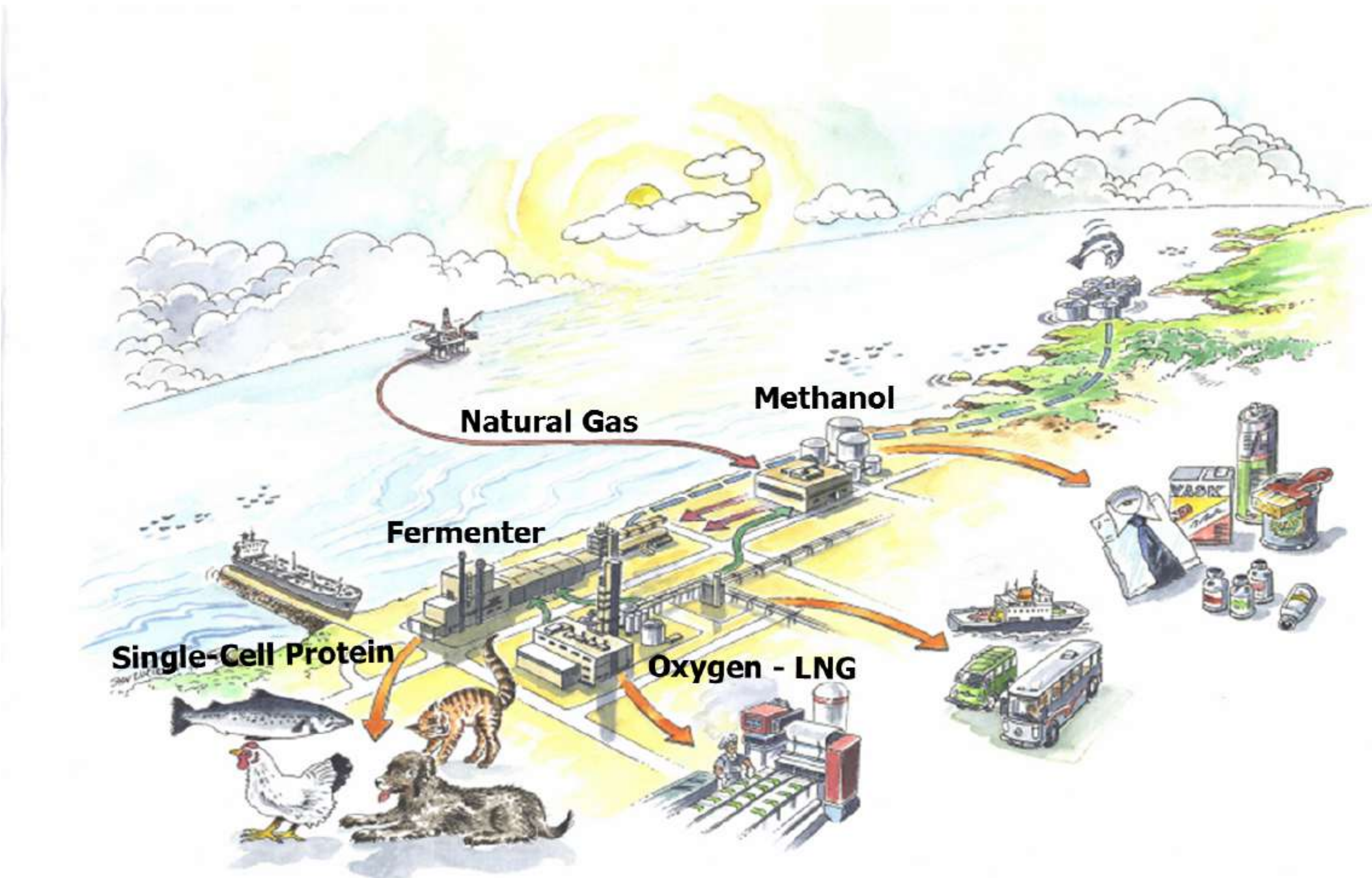

Single-Cell Protein Production in a U-loop Reactor

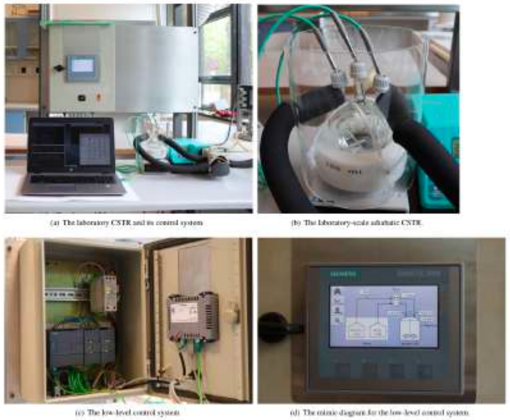

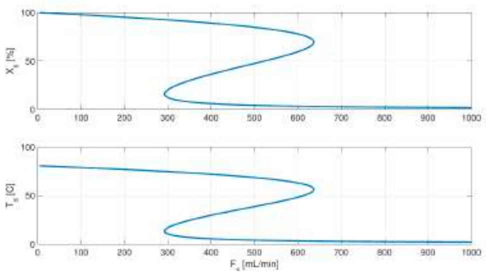

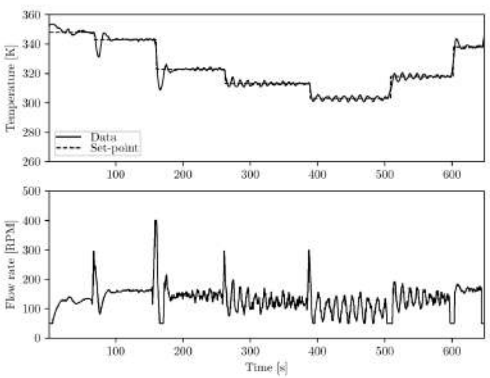

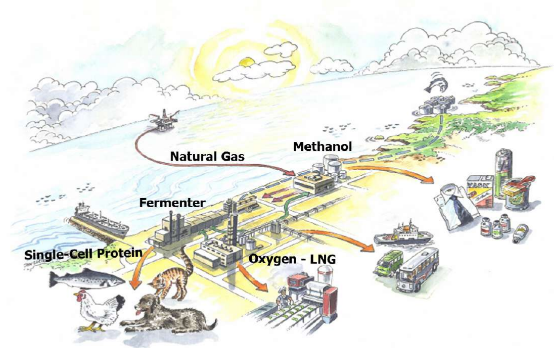

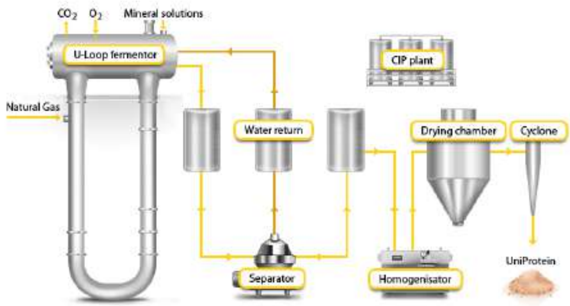

maximize

$$\phi = \int_{t_0}^{t_f} \underbrace{\left(p_X F(t)\bar{C}_X(t)\right.}_{\text{profit per time}} - \underbrace{\left. p_S F_S(t) - p_O F_G(t)\right)}_{\text{injection cost per time}} \mathrm{d}t + p_X \underbrace{\left(\bar{C}_X(t_f)\bar{V} + \int_0^L C_X(t_f,z)A\mathrm{d}z\right)}_{\text{value of the remaining biomass}} - p_X \underbrace{\left(\bar{C}_X(t_0)\bar{V} + \int_0^L C_X(t_0,z)A\mathrm{d}z\right)}_{\text{value of the starting biomass}}$$

Subject to

$$\frac{\mathrm{d}\bar{C}_X}{\mathrm{d}t} = D(\bar{C}_{X,in} - \bar{C}_X(t)) + R_X(\bar{C}_X, \bar{C}_S, \bar{C}_O)$$
$$\frac{\mathrm{d}\bar{C}_S}{\mathrm{d}t} = D(\bar{C}_{S,in} - \bar{C}_S(t)) + R_S(\bar{C}_X, \bar{C}_S, \bar{C}_O)$$
$$\frac{\mathrm{d}\bar{C}_O}{\mathrm{d}t} = D(\bar{C}_{O,in} - \bar{C}_O(t)) + R_O(\bar{C}_X, \bar{C}_S, \bar{C}_O)$$

$$\frac{\partial C_X}{\partial t}(t,z) = -\frac{\partial N_X}{\partial z}(t,z) + R_X$$
$$\frac{\partial C_S}{\partial t}(t,z) = -\frac{\partial N_S}{\partial z}(t,z) + R_S$$
$$\frac{\partial C_O}{\partial t}(t,z) = -\frac{\partial N_O}{\partial z}(t,z) + R_O + \frac{1}{1-\epsilon}J_{gl,O}$$
$$\frac{\partial C_{gO}}{\partial t}(t,z) = -\frac{\partial N_{gO}}{\partial z}(t,z) - \frac{1}{\epsilon}J_{gl,O}$$

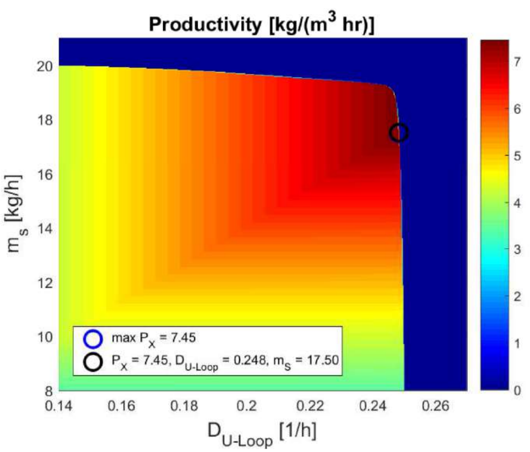

Single-Cell Protein Production in a U-loop Reactor

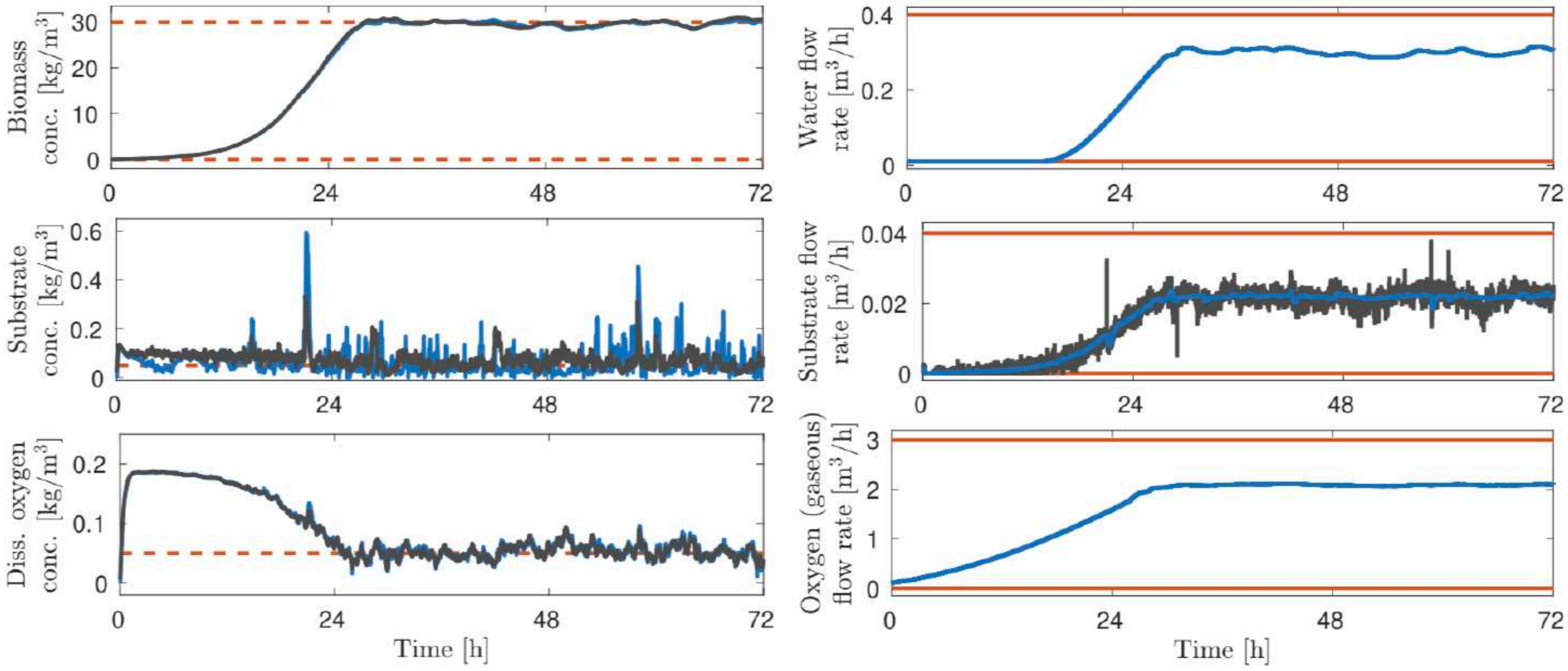

Single-Cell Protein Production in a U-loop Reactor

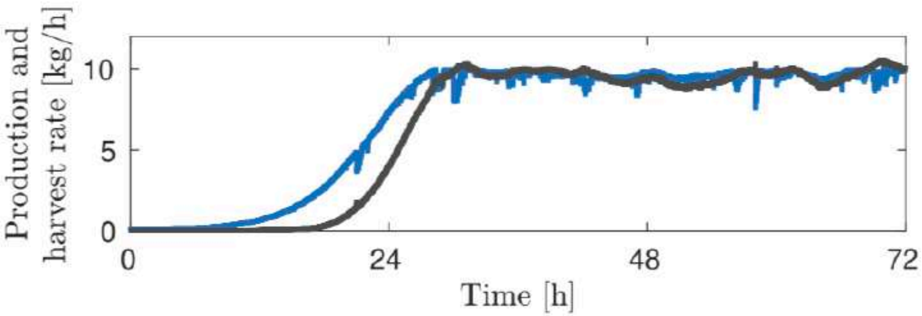

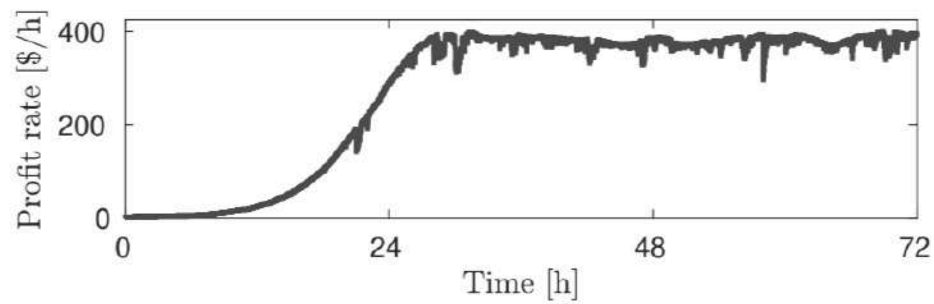

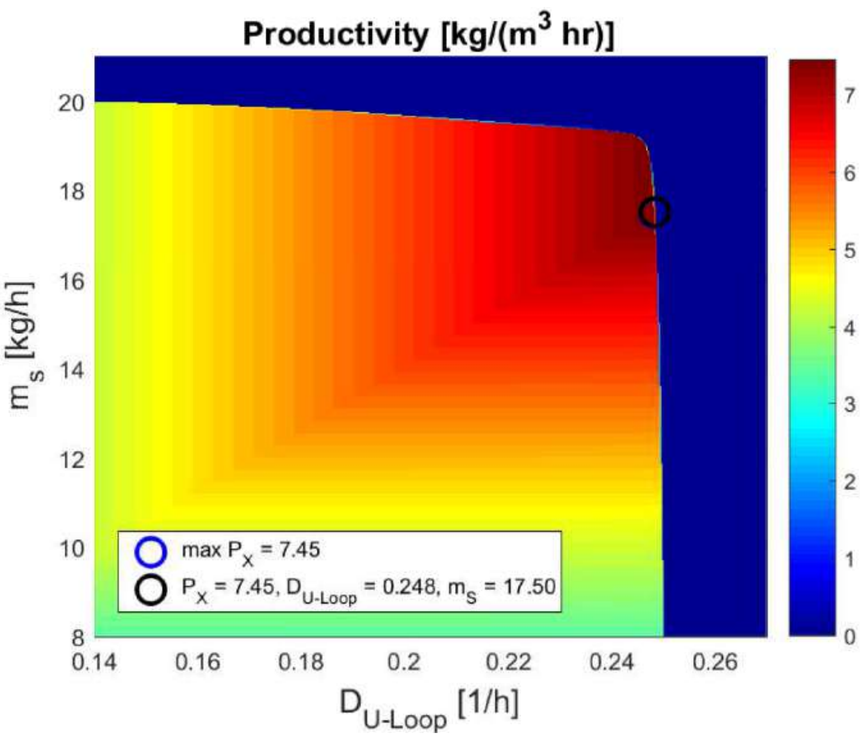

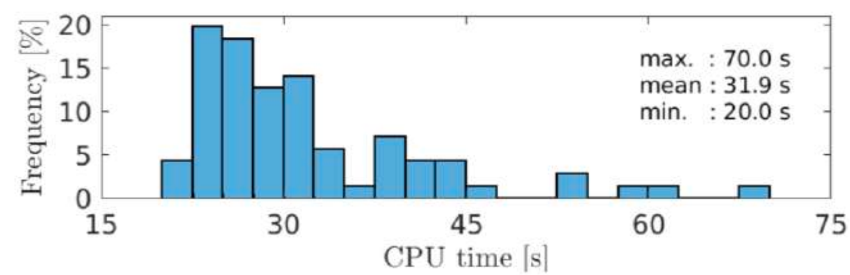

A patent appliction for the NMPC solution has been filed

Productivity increased from 3 kg/m3/h to 7 kg/m3/h

15 mio USD funding from private investors

Energy Smart Homes

and other energy systems facilitating the green transition

The Vision of Energy-Smart Homes

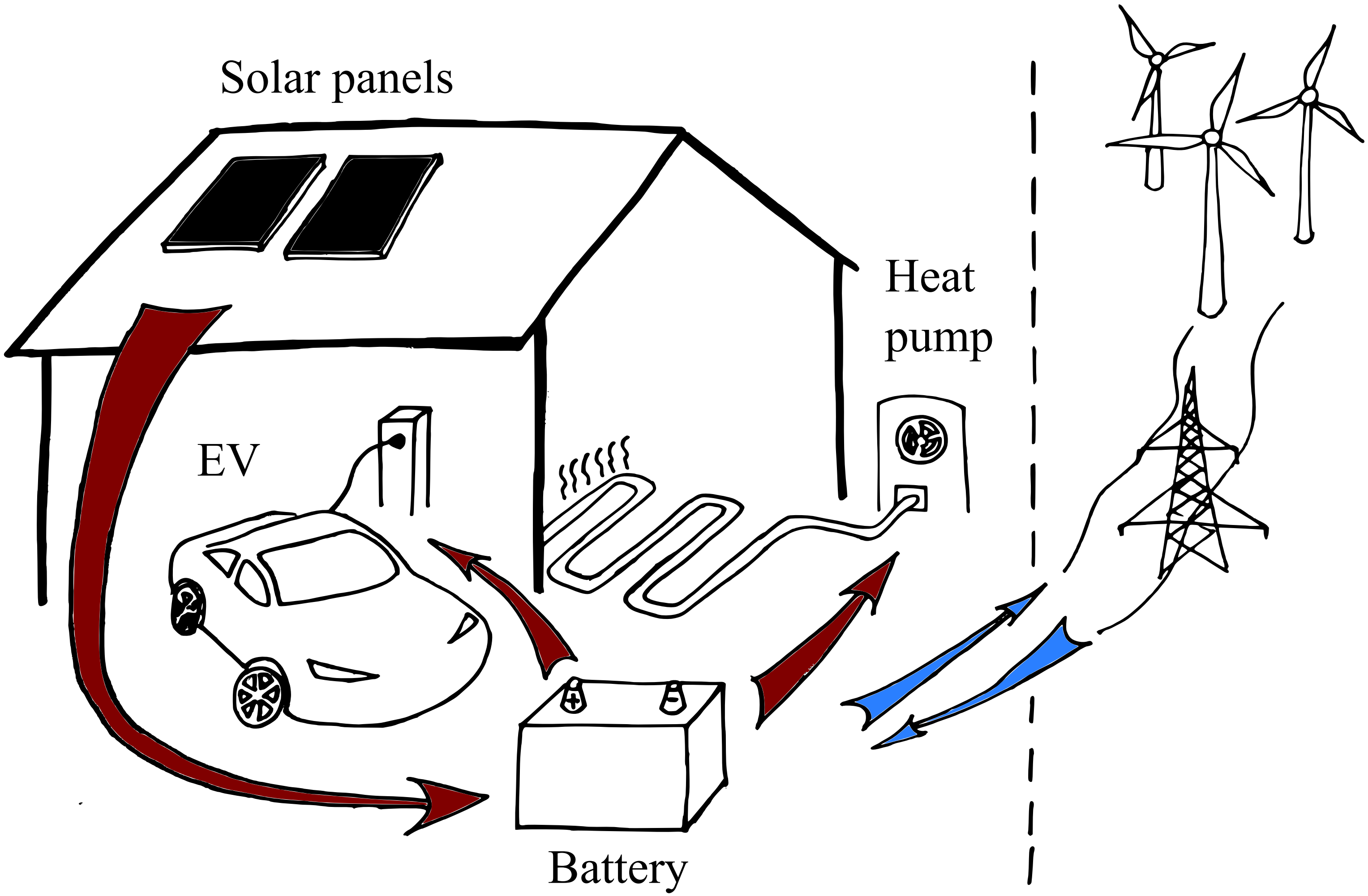

Elon Musk’s vision of an energy-smart home

Scientific advances in Economic MPC to enable smart energy homes

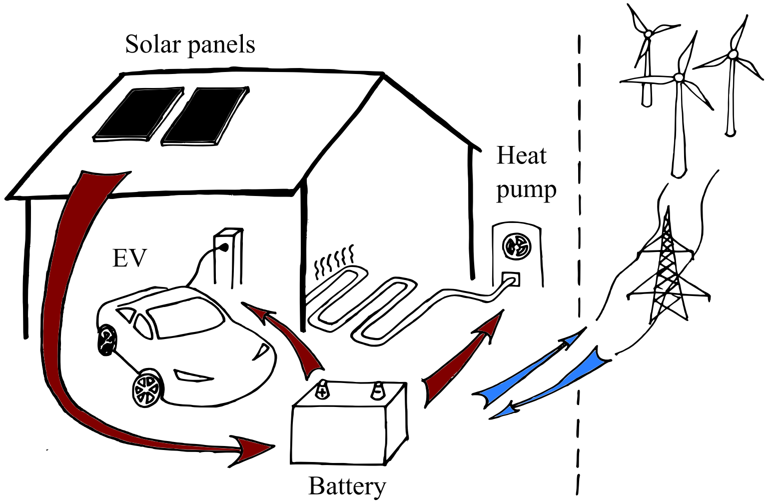

Economic MPC for Smart Energy Homes – a number of scientific advances

- Multi-level soft constraints
- Cost-to-go function – value of energy stored at the end of the prediction horizon
- A simple model for simulation, control and optimization of such systems
- Efficient algorithms and computational technologies

Economic MPC for Building Climate Control

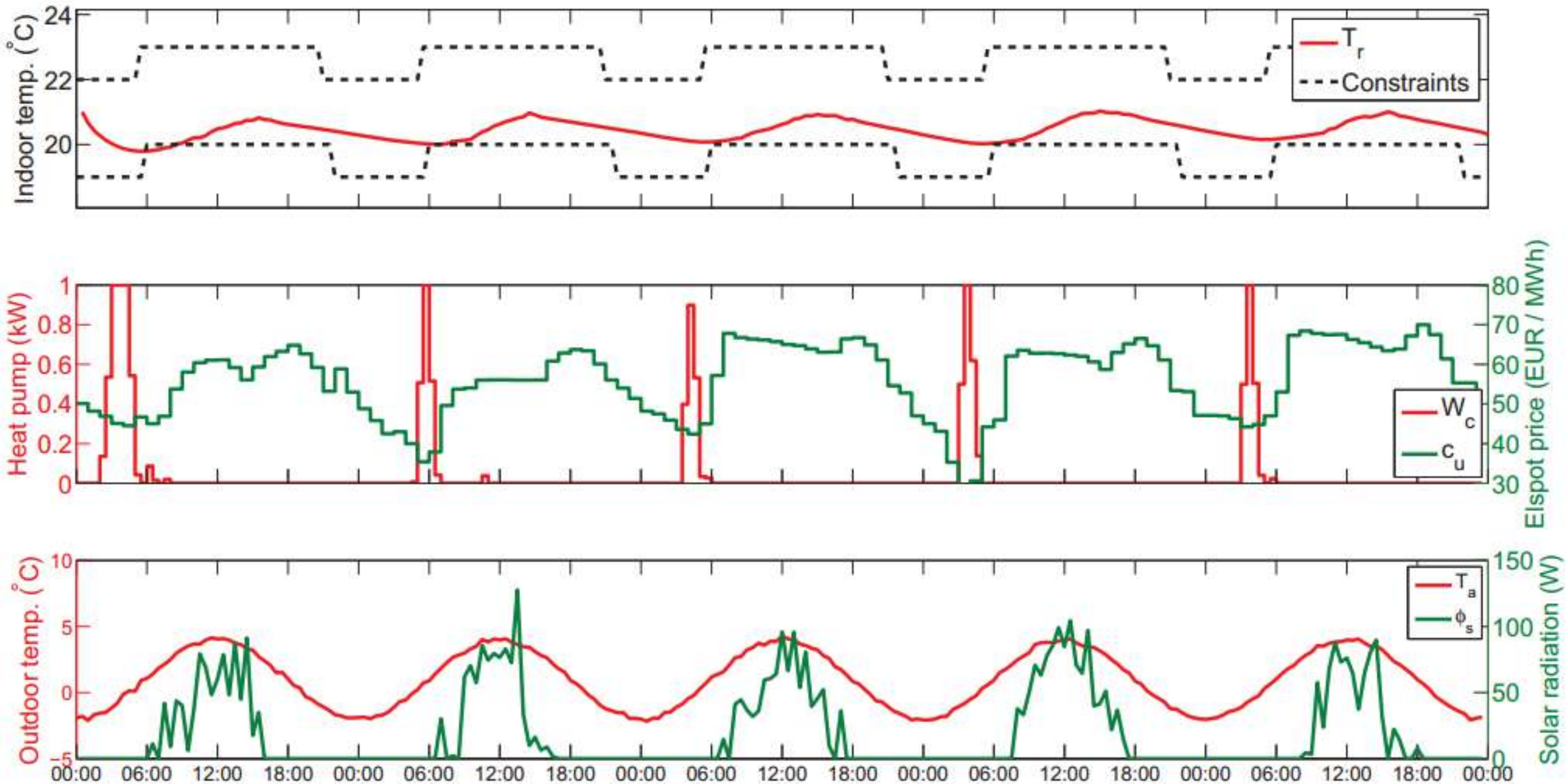

Model Predictive Control for a Smart Energy Home – Simulation Results

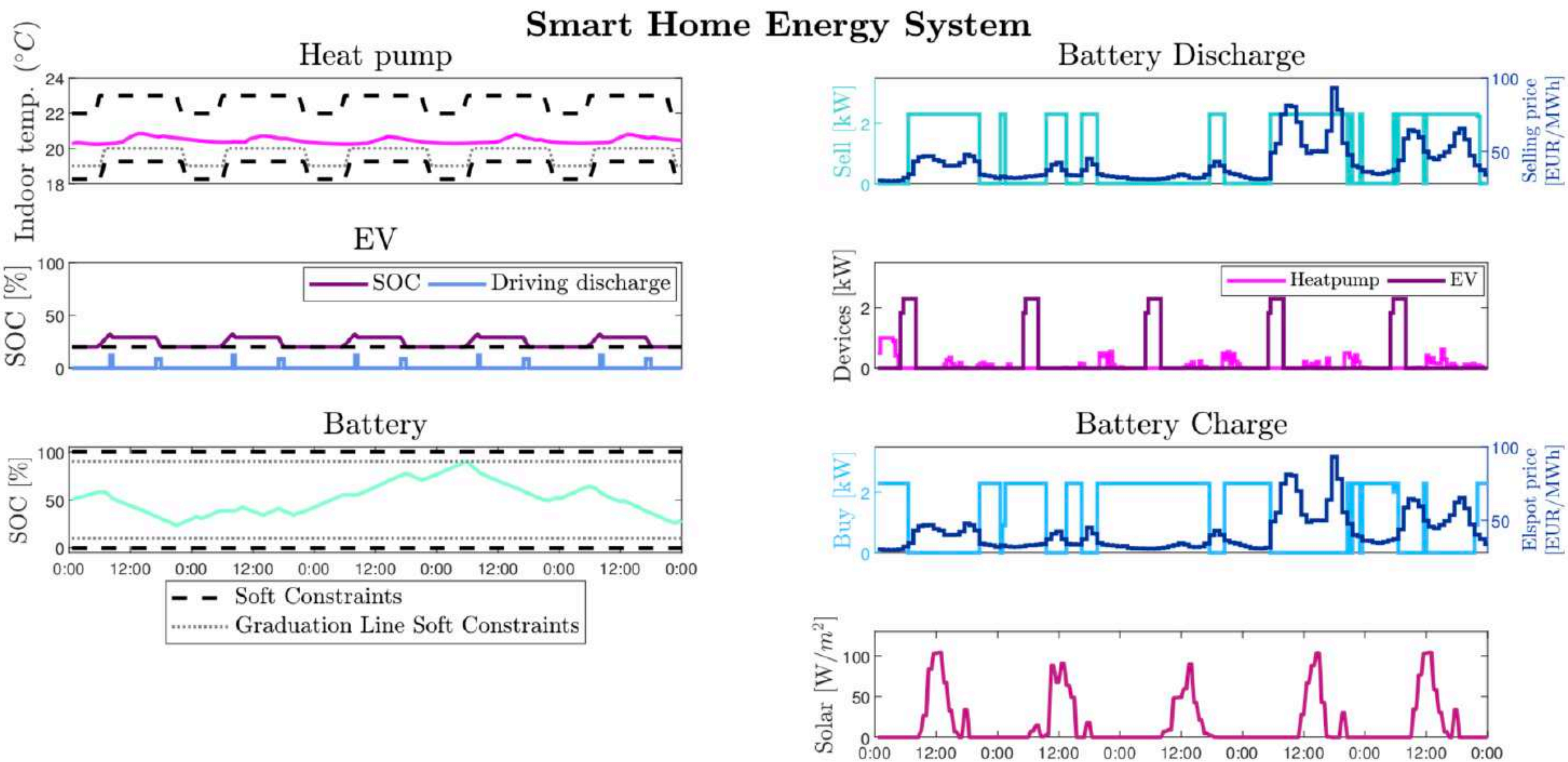

A neighborhood of smart energy homes - Lærkevej

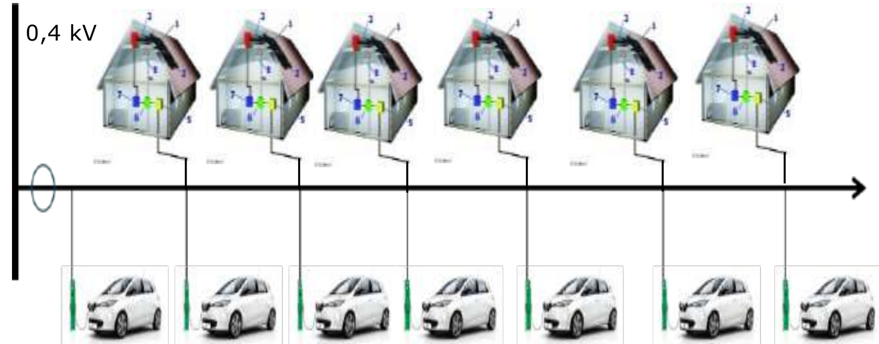

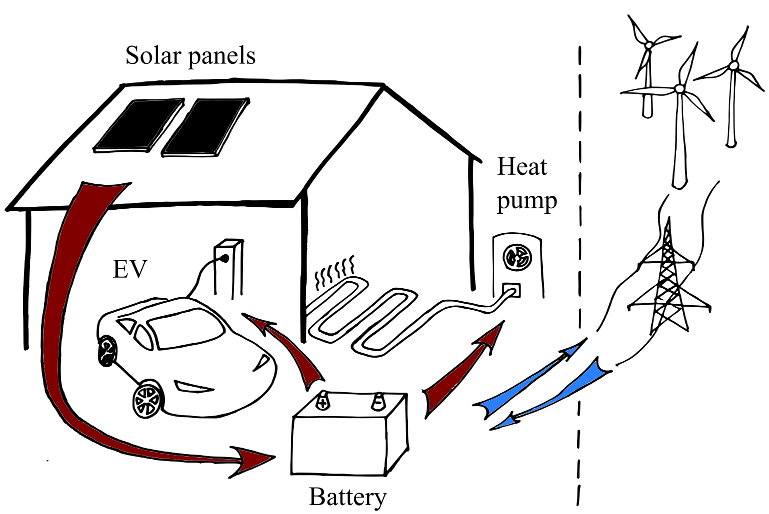

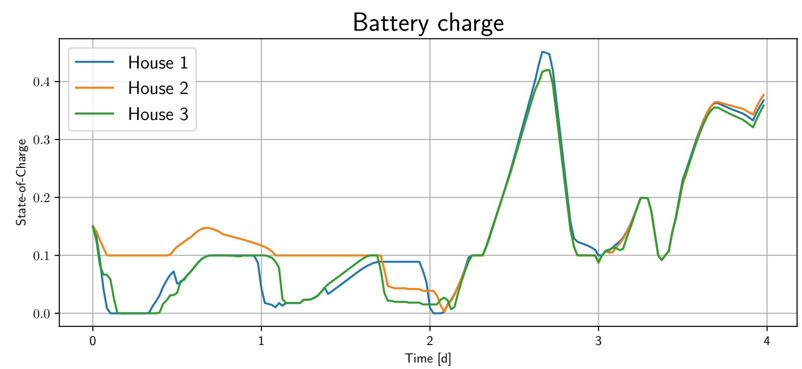

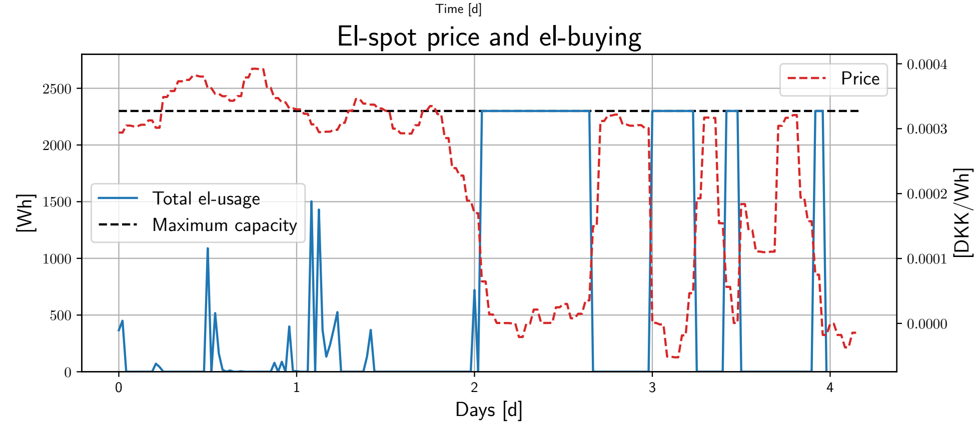

MPC & Energy

- MPC technology implemented in many systems to enable coordinated and efficient operation
- Industrial energy related processes
  - Cement Processes (FLSmidth)
  - Food processes (GEA Process Engineering)
- Energy Processes
  - Energy system control (Orsted)
  - Wind turbine control (Vestas)
- MPC technology is mature and ready to be implemented on large scale for buildings to enable smart cities and smart energy homes.
- MPC technology is the key enabler for integrated and coordinated systems

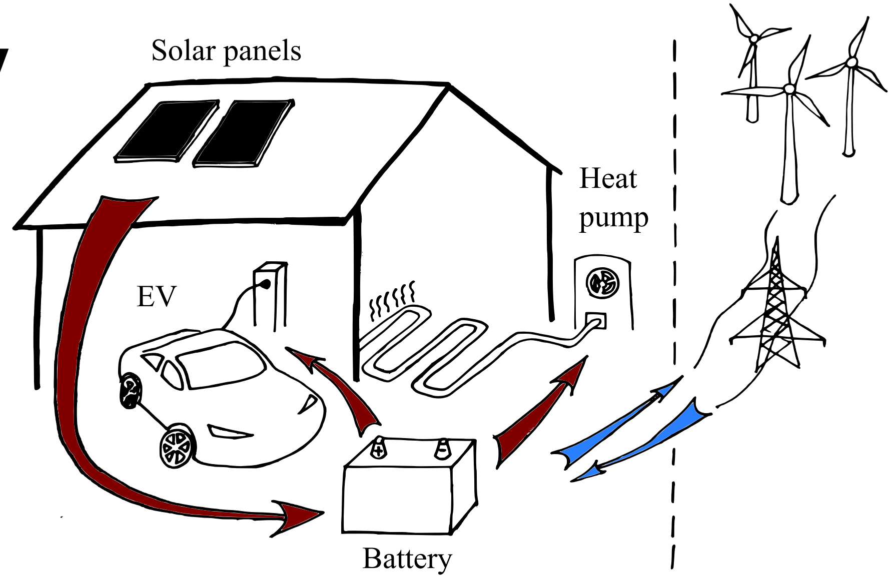

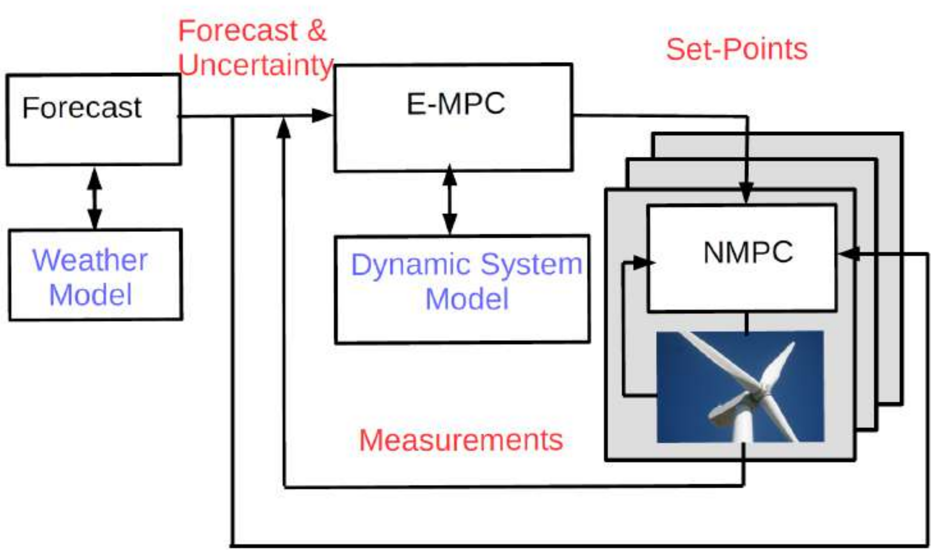

Upstream Oil and Gas

DTU Compute
Department of Applied Mathematics and Computer Science

CERE
Center for Energy Resources Engineering

Digitalization and optimization for upstream oil and gas

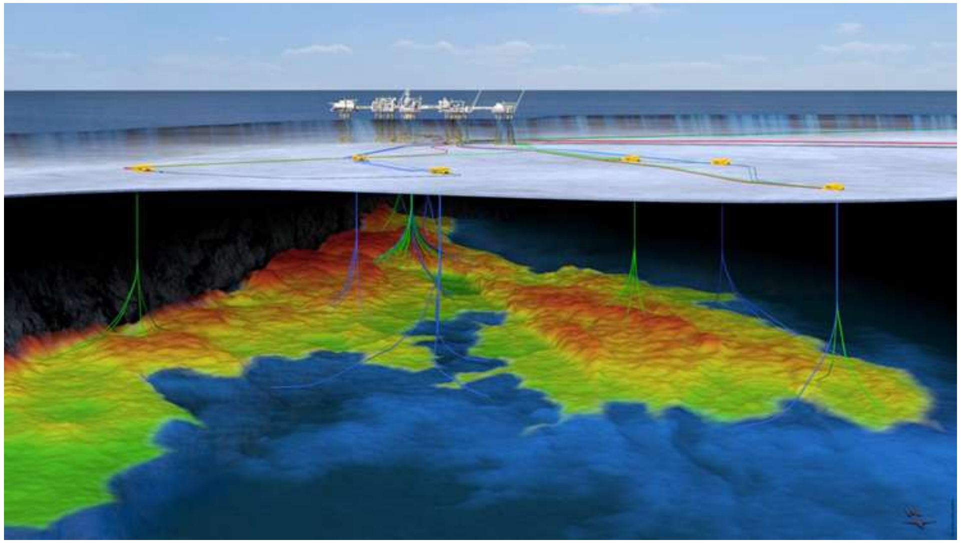

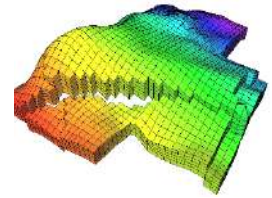

General form of partial differential equations

$$\left.\begin{aligned} \partial_t C_w &= -\nabla\cdot \mathbf{N}^w + Q^w, \\ \partial_t C_k &= -\nabla\cdot \mathbf{N}_k + Q_k, \\ \partial_t u &= -\nabla\cdot \mathbf{N}_u + Q_u \end{aligned}\right\} \quad \boxed{\partial_t C = -\nabla\cdot \mathbf{N} + Q}$$

Optimal control problem

$$\min_{[x(t);y(t);z(t)]_{t_0}^{t_f},\{u_k\}_{k\in\mathcal{N}}} \quad \phi = \int_{t_0}^{t_f} \Phi(y(t),u(t),d(t))dt$$

subject to

$$\begin{aligned} & x(t_0) = \hat{x}_0, \\ & G(x(t),y(t),z(t)) = 0, && t\in\mathcal{T}, \\ & \dot{x}(t) = F(y(t),u(t),d(t)), && t\in\mathcal{T}, \\ & u(t) = u_k,\ t\in[t_k,\ t_{k+1}[, && k\in\mathcal{N}, \\ & d(t) = \hat{d}_k,\ t\in[t_k,\ t_{k+1}[, && k\in\mathcal{N}, \\ & \{u_k\}_{k\in\mathcal{N}} \in \mathcal{U}. \end{aligned}$$

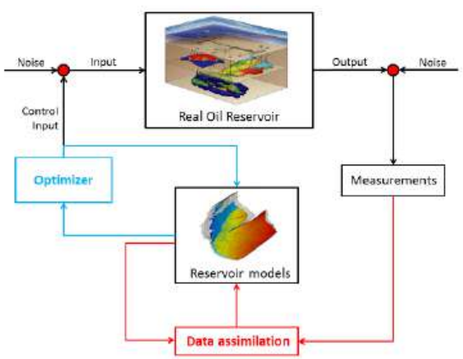

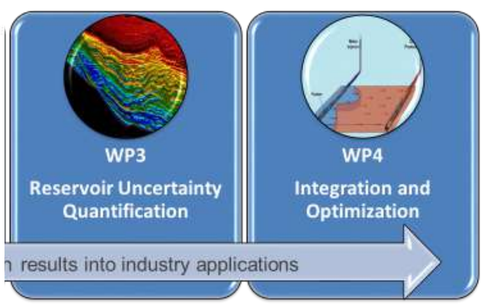

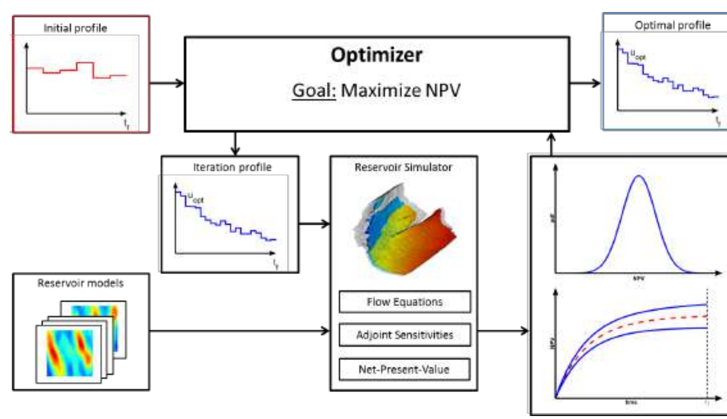

Uncertainty Quantification + Production Optimization =
Optimization under Uncertainty

Slug flow

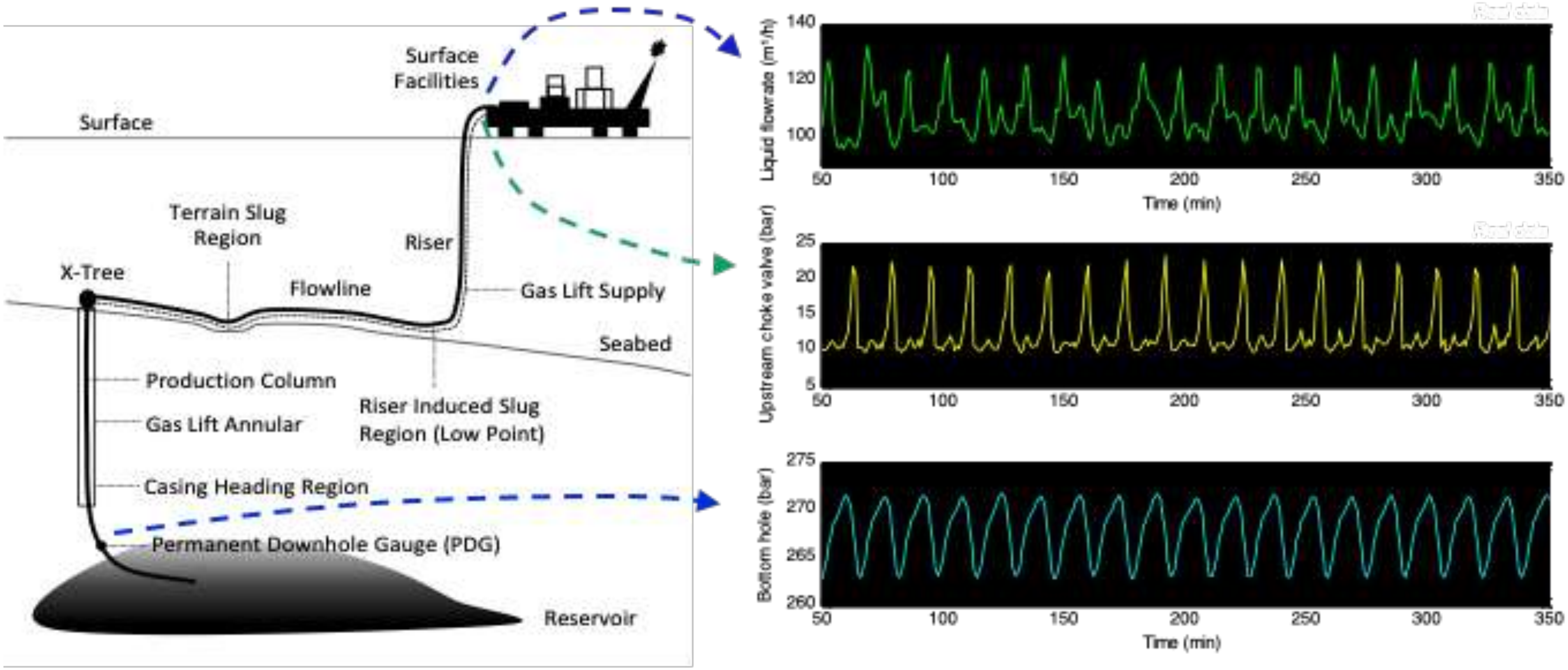

...increase shutdown risks and spread oscillation to the process plant!

Slug flow

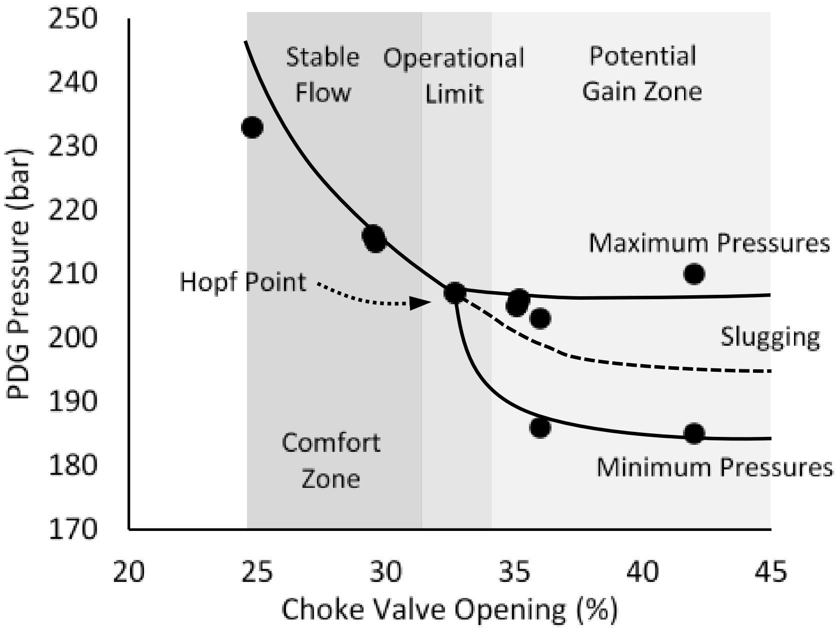

Stable Flow
Operational Limit
Potential Gain Zone
Maximum Pressures
Hopf Point
Slugging
Comfort Zone
Minimum Pressures
PDG Pressure (bar)
Choke Valve Opening (%)
250
240
230
220
210
200
190
180
170
20
25
30
35
40
45

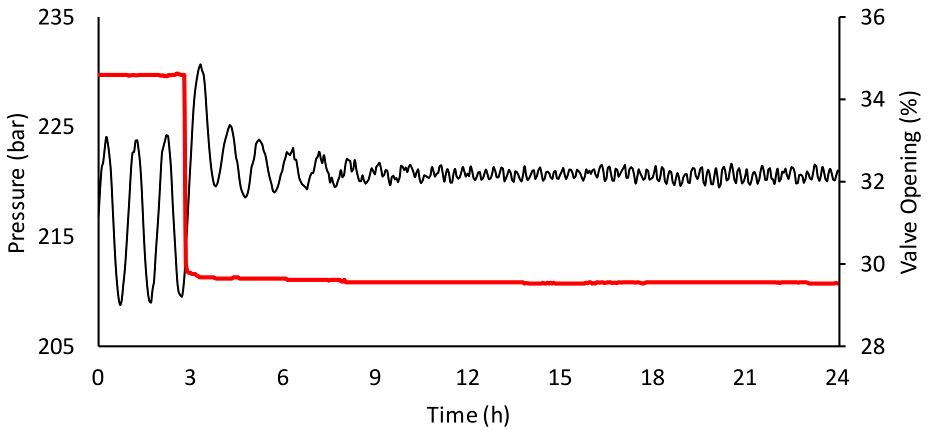

Pressure (bar)
Valve Opening (%)
Time (h)
235
225
215
205
36
34
32
30
28
0
3
6
9
12
15
18
21
24

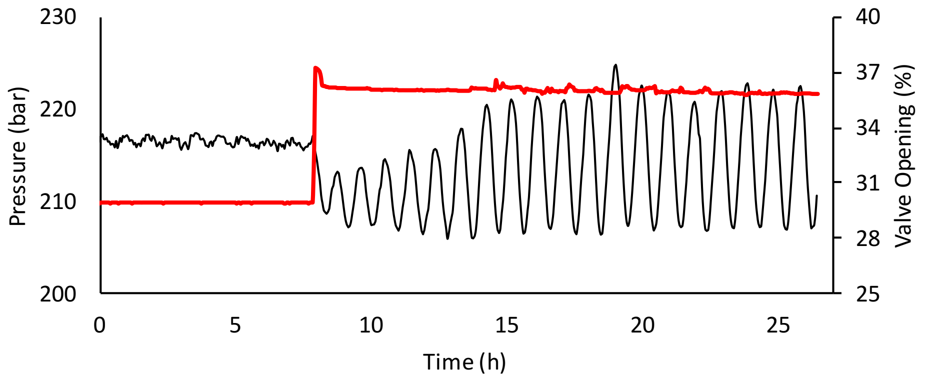

Pressure (bar)
Valve Opening (%)
Time (h)
230
220
210
200
40
37
34
31
28
25
0
5
10
15
20
25

Field deployment

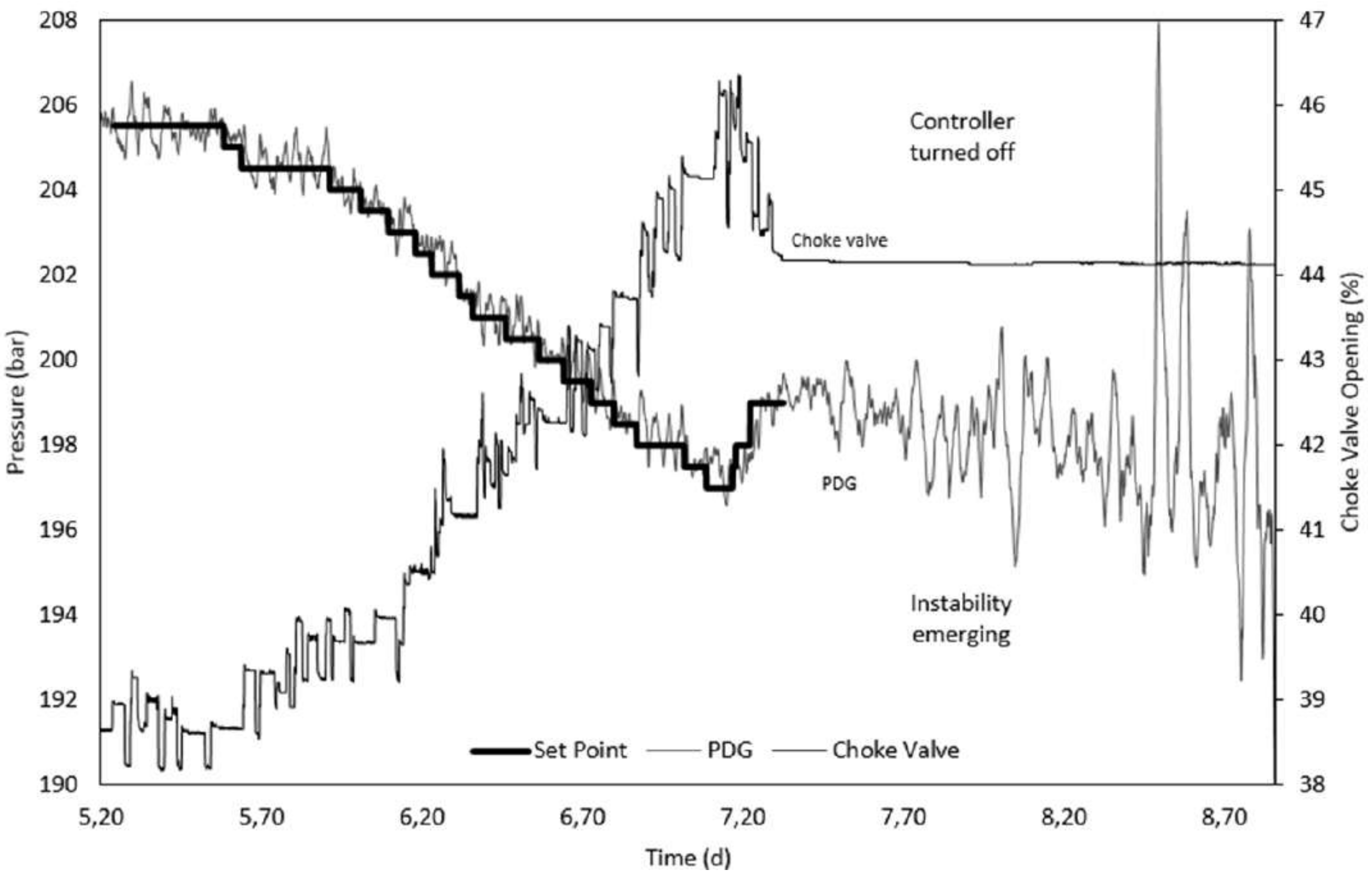

- Reduction of 8,5 bar in the bottom hole pressure (PDG)
- Increase in the choke valve opening from 39% to 46%
- Oil production: 10% higher than before the test
- Financial gain estimated about US$ 5 MM / year (Brent = US$ 60)
- The instabilities came up right after the controller was turned off
- In the second day the well stopped by an unscheduled shutdown caused by the instabilities

Summary & conclusions

DTU Compute & Model Based Control
Lots of opportunities in a connected digital future

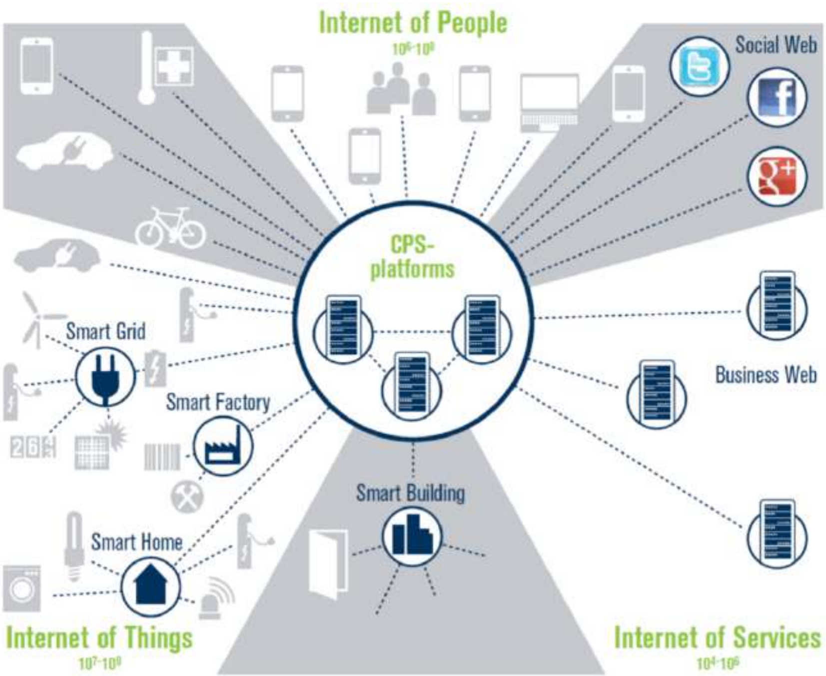

DTU Compute
Department of Applied Mathematics and Computer Science